Identification and characterization of interactors of *RAX1* controlling shoot branching in *Arabidopsis thaliana*

Inaugural-Dissertation

zur Erlangung des Doktorgrades

der Mathematisch-Naturwissenschaftlichen Fakultät

der Universität zu Köln

Vorgelegt von

Fang Yang

aus Chengdu, China

Köln 2007

Gutachter: Prof. Dr. Klaus Theres

Prof. Dr. Wolfgang Werr

Datum der mündlichen Prüfung: 06.02.2008

Index

Abbreviation

AA	amino acid
AD	GAL4 activation domain
AFO	*ABNORMAL FLORAL ORGANS*
AM	Axillary meristem
A.t.	*Arabidopsis thaliana*
AtLAX	*LAX*-related gene in Arabidopsis
AtRHD6	*ROOT HAIR DEFECTIVE 6*
AtRSL1	*RHD SIX-LIKE1*
BD	GAL4 binding domain
bHLH	basic helix-loop-helix
BA1	*BARREN STALK1* from maize
bp	base pair
Col	Columbia
CTK	Cytokinin
CUC	*CUPSHAPED COTYLEDON*
DNase	Deoxyribonuclease
E.coli	*Escherichia coli*
EGL3	*Enhancer of GLABRA3*
FIL	*FILAMENTOUS FLOWER*
FM	Floral meristem
GL1	*GLABRA1*
GL3	*GLABRA3*
GST	Glutathione S Transferase
HAT1	*HD-Zip protein 1*
HDZip	*Homeodomain leucine zipper*
IND	*INDEHISCENT*
IPTG	Isopropyl β- D -1-thiogalactopyranoside

KNAT   *KNOX-Gene* from Arabidopsis

LAS   *LATERAL SUPPRESSOR* from Arabidopsis

LAX   *LAX PANICLE* from rice

LD   Long days

LM   Lateral meristem

Ls   *LATERAL SUPPRESSOR* from Tomato

ORF   Open reading frame

Os   *Oryza sativa (rice)*

RAX   *REGULATOR OF AXILLARY MERISTEMS*

RT-PCR   Reverse transcriptase PCR

SD   Short days

TF   Transcription factor

wt   Wild type

WUS   *WUSCHEL* from Arabidopsis

Y2H   Yeast two hybrid

YAB1   *YABBY1* from Arabidopsis

Zm   *Zea mays (maize)*

1. Introduction

1.1 SAM is the fountain of plant growth

The basic growth axes of flowering plants are established during embryogenesis. On the basis of positional information specified by the apical-basal body axis, the shoot apical meristem (SAM) and root apical meristem (RAM) form at fixed positions early during embryogenesis. After germination, the RAM gives rise to the root system, whereas the SAM is responsible for the development of areal structures of a plant. The SAM may become determinate by forming a terminal flower (sympodial growth), or it may display an indeterminate pattern of growth (monopodial growth) by continuously producing leaves, branches and flowers (Itoh et al., 2006; Kerstetter and Hake, 1997). Shoot branches originate from axillary meristems (AMs) that initiate in the axils of leaf primordia and function like the SAM of the primary shoot. The pattern of shoot branching, as a result of the selective outgrowth of AMs, is a major source of the morphological diversification of flowering plant species.

1.1.1 Organization of the SAM

The SAM consists of a small group of cells from which all the aerial parts above the cotyledons of a plant are derived. SAMs are organized by three functionally different zones with distinct cellular morphologies (Fig. 1a; Steeves and Sussex, 1989; Clark, 1997; Medford et al., 1992; Kerstetter and Hake, 1997). The central zone (CZ), locating at the summit of the meristem, contains a population of slowly dividing stem cells. Cells in the surrounding peripheral zone (PZ) tend to be larger. They divide more rapidly, and eventually form lateral organs and the outer tissue of the stem. Underlying the CZ is the rib meristem (RZ, rib zone), whose cells also divide and expand rapidly and form the central tissue (pith) of the stem (Golz, 2006).

Another structural feature of the SAM of many angiosperms is the stratified appearance of the cell layers (Fig. 1a. Kerstetter and Hake, 1997). The cells of outermost layer(s) of the SAM, the **tunica**, divide in an anticlinal plane (perpendicular to the surface), whereas the cells in the **corpus** layers also divide periclinally. The tunica layer includes the L1 and L2 layers in most dicots, and the corpus comprises the L3 layer, underneath the tunica. In general, the outermost L1 layer gives rise to the epidermis of shoots, leaves and flowers, the L2 layer produces the ground tissues and germ cells, and the L3 layer contributes to the vascular tissues of the stem and the most internal tissues of leaves and flowers (Clark, 1997; Laux and Jurgens, 1997; Poethig, 1997; Schiefelbein et al., 1997).

1.1.2 Establishment and maintenance of the SAM

The SAM is formed during embryogenesis and subsequently gives rise to new organs reiteratively during postembronic development (Steeves and Sussex, 1989). Once established, the SAM harbors a population of stem cells over almost the entire life cycle of monopodial plants (Weigel and Jürgens, 2002). Stem cells in the center of the shoot meristem are the ultimate source from which all tissues of the growing shoot are derived (Clark, 1997; Laux and Mayer, 1998; Meyerowitz, 1997). Molecular and genetic studies revealed key regulators controlling establishment and maintenance of the SAM. The first described gene regulating the SAM identity is the maize *KNOTTED 1* (*KN1*), the founding member of the class-I *KNOX* subfamily of homeobox genes (Kerstetter and Hake, 1997; Kerstetter et al., 1997; Vollbrecht et al., 2000). A gain-of-function mutation or ectopic expression of *KN1* results in meristematic structures in the vicinity of leaf veins (Smith et al., 1992; Sinha et al., 1993). Subsequent loss-of-function studies have demonstrated that *KN1* is essential for shoot meristem formation and maintenance. The *KN1* mRNA is expressed in the corpus of the SAM and developing stem but not in leaf primordia or mature leaves (Jackson et al., 1994; Kerstetter et al., 1997). In *Arabidopsis*, the KNOX I subclass of genes

comprise four members, namely *SHOOT MERISTEMLESS (STM)*, *KNAT1/BP* (KNAT = Knotted in Arabidopsis thaliana; *BP=BREVIPEDICELLUS*), *KNAT2* and *KNAT6*. Based on null mutant phenotypes and expression patterns of transcripts, *STM* has a closer functional similarity to *KN1* than other KNOXI genes (Long et al., 1996; Vollbrecht et al., 2000). Mutants harbouring the strong loss of function alleles *stm-1*, *stm-5* and *stm-11* lack a functional SAM at the base of the cotyledons, and the less severe mutation *stm-2* results in disorganized and short-lived SAM. (Barton und Poethig, 1993; Long et al., 1996; Clark et al., 1996; Endrizzi et al., 1996). Thus, *STM* is essential for embryonic shoot meristem formation and for the subsequent maintenance of SAM organization. *STM* is initially expressed in the central apical cells of the globular embryo, later on in the transcripts are detectable throughout the SAM (including the CZ and PZ), in the interprimordial regions and in newly formed lateral meristems (Grbic and Bleecker, 2000; Long and Barton, 2000).

1.1.3 Shoot meristem maintenance by the *CLV-WUS* feedback loop

Shoot meristems, as the growth pole of a plant, always keep a homeostasis during life which is maintained by a tightly controlled balance between slowly dividing stem cells in the meristem center and cells that are recruited in the periphery and undergo differentiation (Haecker and Laux, 2001). *WUSCHEL* (*WUS*) and *CLAVATA* are identified as components of a negative feedback loop that controls this balance (Schoof et al., 2000). The genes acting in the *CLV* pathway are *CLV1*, *CLV2* and *CLV3* (Clark, 1997; Clark et al., 1993; Kayes and Clark, 1998). Mutations in any of these three genes produce larger SAMs due to an increased number of cells in the CZ suggesting that *CLV* genes suppress stem cell proliferation and/or promote organ formation. *CLV1* is expressed in the L3 layer of the meristem (Clark et al., 1997; Mayer et al., 1998). The transcript of *CLV3* is restricted to the so-called stem cells, through the L1 to L3 layers, and hence is often used as a maker for stem cells in the SAM

(Fletcher et al., 1999; Fig. 1). *CLV3* is postulated to function together with *CLV1* to limit the size of the *WUS* expression domain underneath (Trotochaud et al., 1999).
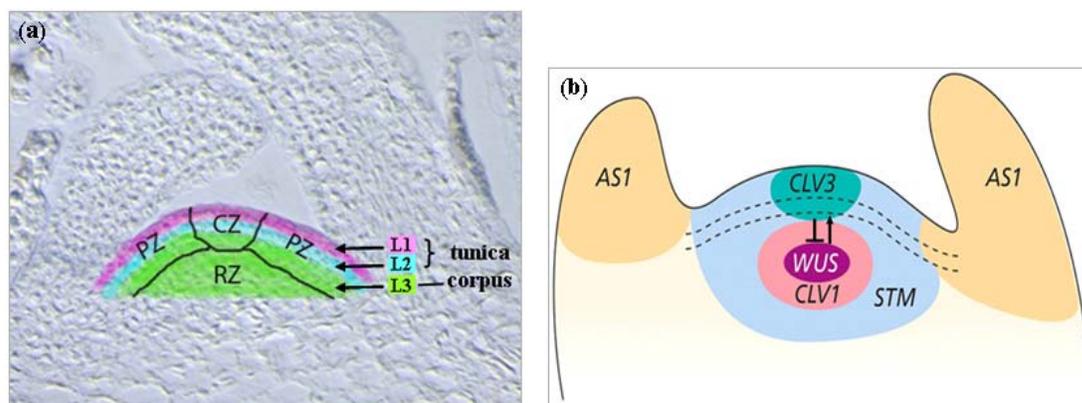
Fig. 1. Histology of the shoot apical meristem (SAM) and the CLV-WUS feedback loop. (a) Three cell layers and three zones of an *Arabidopsis* vegetative SAM. The colored domains depict the different cell layers. In *Arabidopsis*, the tunica corresponds to the outer two cell layers, L1 and L2, whereas the corpus corresponds to the internal layers L3. The black lines represent the approximate boundaries between the different meristematic zones: the peripheral zone (PZ) from which lateral organs are formed, the rib zone (RZ), and the central zone (CZ) acting as a 'source' of cells for the PZ and RZ, but also for its own replenishment with new cells (Golz, 2006). The PZ and the CZ contain both tunica and corpus cells, whereas the RZ locates in the deeper layers of the corpus. (b) A schematic representation showing the *CLV-WUS* feedback required for maintenance of a functional SAM. A positive signal from *WUS* maintains the *CLV3* expression domain and stem cell identity in L1, L2, and L3 layers at the summit of the meristem. A signal from *CLV3* limits the expression domain of *WUS* to the organizing center (OC) (Adapted from Taiz & Zeiger 3rd. Fig 16.28. p364).

WUS encodes a homeodomain transcription factor and is expressed in a small region in the centre of the SAM, called the organizing center (OC) (Laux et al. 1996; Mayer et al. 1998). *wus* mutants are characterized by a stop-and-go growth, indicating that *WUS* is necessary for maintenance of the SAM. *WUS* expression is sufficient to induce the expression of *CLV3* and to promote meristem cell identity of overlying neighbor cells. Activation of *CLV3* results in a down-regulation of *WUS* expression. Such a feedback loop allows the SAM to maintain the equilibrium between stem cell proliferation in the CZ and cell loss due to differentiation in the PZ (Brand et al. 2000; Schoof et al. 2000; Fig. 1b). Double mutant combination of *wus* and *clv* are almost indistinguishable from the *wus* single mutant, consistent with the model that *WUS* is a target for the negative regulation by the *CLV* genes to maintain a constant number of stem cells in the CZ of the SAM (Laux et al., 1996; Schoof et al., 2000).

1.1.4   The SAM and lateral organs

In seed plants, lateral organs such as leaf and floral primordia are formed from the flanks of the SAM, a defined group of founder cells of apical meristems. *KNOX* genes are not expressed in developing primordia and have been shown to function antagonistically to the process of leaf development (Brand et al., 2002; Chuck et al., 1996; Dean et al., 2004; Gallois et al., 2002; Lenhard et al., 2002; Lincoln et al., 1994; Pautot et al., 2001). Several genes are responsible for the initial repression of the *KNOX* genes in lateral organs: *Antirrhinum PHANTASTICA* (*PHAN*) (Waites et al., 1998), maize *ROUGH SHEATH2* (*RS2*) (Timmermans et al., 1999; Tsiantis et al., 1999b) and *Arabidopsis ASYMMETRIC LEAVES1* (*AS1*) (Byrne et al., 2002). Loss of *PHAN/RS2/AS1* functions is associated with the ectopic expression of *KNOX* genes in leaves indicating that these genes repress *KNOX* expression in leaf primordia (Schneeberger et al., 1998). The *PHAN/RS2/AS1* genes are initially expressed in the leaf founder cells and later in the growing leaf primordia.

In addition, members of the *YABBY* (*YAB*) gene family have also been shown to repress the expression of class-I *KNOX* genes in leaves (Kumaran et al., 2002). *YABBY* genes are expressed on the abaxial side of lateral primordia and function in promoting abaxial cell fate of lateral organs (Kumaran et al., 2002; Sawa et al., 1999; Siegfried et al., 1999). Knockout mutations in both *YAB1* and *YAB3* result in lobed leaves expressing *KNOX* genes and ectopic meristems, suggesting an incompatibility between *KNOX* gene functions and proper specification of abaxial cell fate.

Adaxial-specific transcriptional regulators are also important in establishing a connection between leaf polarity and shoot meristem function (McConnell et al., 2001; Otsuga et al., 2001). The class III HD-ZIP family members *PHABULOSA* (*PHB*), *PHAVOLUTA* (*PHV*) and *REVOLUTA* (*REV*) are adaxial-identity promoting factors in developing leaves (Byrne, 2006).

These genes are expressed in the central zone of the SAM, in the vasculature and on the adaxial side of developing leaf primordia. Loss-of-function mutations in *REV* result in a reduced meristematic competency (Talbert et al., 1995). Mutants harboring gain-of-function mutations in *PHB* and *PHV* produce enlarged SAMs and *STM*-expressing ectopic meristems. (McConnell and Barton, 1998). Conversely, simultaneous loss of *PHB*, *PHV* and *REV* function results in leaf abaxialisation and loss of shoot meristem formation/maintenance (Emery et al., 2003).

1.1.5 Hormonal regulation of the SAM function

Recently, several studies lead to a model in which high auxin concentrations in incipient primordia down-regulate the expression of *KNOXI* genes, inducing lateral organ initiation (Benkova et al., 2003; Reinhardt et al., 2000; Reinhardt et al., 2003). Therefore, auxin is supposed to act as a positive regulator for leaf initiation.

The positive role of cytokinin (CK) on SAM function has been addressed by the analysis of triple mutants of three genes encoding CK receptors: *AHK2* (*Arabidopsis HISTIDINE KINASE 2*), *AHK3* and *AHK4/CRE1/WOODEN LEG* (*WOL*) (Higuchi et al., 2004; Nishimura et al., 2004; Riefler et al., 2006). *ahk2 ahk3 ahk4* triple mutants display a dramatic reduction in meristem size. New insights into the regulation of CK in meristem function and maintenance come from functional analysis of *LONELY LOG* (*LOG*) in rice (Kurakawa et al., 2007). The *log* mutant has a smaller vegetative meristem and its floral meristems terminate prematurely. *LOG* is specifically expressed in the shoot meristem tips and encodes an enzyme that controls the final CK biosynthesis step to release active CK.

KNOXI proteins have been shown to negatively regulate gibberellic acid (GA) biosynthesis, causing a suppression of GA activity in the SAM (Chen et al., 2004; Hay et al., 2002;

Sakamoto et al., 2001). The application of exogenous GA suppresses the phenotypes caused by the misexpression of *KNOX* genes (Hay et al., 2002).

1.2 Shoot branches determine the architecture of a plant

The aerial architecture of flowering plants is determined to a large extent by shoot branches established by the formation and outgrowth of axillary meristems (AMs). These meristems subsequently function as shoot apical meristems (SAMs) to provide plants with an unlimited growth potential. In higher plants, AMs form in the axils of leaves (Sussex and Kerk, 2001; Ward and Leyser, 2004). Once established, AMs first produce a few leaves to form lateral buds. These buds have a potential to develop into lateral shoots, or remain dormant until outgrowth is triggered. The outgrowth of lateral buds is controlled by the main shoot apex, which is known as apical dominance. Hence, the degree of branching depends not only on the establishment of an axillary meristem but also upon its subsequent activity.

1.2.1 Formation of axillary meristem

1.2.1.1 Ontogeny of axillary meristem

AMs form at the boundary regions between the SAM and lateral primordia. These 'boundary cells' display distinctive structural characteristics compared to the surrounding cells (Kwiatkowska and Dumais, 2003). However, the ontogeny of the AM is still in a state of debate. To date, there are two opposite models explaining the originS of AMs. The first suggests that AMs initiate de novo separately from the SAM in leaf axils ('*de novo*' formation concept) (Snow and Snow, 1942). This hypothesis is supported by the observation that in the axils of leaves formed in early development there is no morphologically distinguishable AM at the time of leaf primordium initiation. Further support for the '*de novo*' formation of AMs

comes from the study on the *Arabidopsis phabulosa-1d* mutant in which AMs form at the (adaxilaized) abaxial base of leaves (McConnell and Barton 1998). An alternative model suggests that AMs derive from groups of meristem cells that detach from the SAM at the time of leaf primordia initiation and never lose their meristematic identity ('*detached*' meristem concept) (Garrison, 1955; Sussex, 1955). Evidence for this hypothesis comes from the expression of the SAM marker *STM* in the leaf axils immediately proceeding the appearance of a morphological AM (Long et al., 1996). However, the interprimordial expression of *STM* makes it difficult to distinguish between the "detached meristem" and "de novo formation" concepts of AM initiation.

The formation of AM has been suggested to be temporally and spatially specified. In *Arabidopsis*, not all AMs develop at the same time, some may not develop at all (especially those in the cotyledonary nodes) (Aguilar-Martinez et al., 2007). During prolonged vegetative stage, AMs are initiated in an acropetal order, first in the axils of mature leaves distant from the shoot apex and progressing to younger leaves. Once the SAM is transformed from the vegetative to reproductive stage, AMs are initiated in a basipetal order, first in leaf axils closest to the shoot apex (Hempel and Feldman, 1994; Grbic and Bleecker, 2000; Long and Barton, 2000).

1.2.1.2 Regulators of axillary meristem initiation

The characterization of mutants defective in shoot branching makes it possible to investigate the molecular mechanisms of AM initiation. The well-known regulators for AM initiation are orthologous *GRAS* transcription factors from tomato *LATERAL SUPPRESSOR* (*Ls*), *Arabidopsis LATERAL SUPPRESSOR (LAS)*, and rice *MONOCULM1* (*MOC1*) (Greb et al., 2003; Schmitz et al., 2002; Schumacher et al., 1999; Li et al., 2003). Mutations in both *Ls* and *LAS* resulted in a complete lack of side shoots during the vegetative phase of development. This

phenotype is due to loss of the meristematic competence of the cells in the leaf axils. After the transition to reproductive development, axillary shoots are formed and inflorescence branching is not affected in these mutants. Introduction of a genomic fragment carrying the *Arabidopsis LAS* gene into the tomato *ls* mutant led to a full complementation of the mutant phenotype, revealing a conserved working mechanism for AM formation over a large evolutionary distance (Greb et al., 2003). The *Arabidopsis LAS* gene is expressed in a band-shaped domain at the adaxial base of all primordia derived from the SAM. The *Ls/LAS*-orthologous gene *MOC1* in rice controls vegetative as well as reproductive branching. Loss of *MOC1* function resulted in lack of tillers as well as a reduced number of rachis branches and spikelets (Li et al., 2003). *MOC1* is expressed mainly at the leaf axils and the expression extends to the entire tiller buds. Molecular and structural analysis of the barren leaf axils in these mutants suggests that the function of *LAS/Ls/MOC1* is probably to retain the meristematic capacity in a group of cells at the adaxial base of leaf primordia. Loss of *LAS/Ls/MOC1* function results in an inability to sustain this group of cells, hence the phenotypes of these mutants. This conserved genetic function suggests a single general mechanism of AM formation in different plant species.

In *Arabidopsis thaliana*, the functionally redundant genes *CUP-SHAPED COTYLEDON1* (*CUC1*), *CUC2*, and *CUC3* regulate embryonic shoot meristem formation and boundary specification of lateral organs including cotyledons (Aida et al., 1997; Hibara et al., 2006; Takada et al., 2001; Vroemen et al., 2003). Any combination of mutant *cuc* alleles leads to severe cotyledon fusions and cup-shaped structures, which do not contain a SAM. All three *CUC* genes encoding NAC transcription factors are expressed in a narrow strip of cells in the boundary domains between the SAM and lateral primordia, very similar to *LAS*. Such characteristic expression patterns of *CUCs* in the axils of leaf primordia indicate their roles in AM formation. This hypothesis has been proven by two independent studies on *cuc* loss-of-function mutants (Hibara et al., 2006; Raman, 2006). The significant roles of *CUC2*

and *CUC3* in AM formation were described by Hibara (Hibara et al., 2006). *cuc3* mutants were found to be impaired in tertiary shoot formation (axillary shoots from secondary shoots) at a low frequency, whereas the *cuc2 cuc3* double mutant lacked branches in all leaf axils, indicating the redundant functions of *CUC2* and *CUC3* in AM formation. Raman also showed that *CUC3* regulates axillary bud formation (Raman, 2006). Over-expression of *MIR164A* or *MIR164B*, targeting the mRNAs of *CUC1* and *CUC2*, in the *cuc3-2* mutant caused an almost complete lack in axillary bud formation, revealing a functional redundancy of *CUC1, CUC2* and *CUC3* in AM formation.

Recently, the roles for three *Scarecrow like* (*SCL*) genes (*SCL6, 22, 27*) in AM development, but not in AM initiation have been characterized by Schulze (2007). In *scl27-1* mutants grown in short photoperiods, formation of lateral buds was found to be compromised during the vegetative and reproductive phases of development. Any combination of loss-of-function mutations in three *SCL* genes led to an enhancement of the branching defect of *scl22-7*, demonstrating functional redundancy among these three genes. Transcripts of *SCL22* and of *SCL27* were detected in vegetative and reproductive apical meristems, lateral meristems and the vasculatures of shoots and leaves. *SCL6* transcripts were detected in the axils of leaf and floral primordia. The expression of the meristem markers *STM* and *LAS* was detected in the interprimordial regions of apices of *scl22-1 scl27-1* and *scl6-1 scl22-1 scl27-1* mutant plants, demonstrating that the activities of these *SCL* genes are needed for the development of side shoots after the initiation of AMs (Schulze S., 2007).

Another group of regulators controlling early steps of AM formation comprises members of R2R3-type *MYB* transcription factors from tomato and *Arabidopsis*, namely *Blind* and *REGULATORS OF AXILLARY MERISTEMS* (*RAXs*), respectively. In tomato, the allelic *blind* and *torosa* mutants display a strong reduction in AM formation during the vegetative and reproductive developmental stages (Mapelli and Kinet, 1992; Schmitz et al., 2002). The

sympodial shoot is often not formed in these mutants and the plants terminate with a single inflorescence. In addition, the number of floral meristems (FMs) is greatly reduced, and flowers are often fused. In *Arabidopsis*, the *Blind*-homologous *RAX* genes (*RAX1, 2, 3*) have recently been shown to control an early step of AMs formation (Müller et al. 2006; Keller et al., 2006). *rax1-3* mutants fail to form lateral buds during the early vegetative developmental stage. Analysis of double and triple *rax* mutants revealed that *RAX* genes control shoot branching in overlapping zones along the shoot axis. In addition, the severity of branching defects of *rax* mutants was shown to be strongly dependent on day-length conditions. The defects observed under short-day conditions were strongly diminished or vanished in long days. *RAX1* transcripts accumulate in a ball-shaped domain in the center of the boundary region between the SAM and the leaf primordia. *RAX3* displays an expression pattern similar to that of *RAX1* during the vegetative stage, whereas *RAX2* shows a wide expression in the shoot tip (Müller et al. 2006). Double mutant analysis of *ls* and *blind* (*bl*) in tomato as well as of *las-4* and *rax* in *Arabidopsis* suggests that at least two independent pathways control the initiation of AMs (Müller et al., 2006; Schmitz et al., 2002).

LAX PANICLE (*LAX*) and *BARREN STALK1* (*BA1*) were recently characterized as major regulators of shoot and inflorescence branching in rice and maize, respectively (Gallavotti et al., 2004; Komatsu et al., 2003; Komatsu et al., 2001). *LAX* and *BA1* encode homologous basic helix–loop–helix (bHLH) transcription factors. *LAX* transcripts are excluded from the vegetative SAM and accumulate mainly in the boundary regions between the SAM and the new meristems during the reproductive stage. Plants homozygous for strong *lax* alleles have severely reduced panicle branches and completely lack lateral spikelets, demonstrating an important role of *LAX* in regulating reproductive branching. The *LAX* gene also regulates the formation of vegetative branches (tillers), in a redundant fashion with the *SMALL PANICLE* (*SPA*) gene. *lax spa* double mutants are characterized by a complete lack of tillers (Komatsu et al., 2003). Studies on mutants harbouring a loss-of-function mutation in *BA1,* the

LAX-orthologous gene from maize, have uncovered a pivotal role of *BA1* in AM formation during the vegetative and reproductive stages of development (Gallavotti et al., 2004). *ba1* mutants do not form tillers, ears and tassel branches. Accordingly, *BA1* transcripts are detectable at the adaxil bases of new meristems.

1.2.2 Outgrowth of axillary meristem

The outgrowth of lateral buds is well known to be inhibited by signals derived from the main shoot tip, a phenomenon named apical dominance (Chatfield et al., 2000; Horvath et al., 2003). The plant hormone auxin (IAA, Indole-3-acetic acid) is an important cause for the inhibition of axillary bud outgrowth. Studies on the *AUXIN RESISTANT1* (*AXR1*) gene of *Arabidopsis* supply in vivo significance for this fact (Leyser *et al*., 1993; Lincoln *et al*., 1990; Stirnberg *et al*., 1999). Mutations in *AXR1* result in increased shoot branching in both vegetative and floral nodes, and the lateral buds in *axr1* are resistant to inhibition by apically or locally applied IAA.

However, the endogenous level of IAA is not always correlated with the degree of shoot branching, suggesting that additional signals could be involved (Beveridge et al., 1994; Beveridge et al., 2000). Genetic analysis has provided evidence for the presence of a new messenger regulating axillary bud outgrowth. Mutations in the *MORE AXILLARY GROWTH* (*MAX*) *1*, *3*, and *4* genes of *Arabidopsis*, the *RAMOSUS* (*RMS*) *1* and *5* genes of pea, and the *DECREASED APICAL DOMINANCE1* (*DAD1*) gene of petunia result in increased bud outgrowth (Booker et al., 2005; Napoli, 1996; Snowden et al., 2005; Sorefan et al., 2003; Stirnberg et al., 2002; Turnbull et al., 2002). *RMS1, DAD1,* and *MAX4* are orthologous genes. The *max4* and *rms1* mutant buds are resistant to the inhibitory effects of apical auxin, leading to the hypothesis that the MAX/RMS/DAD pathway plays an important role in regulating bud outgrowth (Beveridge et al., 2000; Sorefan et al., 2003). Bennett *et al*.

demonstrated that the MAX pathway controls shoot branching by regulating auxin transport capacity (Bennett et al., 2006). *max* mutants have increased levels of PIN proteins, auxin efflux facilitators, and therefore have increased auxin transport capacity. Thus, the MAX/RMS/DAD pathway may act through auxin signaling in the process of lateral bud outgrowth.

Several *TCP* (*TEOSINTE BRANCHED1, CYCLOIDEA*, and *PCF*) transcription factors were also shown to regulate bud outgrowth. These are *TEOSINTE BRANCHED1* (*TB1*) from maize (Zea mays) (Doebley et al., 1997) and its homologous genes *OsTB1* from rice (Oryza sativa) (Takeda et al., 2003; Hu et al., 2003), *SbTB1* from sorghum (Sorghum bicolor) (Kebrom et al., 2006), and the two *Arabidopsis* homologs *BRANCHED1* and *2* (Aguilar-Martinez et al., 2007). Both *TB1* and *OsTB1* are expressed in AMs and lateral buds, where they function as negative regulators of lateral branch outgrowth (Hubbard et al., 2002; Takeda et al., 2003). Loss-of-function mutations in *TB1* and *OsTB1* (*FINE CULM1*) caused enhanced outgrowth of tillers. *BRANCHED1* (*BRC1*), one of the closest homologs of *TB1* in *Arabidopsis*, is a recently characterized regulator of bud outgrowth*. BRC1* is expressed in different regions of lateral buds throughout axillary bud development (Aguilar-Martinez et al., 2007). Downregulation of *BRC1* leads to branch outgrowth as a result of a relief of bud growth repression. Aguilar-Martinez *et al*. also showed that *BRC1* acts downstream of the MAX pathway and is required for auxin-induced apical dominance. Therefore, *BRC1* acts inside the buds as an integrator of branching signals and translates them into a response of cell growth arrest.

1.3   Aim of this work

The aim of this work was to identify and characterize interactors of RAX1, an early regulator of axillary meristem formation in *Arabidopsis thaliana*. A yeast two-hybrid screening was performed to identify interactors for RAX1 at a large scale. *HAT1 (HD-Zip protein1)* and *YAB1 (YABB1/AFO/FIL)* were two candidates and were focused on analysis in the first part of this study. A further aim of this study was to identify novel regulators of axillary meristem initiation. *AtLAX* (*LAX*-related gene in *Arabidopsis*) was isolated based on its high sequence similarity to *LAX* and *BA1*, two important regulators of shoot and inflorescence branching in rice and maize, respectively. The role of *AtLAX* in axillary meristem formation was characterized. In addition, the genetic interaction between *AtLAX, RAX1* and *LAS*, another axillary meristem regulator, was inspected.

2. Material and Methods

2.1 Materials

2.1.1 Chemicals

The following were main sources of supply for chemicals used in this work:

Ambion, Austin, USA

Amersham Pharmacia Biotec, Braunscheig, Germany

Biozym, Hess.Oldendorf, Germany

Carl Roth GmbH, Karlsruhe, Germany
Invitrogen GmbH, Karlsruhe, Germany

MBI Fermentas GmbH, St. Leon-Rot, Germany

Merck KgaA, Feinchemikalien und Laborbedarf Deutschland, Darmstadt

New England BioLabs GmbH, Schwalbach/Taunus, Germany

Operon, Cologne, Germany

PIERCE, Rockford, USA

QIAGEN, Hilden, Germany

Roche, Basel, Switzerland

Sigma Chemical Co., St.Lois, USA

2.1.2 Expendable materials and reagents

The following were the main suppliers of laboratory expendables used during this work:

Incubation tubes and Petri-dishes: Greiner Lobortechnik; Eppendorf-Netheler-Hiny

GmbH, Hamburg; Sarstedt AG & Co, Nümbrecht

PVDF membranes: Macherey-Nagel GmbH & Co.KG, Düren

Kits for DNA and RNA extraction and purification: Qiagen, Hildesheim

Kits for total RNA extraction from plant: Qiagen, Hildesheim

cDNA synthesis kit: MBI, GmbH, Fermentas

RNA probe transcription kit: Austin, USA

pGEM-Teasy for RNA probe transcription: Invitrogen, GmbH, Karlsruhe, Germany

Gateway cloning kit: Invitrogen, GmbH, Karlsruhe, Germany

SuperSignal West Dura Extended Duration Substrate, Pierce, Rockford, USA

SuperSignal West Pico Chemiliminescent Substrate, Pierce, Rockford, USA

2.1.3 Enzymes

Enzymes used during the course of this work were from following suppliers:

Invitrogen GmbH, Karlsruhe, Germany

New England BioLabs GmbH, Schwalbach/Taunus, Germany

MBI Fermentas GmbH, St. Leon-Rot, Germany

Roche, Basel, Switzerland

Sigma Chemical Co., St.Lois, USA

KOD hot start DNA polymerase, Novagen, Toyobo, Japan.

2.1.4 Antibodies

Anti-Digoxigenin-AP Fab-Fragments (from sheep), Roche, Basel, Switzerland

Anti·His HRP conjugates, Hildesheim, QIAGEN

2.1.5 Organisms

2.1.5.1 Bacteria

The following *Escherichia coli* strains were used during the course of this work. For cloning specific DNA fragements into vectors, DH5α (Hanahan, 1983) was transformed. For large scale fused proteins expression, BL21 (Stratagene) was used. The chemical competent cells were prepared as described by Sambrook und Russell (2001).

DH5 α	F-, end A1, hsdR17 (rk-, mk+), gyrA96, relA1, supE44, L-, recA1, 80dlacZM15, Δ(lacZYAargF) U196	Hanahan, 1983
DB3.1	B F− *ompT hsdS*(rB− mB−) *dcm*+ Tetr *gal l* (DE3) *endA* Hte *metA::Tn5*(KanSr) *[argU proL* Camr]	Stratagene
BL21- CodonPlus (DE3)-RP-X	B F− *ompT hsdS* (rB− mB−) *dcm*+ Tetr *galλ* (DE3) *endA* Hte *metA::Tn5* (KanSr) *[argU proL* Camr]	Stratagene

For plant transformation, *Agrobacterium tumefaciens* was used.

GV3101	Virulence Plasmid: pMP90RK (Koncz und Schell, 1986) Selection markers: Rifampicin, Gentamycin and Kanamycin.

PMP90RK was included as helper to integrate into plant genome when the binary vectors contain Carb selective marker. Antibiotics used for selection: Rif, Gent, Kan, Carb.

Antibiotics and plant* selection

Antibiotics	Working concentration	Solvent
Ampicillin (Amp)	100 mg/L	H_2O
Carbenicillin (Carb)	100 mg/L	H_2O
Gentamycin (Gent)	50 mg/L	H_2O
Kanamycin (Kan)	50 mg/L	H_2O
Rifampicin (Rif)	100 mg/L	DMSO
Spectinomycin (Spec)	100 mg/L	H_2O
Basta *	25 mg/L	H_2O

2.1.5.2 Plants

The phenotype investigation in this work were carried out on model plant *Arabidopsis thaliana*, belonging to the ecotypes Columbia, Landsberg and Wassilewskija. Seeds for the different ecotypes were obtained from the Nottingham Arabidopsis Stock Centre (NASC).

The following *Arabidopsis thaliana* mutants were used during this work:

Mutant	Allele	Type of mutation	Genetic background	Source
atlax	*atlax-1*	Null allele; A T-DNA insertion at the beginning of the bHLH domain (156bp after ATG)	Col	N580565
	atlax-2	Null allele; A T-DNA insertion at 396bp after ATG (118bp behind of the bHLH domain).	Col	N524760
bhlh85	*bhlh85-1*	A T-DNA insertion at 107bp upstream of ATG.	Col	N548849
bhlh86	*bhlh86-1*	A T-DNA insertion at 164bp upstream of ATG.	Col	N465407
bhlh87	*bhlh87-1*	Null allele; A T-DNA insertion at 486bp after ATG.	Col	N566339

bhlh88	*bhlh88-1*	Null allele; A T-DNA insertion at 543bp after ATG (exactly at the end of the bHLH domain).	Col	GABI297B10
hat1	*hat1-1*	T-DAN insertion in the 2nd intron	Col	N506022
lateral suppressor	*las-4*	Null allele; frameshift arising from deletion of 20bp and addition of a single nucleotide in the begining of the ORF	Col	Greb *et al.,* 2003.
rax1	*rax1-3*	T-DNA insertion in the end of ORF.	Col	Müller *et al.,* 2006
yab1	*fil-8 (afo-1)*	Ds insertion in the 4th exon.	Ler	Y. Esheld (Kumaran *et al*, 1999)
	fil-1	G to A change in splice site acceptor sequences.	Ler	(Siegfried et al., 1999).

2.1.6   Vectors

2.1.6.1   E.coli vectors

The following vectors were used to clone specific DNA fragements and express fusion proteins *in vitro* during this work:

GEM4Z	Vector for cloning and transcription of DNA fragment under the T7 promotor.	Promega
pGEM-Teasy	Vector for cloning of PCR products and their transcription under the T7 Promotor .	Promega
pDONR201	Vector for cloning of DNA-Fragmenten for use in Gateway System	Invitrogen
pDONR221	Vector for cloning of DNA-Fragmenten for use in Gateway System	Invitrogen
pET28a	Vector for protein expression with N-terminal His$_{(6)}$-Fusion	Novagen
PGEX4T1	Vector for protein expression with N-terminal GST-Fusion	Pharmacia

2.1.6.2   Yeast vectors

To investigate protein interactions in yeast, the following vectors were used during this work:

PAS-attR-new   Vector for protein expression fused with GAL4-BD

(kindly provided by J. Uhrig)

PACT-attR   Vector for protein expression fused with GAL4-BD

(kindly provided by J. Uhrig)

pGADT7   Vector for protein expression fused with GAL4-AD   Clontech

pGBKT7   Vector for protein expression fused with GAL4-BD   Clontech

pCL1   Positive control for yeast two hybrid system,   Clontech

coded for GAL4-transcription factor

pGBKT7-53   Positive control for yeast two hybrid system,   Clontech

coded for fusion protein between p53 from mouse

and the Gal4-BD

pGADT7-T   Positive control for yeast two hybrid system,   Clontech

coded for fusion protein between SV40 T-antigen

and the Gal4-AD

pGBKT7-LamC   Negative control for the yeast two-hybrid system,   Clontech

coded for fusion protein between Lamin C from

humans and the GAL4-BD

2.1.6.3   Plant vectors

For transformation of *A. thaliana*, the following binary vectors were used:

pGPTV-Bar-35S   35S promoter carrying binary vector (Cardon et al., 1999). GV3101 was transformed with constructs in this vector backbone.

pGPTV-Bar-*AscI*   GUS carrying binary vector (Überlacker *et.al,*1996). GV3101 was transformed with constructs in this vector backbone.

pXLSG-strepII   C-terminal strepII-tag fusion binary vector harboring attR1, R2

sites for Gateway cloning (Witte et al., 2004). GV3101+pMP90K was used for plant transformation.

2.1.7 Libraries for yeast two-hybrid screening

To identify the interaction partners of RAX1 protein, cDNA libraries screening is powerful and handy way using yeast two hybrid method. The following are two kinds of prey libraries used in this study:

Library	Material	Density	Sourse
Apex cDNA library	Shoot tips from both vegetative and reproductive stages	$\sim 1 \times 10^6$	Hans Sommer
Transcription factor (TF) library	Annotated transcription factors	1002	REGIA (Paz-Ares et al., 2002)

2.1.8 Oligonucleotides

The oligonucleotides used in this study were mainly synthesized in Operon and Invitrogen.

Oligonucleotides used in the part of yeast two-hybrid screening:

Name	5'-3' sequences	Locus
HAT1-rev	GAA GAT CTA TCT AGA GTG ATG	At4g17460
HAT1-841R	CCA AAG CCA GCT TCT GTT Tc	At4g17460
HD-ZIP-EcoRIfo	GAT GAA TTC ATG ATG ATG GGT AAA GAG GAT	At4g17460
HD-ZIP-NotIre	CAT GCG GCC GCT TAA GAC CTA GGA CGC ATC A	At4g17460
HD-ZIP-ORFre	CTT CTG TTT GGG ATT GAG AGT	At4g17460
M37-1036F	ATT CAC TAA CGA GAG AAA TGG GAA	At5g23000
M37-2549R	CAA GAG AGT CTA GAA GAA CTA GGA G	At5g23000
M37-1987F	CAA TCC CAT CTT CTT CTT ACA ATC C	At5g23000
M37-2489R	GCT ACC CAT GCT TTT GTT CTC	At5g23000
myb37-EcoRIF	CAT GAA TTC GGA AGA GCT CCG TGT TGC GAC	At5g23000
myb37-XhoIR	CAT CTC GAG CTA GGA GTA GAA ATA GGG CAA GC	At5g23000
myb37-XhoIre	CAT CTC GAG TCA GAG TTT CTT CCT TAG CTT TGT G	At5g23000
YAB1-EcoRI-F	GTA GAA TTC ATG TCT ATG TCG TCT ATG TCC TC	At2g45190
YAB1-XhoI-R	GAT CTC GAG TTA ATA AGG AGT CAC ACC AAC G	At2g45190
YAB1-ORF-fo	TGT GGT TGC TGT ACC AAT CT	At2g45190
YAB1-ORF-re	GGA CTC TCT GTC TTT TCT CTG	At2g45190
YAB1-1309F	GTC TCT TTC TGT CTG AGT TTT TG	At2g45190

YAB1re   AGA AAC CAC AAC TTT TGG ACA T   At2g45190

Oligonucleotides used in the part of bHLH140 functional analysis:

Name	5'-3' sequences	Locus
bHLH37-998F	GGA GGA TGG ATA ACT CCC AC	At3g50330
bHLH37-1699R	ATC ATC TAA GAA TCT GTG CAT TTC C	At3g50330
bHLH40F	CAA CCA CAG CCC CAA AAG A	At4g00120
bHLH40R	TCT TCT CGC TGA TCC TTT CC	At4g00120
bHLH43-for2	TGA ACC CAT CTC TCT TCC AAA	At5g09750
bHLH43-rev2	GGC GGT GAA ACC CAT GAC	At5g09750
bHLH52-for2	CAA GAG CAA CCG CAA CAT C	At1g30670
bHLH52-rev2	AAG ATG CAT TCT TCG GCT TT	At1g30670
bHLH53-for2	TTG CTT TAT TCC CGA GAT GG	At2g34820
bHLH53-rev2	AAA TAT TCG GGG TTC TGC AA	At2g34820
bHLH54-for2	TGG AGT CTC TCT TGG GGA TG	At1g27740
bHLH54-rev2	GTA AGC CAA TGG TGC GTA CA	At1g27740
bHLH83F	ATC CGG TGA AGA TCA TCA CAA	At1g66470
bHLH83R	AGC GGA TTT AGG CGA AAG AG	At1g66470
bHLH84F	TCT CCC CTC CAA GGA TTT GT	At2g14760
bHLH84R	AGA GAA GCA AAA GCC ACC A	At2g14760
bHLH85F	AGC AAC AAC CTC GGA GGA A	At4g33880
bHLH85-For2	TGA AGC CGG TAG CTT CTG TT	At4g33880
bHLH85-proF2	ATT ACT CGG ATG CTA ACG AAA C	At4g33880
bHLH85R	CCA TTG TCT CAT TTT GGT TCT CTT	At4g33880
bHLH85-T7R	CGA TAA TAC GAC TCA CTA TAG GGC CAT TGT CTC ATT TTG GTT CTC TT	At4g33880
bHLH085-T7R2	TAA TAC GAC TCA CTA TAG GGA TGT CCA TCC CAT TGA AGC	At4g33880
bHLH86-for2	ATT GCG GAT TAG ACG AAG GA	At5g37800
bHLH086F	TGC TTC ATC ATT CTT CAC CTT T	At5g37800
bHLH086-T7F	TAA TAC GAC TCA CTA TAG GGT GCT TCA TCA TTC TTC ACC TTT	At5g37800
bHLH86-proF	TGA TCT CAT GCC AGC TTC C	At5g37800
bHLH086R	GAA AGT TGT GTG TTC TCT CCC	At5g37800
bHLH086-T7R	TAA TAC GAC TCA CTA TAG GGT GCT TCA TCA TTC TTC ACC TTT	At5g37800
bHLH86-rev2	AAA ACT CAT CGG CTG CAA GT	At5g37800
bHLH87-348F	ATG GAA GGA TTG GAA TCT GTG T	At3g21330
bHLH87-1145R	CTC CAC AAT CTC TAA CCC GAA	At3g21330

bHLH087-1461R	TCA AAA GTT TAT AAT CTG TCA ACA CTC	At3g21330
bHLH88F	ACT AAC CCT TCT TCT ATC TCT CC	At5g67060
bHLH88-T7R	TAA TAC GAC TCA CTA TAG GGC TCT CGC TTA TTC TCT CCC TT	At5g67060
bHLH88-116F	ACC CAT TTT ATC AGC TTC TCC A	At5g67060
bHLH88-519R	CTC CTC TTC GGT GGC TTA AC	At5g67060
bHLH139F	TGC AAT GCT CCA AAT GAG AC	At5g43175
bHLH139-T7R	CGA TAA TAC GAC TCA CTA TAG GGG CTA TCC CTC TGT TGG CTT T	At5g43175
bHLH137-1040F	GGG GAC AAG TTT GTA CAA AAA AGC AGG CTC AAT GGA TGA TTT CAA TCT TCG TAG	At5g01310
bHLH137-1347F	GCT TCT CTT CAT AAA CGA CCA C	At5g01310
01310-1551R	CGA GTC ACG TTC TTG CTC A	At5g01310
bHLH140-1931R	CAA ATT TAC ATT AAA ACG CCT GTT TAT C	At5g01310
bHLH140-Acc65Ire	CTA GGT ACC GGA CGA GTC ACG TTC TTG CTC A	At5g01310
bHLH140-BamHIre	GAT GGA TCC ATG GAT GAT TTC AAT CTT CGT AGC	At5g01310
bHLH140-EcoRIfo	GAT GAA TTC ATG GAT GAT TTC AAT CTT CGT AGC	At5g01310
bHLH140-NotIre	CAT GCG GCC GCC TAG GAC GAG TCA CGT TCT TGC	At5g01310
bHLH140GW2	GGG GAC CAC TTT GTA CAA GAA AGC TGG GTT GGA CGA GTC ACG TTC TTG CT	At5g01310
Atls2427F	TCC TCT CCC TTA ACT CTT CTC C	At1g55580
Atls2717R	CCG TTA AAT GAC CGA ACC GA	At1g55580
CUC3-1610F	TGG AAA GCT ACC GGC AAA	At1g76420
CUC3-1983R	ATT GAA CAC TCT GCA AAT CA CC	At1g76420
LDs10	GGG AAT TCT TTT ACC GAC CGT TAC CGA C	Ds-element
M37-1036F	GGG GAC AAG TTT GTA CAA AAA AGC AGG CTA TTC ACT AAC GAG AGA AAT GGG AA	At5g23000
M37-1688F	AAA ATC ACG AGC TAC ATT GAT TCC	At5g23000
M37-2624R	TTC TCT CTC CTC CCA TAC CCC ATC AAA TC	At5g23000
Myb37-GW2	GGG GAC CAC TTT GTA CAA GAA AGC TGG GTA GGA GTA GAA ATA GGG CAA GCA	At5g23000
T-DNA-LB-Rev	GTT ACT AGA TCG ACC GGC A	T-DNA
T-DNA-LBfo	CCA AAC TGG AAC AAC ACT CAA	T-DNA
T-DNA-RBre	GCG GTT CTG TCA GTT CCA A	T-DNA
T-DNA-RBre2	GAA ATC ACC AGT CTC TCT CTA CA	T-DNA

Molecular markers for identification of mutant alleles:

Allele	Markers	Polymorphism
atlax-1	T-DNA-LB-Rev+bHLH140-1931R;	Produces an ~1200bp T-DAN band

	bHLH140-EcoRIfo+bHLH140-1931R	Produces an 860bp WT band
atlax-2	T-DNA-LB-Rev+bHLH140-1931R; bHLH140-EcoRIfo+bHLH140-1931R	Produces an ~970bp T-DNA band Produces an 860bp WT band
bhlh85-1	T-DNA-LB-Rev+bHLH85pro-F2 bHLH85pro-F2+bHLH85R	Produces a ~900bp T-DAN band Produces an 830bp WT band
bhlh86-1	GABI-Left+bHLH86R bHLH86-proF+bHLH86R	Produces an ~870bp T-DAN band Produces a 930bp WT band
bhlh87-1	SALK-LB1+bHLH087-1461R bHLH087-348F+bHLH087-1461R	Produces an ~800bp T-DAN band Produces a 1139bp WT band
bhlh88-1	GABI-Left+bHLH088-116F bHLH088-116F+bHLH88-rev2	Produces an ~600bp T-DAN band Produces a 640bp WT band
hat1-1	T-DNA-LB-Rev+HD-Zip-EcoRIfo HD-Zip-EcoRIfo+HAT1-841R	Produces an ~1000bp T-DAN band Produces a 670bp WT band
las-4	Atls2427F+Atls2717R	Produces a 270bp mutant band Produces a 290bp WT band
rax1-3	T-DAN-LB-Rev+M37-1688F; M37-1688F+M37-2624R	Produces an ~930bp T-DAN band Produces a 637bp WT band
fil-8	LDs10+YAB1re YAB1-1309F+YAB1re	Produces an ~970bp Ds band Produces a 1051bp WT band

2.1.9   Plasmids

Listed below are the plasmids used in this study:

Construct	Insertion	Vector	Cloning sites	Antibiotics
BD-RAX1	full length cDNA of *RAX1*	pAS-attR	gateway	Amp
AD-RAX1	full length cDNA of *RAX1*	pACT-attR	gateway	Amp
pFY10 (GST-RAX1)	full length cDNA of *RAX1*	pGEM-4T-1	BamHI/XhoI	Amp
pFY19 (His-RAX1)	full length cDNA of *RAX1*	pET28a	BamHI/XhoI	Kan
pFY30 (His-HAT1)	full length cDNA of *HAT1*	pET28a	EcoRI/NotI	Kan
pFY63 (anti-HAT1)	1-486 relative to the ATG	pGEM-Teasy	T-easy (antisense)	Amp
pFY51 (anti-YAB1)	160-433 relative to the ATG	pGEM-Teasy	T-easy (antisense)	AmP
pFY62 (AD-YAB1)	full length cDNA of *YAB1*	pGADT7	EcoRI/XhoI	Kan
pFY35	full length cDNA of	pET28a	EcoRI/XhoI	Kan

(His-YAB1)	YAB1				
anti-AtLAX	215-510 relative to the ATG	pGEM-Teasy	T-easy (antisense)	AmP	
anti-bHLH86	216-516 relative to the ATG	pGEM-Teasy	T-easy (antisense)	AmP	
anti-bHLH87	1-1145 relative to the ATG	pGEM-Teasy	T-easy (antisense)	AmP	
sense-bHLH87	1-1145 relative to the ATG	pGEM-Teasy	T-easy (sense)	AmP	
anti-bHLH88	116-519 relative to the ATG	pGEM-Teasy	T-easy (antisense)	AmP	
pFY98b *(35S:AtLAXSRDX)*	*AtLAX* with 60bp 5'UTR fused with SRDX	pBar-35S	SmaI/SbfI	Kan	
pFY92 *(35S:AtLAX)*	full length cDNA of *AtLAX*	pXLSG-StrepII	gateway	Amp	
pFY48 (His-AtLAX)	full length cDNA of *AtLAX*	pEF28a	EcoRI/NotI	Kan	
pFY49 (GST-AtLAX)	full length cDNA of *AtLAX*	pGEX-4T-1	EcoRI/NotI	Amp	

2.1.10   Computer programmes and Databases

DNA sequence analyses.and restriction enzyme site searching were done by using Wisconsin GCG software (Genetics Computer Group, 1997), Clone Manager6.0 software package. The databases of National Center for Biotechnology Information (NCBI), Bethesda, USA and the Arabidopsis Information Resource (TAIR) (Huala *et al.,* 2001) were used for DNA sequence searches and comparisons. The SIGnAL "T-DNA Express" Arabidopsis Gene Mapping Tool (http://signal.salk.edu/cgi-bin/tdnaexpress) was used to search for T-DNA knockout mutant lines.

2.2   Methods

All general molecular biology laboratory methods not mentioned here are as described by Sambrook and Russell (2001).

2.2.1   Isolation of Genomic DNA

Isolation of genomic DNA from plants for genotyping and segregation analyses was done using the quick-prep protocol (Edwards *et al.,* 1991). High quality genomic DNA for mapping, cloning and genotyping was extracted using the *DNeasy® 96 Plant Kit* (Qiagen, Hilden,) and *BioSprint® 96* automated DNA extraction apparatus (Qiagen, Hilden).

2.2.2   Isolation and Purification of Plasmid DNA

Plasmid DNA from bacteria was isolated using either the *Plasmid Mini kit* or *Plasmid Midi kit* (Qiagen, Hilden).

Purification of PCR products and vectors were done using *Qiaquick PCR Purification* kit (Qiagen, Hilden).

2.2.3   Isolation of RNA from plants

RNeasy Plant Mini Kit (Qiagen, Hilden) was used for isolation of total RNA from plants. Subsequently, 5ug RNA was submitted to DNase digestion using DnaseI (Ambion, Cat# 1906) in 50µl reaction to get a concentration of 100ng/µl.

2.2.4   cDNA synthesis / RT-PCR

For first strand cDNA synthesis, *RevertAid^{TM} H Minus First Strand cDNA Synthesis Kit* (GmbH, Fermentas) was used to transcribe the isolated total RNA according to manufacturer's protocol. Approximately 500ng of total RNA was used for this reaction. 0.5 to 1µl of the synthesized cDNA was used subsequently for a 50µl PCR.

2.2.5   Polymerase Chain Reaction

Unless otherwise specified, PCR reactions were set as following: 5 µl 10xPCR Buffer, 2.0 µl of 50 mM MgCl, 0.5 µl dNTP (25 mM of each nucleotide), 0.2 µl *Taq*-Polymerase and 1 µl of each Primer (10 pmol/µl) in a 50 µl reaction made up with ddH$_2$O. 10-100 ng of DNA was used as starting DNA template. The *Taq* polymerase was synthesized according to the protocol standardized by Pluthero (1993). Unless specified otherwise, reactions were accomplished using the PCR programme in a T3 Thermocycler by Biometra or the Biozym Multicycler PTC 225: 94°C for 2 min -> 28 to 38 cycles of 94°C for 15 sec, 56-60°C for 30 sec, 72°C for 1 min/kb -> 72°C for 6 min. For cloning work, the amplification of DNA fragments was done using KOD hot start DNA polymerase (Navogen, Japan). KOD hot start DNA polymerase possesses a 5' to 3'-exonuclease activity. Thus, the PCR products do not have 3'-dA-nucleotid overhang.

2.2.6   RNA in situ hybridyzation

2.2.6.1   Description of probes

The *LAS* probe contained the nucleotides 2 to 1348 relative to the ATG (Greb *et al.,* 2003) and the *RAX1* probe was specific for the third exon and contained the nucleotides 934 to 1436 relative to the ATG (Muller et al., 2006). The *HAT1* and *YAB1* antisense probes contained the very specific regions, the nucleotides 1-486 and 160-433, respectively, relative to the ATG. The *AtLAX*-specific probe was transcribed from the coding region 215-510 relative to the ATG. Similarly, probes for *bHLH86, bHLH87,* and *bHLH88* were also transcribed outside of the conserved region and contained the nucleotides 216-516, 1-1145 and 116-519, respectively, related to the ATG. All these probes were cloned into pGEM-Teasy vector in antisense orientation relative to the T7 promoter. Linearised plasmids were used as templates for probe synthesis with T7 RNA polymerase (Ambion). The nucleotides of sense probes were identical to that used for anti-sense probes.

2.2.6.2   Preparation of tissue sections and hybridization

Sample preparations and in situ hybridizations of 8-mm sections were done as described by (Coen et al., 1990) with slight modifications. 0.03% Tween-20 was added to the fixative, and dewatering of the fixed material was done without NaCl. Plant material was

embedded in Paraplast+ (Kendall) in the ASP300 tissue processor (Leica). Probes were not hydrolyzed. After the color reaction, slides were mounted in 30% glycerol and photographed using differential interference contrast microscopy.

2.2.7 DNA sequencing

DNA sequencings were accomplished by the MPIZ service unit Automatic DNA Isolation and Sequencing (ADIS) using Applied Biosystem (Weierstadt) *Abi Prism 377 and 3700 Sequenzer* by means of *BigDye-terminator chemistry*.

2.2.8 Incubation conditions for bacteria

E. coli were incubated in LB medium at 37°C over night (Sambrook and Russell, 2001) and Agro bacteria in YEP medium at 28°C for 2-3 days with proper antibiotics.

2.2.9 Incubation conditions for yeasts

Yeasts were incubated on full medium (YPAD) or selective medium (SD/-dropout) at 30°C for 3-5 days. The yeasts on solid medium can be store at 4°C up to 3 months. Liquid cultures were generally incubated overnight on the shaker with 200rpm.

2.2.10 Bacteria transformation and selection

Transformations of vectors in *E.coli* were carried out by heat-shock treatment of chemical competent cells as described by Hanahan (1983). In cases where heat-shock transformations were inefficient, electro-transformations were performed using electro-competent cells (ElectroMAX DH5alpha-E Cells, Invitrogen) as described by Dower *et al.* (1988). Agro bacterial competent cells were transformed using approximately 1µg of plasmids. Subsequently, the cells were incubated for 5 minutes each on ice, in liquid nitrogen and at 37°C for heat shock. After the addition of 800µl YEP, the cells were incubated on a shaker at 28°C for 3 hours, and then plated out on solid YEP medium with proper antibiotics. The concentration of antibiotics used in this study refers to Table in *Metrials.*

2.2.11   Plant transformation and selection

The agrobacteria-mediated transformation of *A. thaliana* was performed according to the Floral Dip method by Clough and Bent (1998). For the selection of transgenic plants in the T1, 250 mg/l Glufosinat (BASTA®, Hoechst) was sprayed on the plants.

2.2.12   Growth conditions for plants

Arabidopsis thaliana seeds were stratified at 4°C for 2-3 days before sowing, so as to obtain uniform germination rate. Plants were grown at a daytime temperature of 20 - 25°C and a night temperature of 10 - 15°C in the greenhouse, or in a growth chamber (Mobylux GroBanks, CLF Plant Climatics, Germany) at a daytime temperature of 23°C and a night temperature of 18°C. Plants were either grown to maturity in short days (8 h light, 16 h darkness) or long days (16 h light, 8 h darkness), or were grown for the first 28 days in short day conditions, and then shifted to long day conditions to facilitate bolting and flowering. In case of T1 and T2 transgenic plants subjected to BASTA selection, the trays sown with seeds were first placed in a cold chamber at 4°C for a few days and then directly shifted to long day conditions (16 h light, 8 h darkness).

2.2.13   Scanning Electron Microscopy

Scanning Electron Microscopy (SEM) was performed with assistance from Rolf-Dieter Hirtz on a DSM 940 (Zeiss). Tissue were first frozen in liquid nitrogen and subsequently coated with a gold layer under vacuum.

2.2.14   Methods for yeast-two-hybrid system

2.2.14.1 *Transformation of yeast (LiOAc method)*

Inoculate one colony in 10 ml medium (YPAD or SD/-dropout with 2% glucose), 30°C overnight with 220rpm. Next day, dilute dense o/v culture with 50 ml fresh medium till OD_{600}= 0.2-0.3, let them grow for another 4-5 h till OD_{600} reaches 0.4 but less than 0.6 with vigorous shaking. Collect the cells by spinning down 5 min with 4000rpm at room

temperature, decant supernatant and resuspend pellet in ~25ml sterile water by shaking softly. Spin down again for 5 min and resuspend in 10ml of 0.1mM LiOAc (pH7.5 with diluted acetic acid). Decant supernatant and resuspend the cells in the remaining liquid by vortexing. Thus, these cells were used for 5-10 transformations by adding 300µl premixture (240µl of 50% PEG3350 or PEG400, 36µl of 1M LiOAc pH7.5, and 25µl of 2mg/ml ssDNA in TE) per reaction. Denature the ssDNA at 95°C for 5 min prior to use, and then put it on ice. Then 0,5µg~1µg DNA was added into ~300µl transformation mixture and cells. The reaction was incubated at 30°C for 30min followed by heat shock at 42°C for 2min or up to 25min, without shaking during all the incubations. Then collect cells by spinning down for 10 seconds with 6000rpm, and resuspend cells in 150µl sterile water and select transformed cells on selective SD/ plates by incubation at 30°C for 3-5d.

2.2.14.2 cDNA library screening

The *Arabidopsis* apex cDNA library was kindly provided by Simona Masiero and Hans Sommer (Max Planck Institute, Köln, Germany). Yeast strain Y187 containing the bait vector pAS-RAX1 was incubated for overnight at 28˚C. AH109 transformed with empty pGADT7 (AD w/o) was incubated as a negative control. Check the OD_{600} ($0.8< OD_{600}<1.2$) on the next day, and then collect the cells by centrifuging at 1500-2000 rpm for 10 min at 25˚C. Resuspend cell pellets into 25 ml 2 x YPAD medium and mix with 300 ul of cDNA library aliquot for mating. The mating was done in 2-L flask containing 50 ml 2 x YPAD culture for overnight (20-24h) at 28˚C with 40 rpm. In parellel, 12.5 ml of overnight AD (w/o) culture was mated with 12.5 ml bait overnight culture as a negative control. On the third day, spin down overnight mating culture by centrifuging at 1500-2000 rpm for 10 min after determinating the mating efficiency by plating 10µl, 1µl and 0.1µl of mating culture onto SD/-LW unselective plates. Resuspend pellets in 25 ml of 0.5 x YPAD (1 x YPAD: 0.9% NaCl = 1 : 1), and plate onto the selective plates SD/-Ade/-His/-Leu/-Trp + 5mM 3-AT (SD/-AHLW+3-AT). Resuspend 1 ml of negative mating culture in 1 ml of 0.5 x YPAD, and plate onto a selective plate SD/-AHLW+3-AT. The plates were incubated at 28˚C for 5-7 days.

2.2.14.3 REGIA transcription factor (TF) library screening

Prepare 10ml of overnight bait culture by inoculating single colony in SD/-dropout medium with 4% Glucose. Thaw the TF library in water bath at 42°C, followed by an incubation of library in 19ml of YPAD with 4% Glucose for 1h at 30°C. When the OD_{600} of bait and library reach 0.5-0.8, mix 2OD bait and 2OD library and spin down for 5min with 4000rpm at RT. Resuspend the pellet in 2ml of YPAD with 10% PEG6000 and incubate overnight at 30°C with 80rpm. Next day, collect the overnight mating culture (max 4000rpm, max 5min) and resuspend in 100ml of SD/-LWH+5mM 3-AT+0.05% Gelrite. To test the mating efficiency, distribute 10ml resuspension into SD/-LW+0.05% Gelrite medium and count the colonies after 3 days. Pour the rest in 3 petridishes and incubate at 30°C for up to one week. Pick up single colony into water and stamp it onto a SD/-LWH+5mM 3-AT agar plate.

2.2.14.4 Plasmid rescue from yeast cells

One big colony was resuspended in 100µl H_2O, spin down (13,000rpm for 10min) and resuspendeded in 200µl of lysis buffer (100mM NaCl, 10mM Tris.Cl pH8.0, 1mM EDTA, and 0.1% SDS), followed by addition of mixture of Phenol : Chloroform : Isoamyl Alcohol (25:24:1). Vortex the cell mixture with 200 µl of glass beads (Sigma), and then spin down to get rid of the cell debris (13,000rpm, 10min, RT or 4°C). For 150µl supernatant, 15µl of 3M NaAc and 450µl of 100% ethanol were added to precipitate plasmids. Wash the pellet with 70% ethanol, dry the pellet for 5 min at 37°C and dissolve it in 30µl H_2O.

2.2.15 Recombinant protein expression and purification

All proteins used in this study were induced with an IPTG concentration of 0.1mM and expressed at a temperature of 28°C for 4h. Prepare 15ml overnight culture and dilute into 300ml fresh LB medium with antibiotics till the OD_{600} reaches 0.2-0.3. Incubate additional 30-45min with vigorous shaking at 37°C to increase the OD_{600} to 0.4-0.6. Before the induction, 1ml culture was taken out to control the induced cell lysate later on. Induced a fusion protein expression by adding IPTG to a final concentration of 0.1mM and incubating for another 4h at 28°C. Pellet the culture at 4000 x g for 20 min at 4°C, and store the

pellet at -70˚C or continue with purification.

2.2.15.1 Purification of His-fusion protein

Resuspend the cells in 5ml lysis buffer/gram weight (50mM NaH$_2$PO4, 300mM NaCl, 10mM imidazole, 0.1% Triton X-100, pH8.0), and incubate the mixture on ice for 30 min after adding PMSF and DTT to 1mM each, and lysozyme to 1 mg/ml. Sonication was done on ice for 3x1min till the lysate becomes clear with presence of 10 mM EDTA. After centrifuging cell lysate at 15,000 x g for 30 min at 4 °C to pellet the cellular debris, the supernatant containing His-tagged protein and other unspecific proteins from bacteria was co-incubated with 50% Ni-NTA Agarose (QIAGEN) for 1h or O/V at 4°C by gently shaking (1ml slurry for 4ml supernatant). The lysate-Ni-NTA mixture was then loaded onto column with bottom cap removed. His-tagged protein can be extracted from unspecific protein mixture by washing 3 times with wash buffer (50mM NaH$_2$PO4, 300mM NaCl, 20mM imidazole, pH8.0), and then can be eluted in 4x500µl elution buffer (50 mM NaH$_2$PO4, 300 mM NaCl, 20 mM imidazole, pH to 8.0). Thus, the His fusion protein is purified and ready to be used for pull down binding assay.

2.2.15.2 Purification of GST-fusion proteins

Resuspend cell pellet (from 100-150ml culture) in 5ml ice-cold STE buffer (10mm Tris-Hcl, PH 8.0, 1MM EDTA, 150MM NaCl). Incubate mixture on ice for 15min after adding 50 µl of 100mM PMSF (just before adding lysozyme cause PMSF is not stable in water) and 50µl of 10mg/ml lysozyme solution. Sonication was done on ice for 3x1min (or more till solution becomes clearer) immediately after adding 50 µl of 1M DTT and 700µl of 10% Sarkosyl. After centrifuging for 30min at 1300rpm (4^{0}C), Triton X-100 was added to the supernatant in a new 10ml conical tube to reach 2% of final concentration by topping up with STE buffer to 10ml. Thus, the bacterial lysate can be aliquoted (1ml) and stored at -80^{0}C. To purify GST-tagged proteins, resuspend one aliquot cell lysate in 30µl GST^{TM}·bind resin (Novagen) pre-washed with 1ml PBS buffer, followed by incubation with agitation at RT for 1h or O/V at 4^{0}C. Wash beads with 1% Triton in PBS for 3-5x1ml to get rid of unspecific proteins, then the bound GST fusion proteins can be eluted from beads by incubating with

30μl elution buffer (0.2 M Tris-HCl, pH 6.8, 8% SDS, 40% glycerol, 100mm DTT, 0.004% bromphenol blue) at 37^{0}C for 30min, then subjected onto SDS-PAGE gel to check the quality and quantity. For a pull down assay, subject the washed beads to the purified His-tagged proteins.

2.2.16   GST pull down assay

Mix some purified His-prey fusion protein (~20μl) or certain amount of supernatant after sonication with glutathione-beads to which a GST-tagged fusion parotein bind in 500 ul binding buffer (50 mM Tris–HCl, pH 7.5, 150 mM NaCl, 1 mM EDTA, and 0.5% Triton X-100) and co-incubate at 4^{0}C for 2 h with gentle shaking. Wash beads three times with wash buffer (the same as binding buffer), then resuspend in 20ul of 2xSDS loading buffer, and subjecte to SDS–PAGE gel for western blot detection after cooking at 70^{0}C for 15min.

2.2.17   Western blot analysis

Western blotting, sometimes called immunoblotting, is a reliable method to check the presence of a specific protein. The detection is based on the molecular weight of a protein and the interaction of the protein with its specific primary antibody or tag-specific antibody for tagged protein. In this study, western blot was performed to test expression of GAL4-fusions protein in yeast cells and to detect the presence of pulled-down protein by GST-fused protein.

After electrophoresis, equilibrate gel in transfer buffer (190mM glycin, 25mM Tris, 20% methanol, 0.05% SDS) for 20min with softly shaking. Equilibrate PVDF membrane (0.45 µm, Millipore) in transfer buffer for 20min after incubation of membrane in 100% methanol for 15sec and in water for 2min. Just before blotting, saturate the filter paper (two pieces of thick filter paper or four pieces of thin filter paper for one side) by soaking in transfer buffer for 2min. Assemble semi-dry electrophoretic transfer (Biorad) as following order: pre-soaked filter paper -> PVDF membrane -> equilibrated gel -> pre-soaked filter paper. Transfer mini gels for 50-60 min at 20V.

To detect GAL4 protein expression in yeast cells, incubate the membrane in 1xANT buffer (150mM NaCl, 50mM Tris-Cl, pH 8.0, 0.002% NaN_3) for 2x10min, then block in 1xANT/20% NCS for 1.5h at RT before adding 1st antibody (1:1000, anti-GAL4-BD or anti-GAL4-AD from mouse, Biotechnology) in the blocking buffer for o/v at 4^0C. Wash the membrane 4x15min in 1 x ANT/0.05% Tween-20. The 2nd antibody (1:3000, anti-mouse, Bio-Rad) was co-incubated with the membrane in the 1 x ANT/20% NCS buffer for 2h, followed by another 3x15min washing in 1 x ANT/0.05% Tween-20. The antigen (expressed GAL4 fusion protein) recognized by specific antibody was then detected by staining the blot in darkness in 10ml TE with 45µl NBT (110mM in 70% DMF) and 35µl BCIP (90mM in DMF) for 10min up to 30min.

To detect pulled-down protein (His-tagged protein) after pull down binding assay, chromogenic method using Penta·His HRP conjugates (QIAGEN, Cat no. 34460) was applied. Block the blot for 1h in blocking buffer (10mM Tris-Cl, pH 7.5, 150mM NaCl, 3% BSA) after washing 2x10min in TBS buffer (10mM Tris-Cl, pH 7.5, 150mM NaCl). Before antibody incubation, wash the membrane first 2x10min in TBS-Tween/Triton buffer (20mM Tris-Cl, pH 7.5, 500mM NaCl, 0.05% Tween 20, 0.2% Triton X-100) and then 1x10min in TBS buffer at RT. Incubate the membrane with the presence of antibody Penta·His HRP conjugate (1:1000-1:2000) in blocking buffer for 2h at RT to recognize the His-fusion protein, followed by washing membrane for 5x10min in TBS-Tween/Triton buffer first and then in TBS buffer for 10min at RT. His-tagged protein can now be detected specifically using HRP staining buffer (1:1 volume of SuperSignal West Dura Extended Duration Substrate and SuperSignal West Pico Chemiliminescent Substrate, Pierce).

3.   Results

3.1   Yeast two-hybrid screening for RAX1 interacting proteins

RAX1 (*REGULATOR OF AXILLARY MERISTEMS1*), a R2R3-type MYB transcription factor, is recently identified as an important regulator during the early steps of axillary meristem (AM) initiation in *Arabidopsis thaliana* (Keller et al., 2006; Müller et al., 2006). *RAX1* (*MYB37*) is a homologue of the *Blind* (*Bl*) gene regulating the formation of all lateral shoot and inflorescence meristems in tomato (Schmitz et al., 2002). This gene belongs to a family harbouring another five members also showing high sequence similarity to the *Bl* gene, namely *MYB36, MYB38 (RAX2), MYB68, MYB84 (RAX3),* and *MYB87.* Genetic analysis has demonstrated that *RAX1, RAX2,* and *RAX3* are partially redundant in function and control the formation of axillary meristems in overlapping zones along the shoot axis (Keller et al., 2006; Müller et al., 2006). *RAX1* promotes early stages of axillary meristem (AM) formation and functions to establish or maintain an environment conductive for stem cell organization in the course of AM formation (Keller et al., 2006). The transcript of *RAX1* is detectable in a circular domain at the adaxial center of the boundary region between the SAM and the leaf primordia. As this is the position of the newly forming AM, the specific adaxial expression pattern of *RAX1* correlates tightly with its function in the process of axillary meristem initiation.

However, the molecular mechanism of how *RAX1* regulates meristem initiation remains elusive. A large body of evidence shows that protein(s) often interact with other proteins (termed interactors), to exert their biological functions. So, the study of RAX1 interactors may shed light on understanding how *RAX1* regulates axillary meristem formation.

The yeast two-hybrid (Y2H) system is a convenient method to detect protein-protein interactions and is especially useful for large scale screens for potential interactors (Fields and Song, 1989). The principle of this method is shown in Fig 3.1-1. The bait gene is expressed as a GAL4 DNA binding domain fusion protein (GAL4-BD), and a prey gene (cDNA of candidate gene or cDNAs from a library) is fused to a GAL4 activation domain

(GAL4-AD). If the bait and the prey interact with each other, the GAL4-BD and GAL4-AD are brought into proximity. This event will subsequently activate reporter genes driven by a promoter containing GAL4 binding sequences, which results in the growth of cells on media lacking essential amino acids. The cDNA clone(s) encoding the interacting fusion protein(s) can then be isolated from yeast and sequenced.
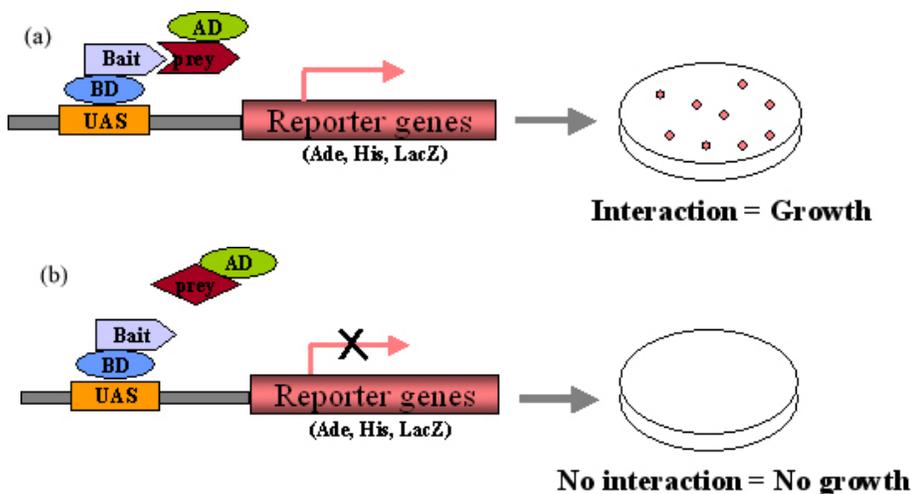
Fig. 3.1-1. Principle of the yeast two-hybrid system. The BD-bait fusion and AD-prey fusion are co-expressed in yeast cells. The interaction between the bait and a prey brings the GAL4-BD and GAL4-AD close together resulting in the activation of reporter genes. The expression of reporter genes allows growth of cells on selective plates (a). Without an interaction reporter genes are not activated, leading to a failure of cells to grow on selective plates (b).

However, the yeast-two-hybrid system has several drawbacks. Firstly, the fusion proteins need to be translocated to the nucleus where the interaction facilitates the activation of reporter genes. Therefore, it may not represent the *in vivo* environment. Secondly, interactions that are dependent upon post-translational modifications, such as protein phosphorylation, may not be easily detected. Moreover, proteins with intrinsic activation properties may create false positives. Therefore, it is always necessary to confirm an interaction detected in an Y2H system using other *in vivo* or *in vitro* methods. Among the methods to confirm protein-protein interactions *in vivo*, bimolecular fluorescence complementation (BiFC, e.g. split-YFP) (Walter et al., 2004), co-immunoprecipitation (Co-IP), and fluorescence resonance energy transfer (FRET) are most common. Meanwhile, GST-pull down assay (Glutathione S Transferase), far-western analysis, and tandem affinity purification coupled to MS (TAP-MS) are effective methods to detect and

confirm the direct interactions *in vitro* (Piehler et al., 2005). In this study, a GST-pull down assay was employed to confirm the interactions identified in the yeast two-hybrid screening.

GST

bait

pGEX

prey

His

pET

Expression and purification

Unspecific proteins + GST-bait

His-prey + Unspecific proteins

Pull down

GST-binding beads

Unspecific proteins

Wash and elute

Input   GST   GST-bait

← Detected by anti-His
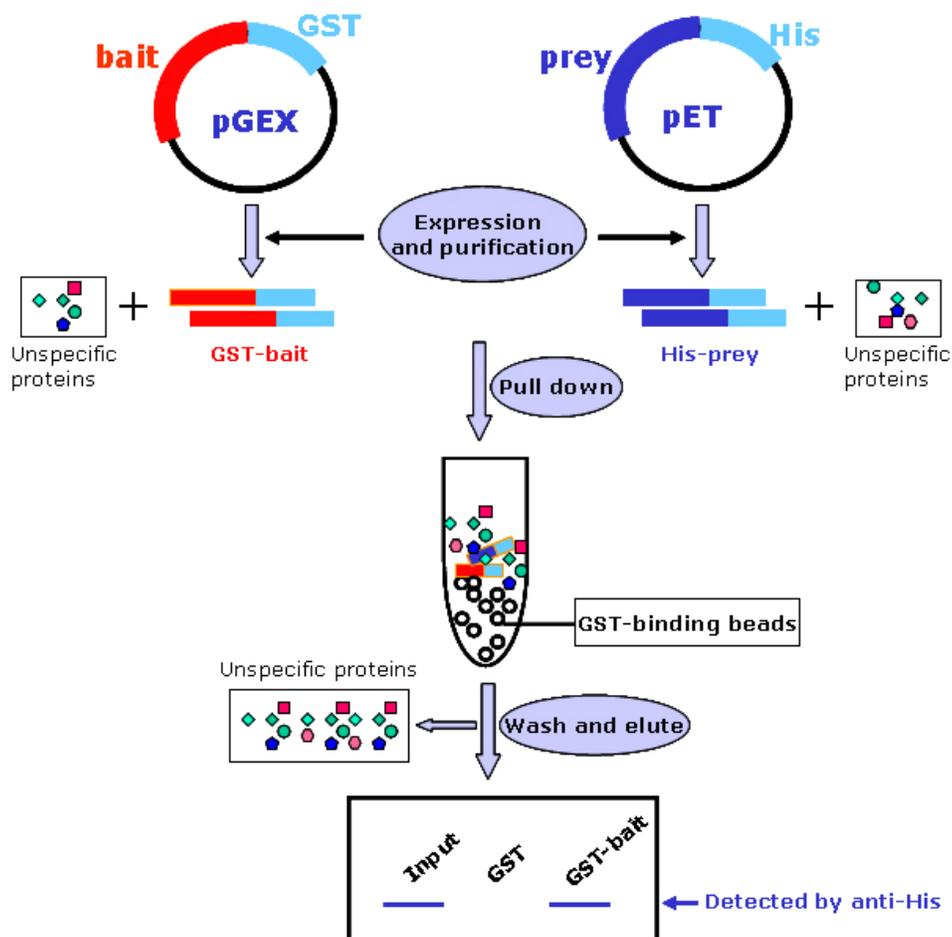
Fig. 3.1-2: The principle of GST-pull down assay. GST-bait fusion and His-prey fusion proteins are expressed in *E.coli* and purified using supports, which have the ability to capture GST- and His-tagged proteins, respectively. Two purified tagged proteins are co-incubated in the presence of glutathione beads to which the GST-bait protein has affinity, followed by washing to remove unbound proteins and elution of the putative interactor (His-prey protein) of GST-bait. Finally, the western blot is employed to detect the His-tagged prey protein using anti-His antibody. Input: 10% of purified His-prey protein as a control for the size of detected band; GST: negative control by co-incubating GST alone with His-prey fusion; GST-bait: pull down reaction by co-incubating GST-bait with His-prey fusion.

The principle of the GST-pull down assay used in this study is shown in Fig 3.1-2. The bait protein is tagged with GST to form a recombinant GST-bait fusion protein which has a high affinity for glutathione. The prey protein is fused to a His tag so that the His-prey fusion protein can bind to nickel beads (Ni^{2+}-NTA). Both GST-bait and His-prey

recombinant proteins are over-expressed in *E.coli* (BL21) or in living plant cells (Arabidopsis or Tobacco), and are subsequently purified using glutathione beads and Ni^{2+}-NTA beads, respectively. Those two purified proteins are then co-incubated in the presence of glutathione beads and followed by a series of washing steps to remove the non-bound unspecific proteins produced by *E.coli* cells. Finally, the bound GST-bait protein and interacting the His-prey protein are eluted from GST beads and subjected to SDS-PAGE gel, followed by western blot analysis to detect the interacting prey protein by anti-His antibodies (Kaelin et al., 1991).

3.1.1 Y2H screen using full-length RAX1 protein as a bait

To identify protein(s) that may interact with RAX1 by yeast two-hybrid screen, the *RAX1* ORF was sub-cloned into the pAS-attR gateway destination vector and then transformed into the *Saccharomyces cerevisiae* strain AH109 or Y187 to generate a bait strain. Prior to the yeast two-hybrid screening experiment, the auto-activation activity of the bait was tested. For this BD-RAX1 in the yeast strain AH109 was co-transformed with the empty GAL4-AD vector pACT-attR. The transformed cells were at first grown on minimal selective medium SD/-Leu-Trp (SD/-LW) to select against only the bait and prey plasmids for 3 days, and then restreaked onto a selective medium of SD/-Ade-His-Leu-Trp+5mM 3-AT (SD/-AHLW+5mM 3-AT) for another 3-5 days to select for protein interaction or auto-activation of a bait protein. As shown in Fig 3.1-1, the cells co-transformed with BD-RAX1 and empty GAL4-AD can grow on the non-selective plates (SD/-LW), but not on the selective plates (SD/-AHLW+5mM 3AT). This indicates that the full length RAX1 protein does not have an auto-activation activity. Moreover, the positive control cells harbouring BD-p53 (p53 from mouse) and AD-T antigen (SV40 T-antigen) showed healthy growth in contrast to the absence of growth of negative control cells co-transformed with BD-LamC and AD-RAX1. Thus, the full-length RAX1 protein was used as a bait to screen for putative interactors in a transcription factor (TF) library.
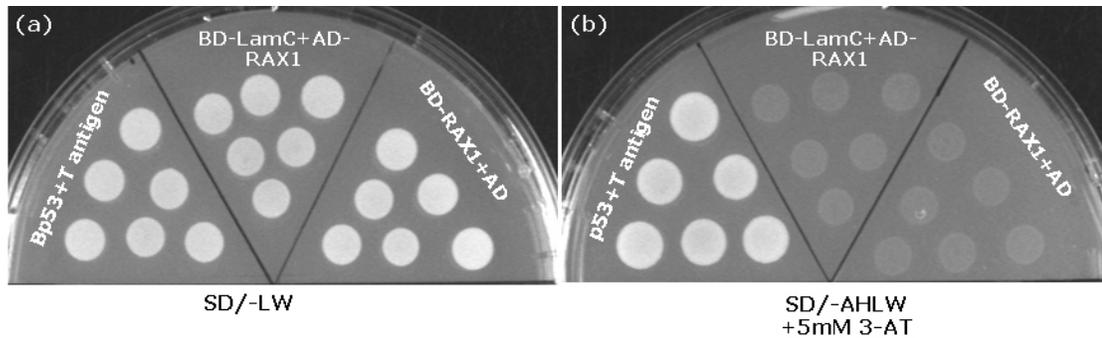
Fig. 3.1-1: Autoactivation test of RAX1. Yeast strain AH109 was transformed with the indicated plasmids. (a) Growth of transformed yeast cells on a non-selective medium after 3 days incubation. (b) Yeast from (a) were restreaked onto a selective medium. The absence of growth of cells bearing BD-RAX1 GAL4-AD indicated absence of autoactivation activity of RAX1 after 5 days incubation on the selective medium.

3.1.1.1 A transcription factor library screening

RAX1 is a transcription factor regulating axillary meristem formation in *Arabidopsis* (Keller et al., 2006; Müller et al., 2006). Many of examples show that transcription factors can form multimers, e.g. heterodimers or homodimers to modulate gene expression. To identify transcription factor(s) which potentially interact with RAX1, a yeast two-hybrid screening against a transcription factor (TF) library (REGIA, REgulatory Gene Initiative in Arabidopsis, Paz-Ares et al., 2002) was performed using full length RAX1 protein as a bait.

The REGIA TF library contains the open reading frames (ORF) of 1002 different transcription factors of *Arabidopsis thaliana* in the gateway donor vector pDONR201. Before the library screening, an LR reaction was performed to clone all the insertions from the entry clones into the expression vector pACT-attR, leading to the generation of destination clones. These clones were subsequently transformed into the yeast strain Y187 to obtain the prey strain (kindly supplied by Klaus Richter), which was then mated with the bait strain AH109 harbouring BD-RAX1. After one-week incubation on SD/-LWH+5mM 3-AT+0.05% Gelrite selective medium, more than 150 colonies from about 1×10^5 diploid yeast cells were found to be growing.

PCR amplification from ninety-six plasmids rescued from yeast clones showed thirty-six insertions with different sizes and these amplifications were subsequently subjected to sequencing. As shown in Table 3.1.1, five different TFs were present in the 36 selected clones: *HD-ZIP protein 1* (*HAT1*), *WUSCHEL* (*WUS*), WOX2, TCP3 and a CCAAT-binding factor. *WUS* is expressed specifically in the organizing center (OC) underneath the stem cells (Mayer et al., 1998), whereas the *RAX1* transcripts accumulate at the adaxial bases of leaf primordia in the apex (Keller et al., 2006; Müller et al., 2006). These distinct expression patterns of *WUS* and *RAX1* suggest that these two proteins do not interact in planta. Among the other TFs identified in this screen, the CCAAT-binding factor and WOX2 are not expressed or expressed at a very low level, respectively, in the shoot apex (Genevestigator data). *TCP3*, which was recently shown to control the morphology of shoot lateral organs via negative regulation of the boundary-specific genes, has very low expression in the shoot apex, at least before the bending cotyledon embryo stage (Koyama et al., 2007). Consequently, these four TFs were not included in further analysis. The main focus was directed towards the *HD-ZIP protein 1* (*HAT1*), given its moderate expression level at the shoot apex (Genevestigator data) as well as the important functions of members from another HD-ZIP subgroup (*REV, PHB, PHV* from HD-ZIP class III) in shoot meristem formation and lateral organ initiation (Prigge et al., 2005).

Gene	Description	Expression*
At4g17460	homeobox-leucine zipper protein 1 (HAT1) / HD-ZIP protein 1	moderately expressed in the shoot apex
At2g17950	WUSCHEL protein	specifically expressed in the organizing center of shoot apex (Mayer et al., 1998)
At5g59340	homeobox-leucine zipper transcription factor family protein, WOX2	lowly expressed in the shoot apex, high expressed in seed
At1g53230	TCP family transcription factor 3 (TCP3)	expressed at a low level in the shoot apex, highly expressed in leaf (Koyama et al., 2007)
At1g72830	CCAAT-binding factor	not expressed in the shoot apex

* according to Genevestigator data

Table 3.1.1. **Results of TF library screening for interactors of RAX1**. Sequencing revealed five different genes were present in 36 selected clones.

3.1.1.2 Analysis of interaction between HAT1 and RAX1 proteins

To confirm the interaction between HAT1 and RAX1, HAT1-harbouring plasmid was isolated from yeast and co-transformed with BD-RAX1 or empty GAL4-BD vector as a negative control. Yeast cells harbouring BD-RAX1 and AD-HAT1 but not the cells harbouring AD-HAT1 and GAL4-BD empty vector were growing on selective medium SD/-AHLH+5mM 3AT (Fig 3.1.1-1a), which corroborated the interaction between RAX1 and HAT1 observed during library screening.

Next, a pull down assay was performed to further confirm the interaction of these two proteins detected in yeast. The full-length protein sequences of both HAT1 and RAX1 were N-terminally fused to a His tag and to a GST tag, respectively. Subsequently, the GST-RAX1 and the His-HAT1 fusion proteins were expressed in *E.coli* BL21 and purified using GST beads and Ni-NTA slurry, respectively (see Material and Methods). The two purified proteins were then co-incubated with glutathione beads and stringently washed. After SDS-PAGE, the western blot analysis showed that the His-HAT1 fusion protein was pulled down by the GST-RAX1 (Fig 3.1.1-1b, lane 3), but not by GST protein alone (Fig 3.1.1-1b, lane 2). This provides further evidence for the interaction between RAX1 and HAT1.
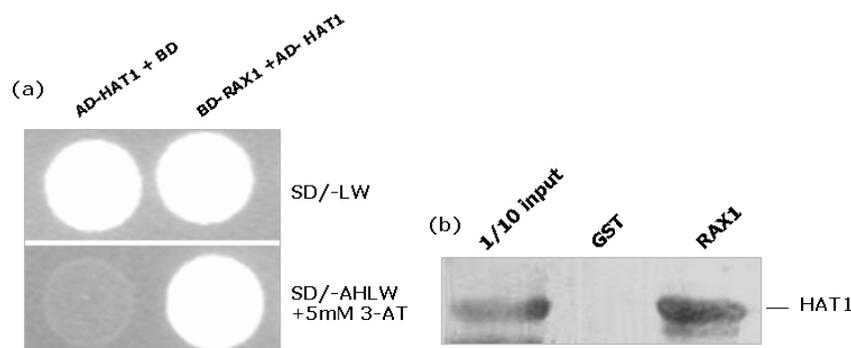
Fig. 3.1.1-1 Interaction between HAT1 and RAX1. (a) HAT1 interacted with RAX1 in yeast. Transformed yeast cells with the indicated plasmids grew on non-selective medium for 3 days (upper panel) and were transferred onto selective medium (lower panel). The growth of the cells harbouring BD-RAX1 and AD-HAT1 in contrast to absence of growth of the cells harbouring AD-HAT1 and empty GAL4-BD indicated the interaction of the two proteins. (b) *In vitro* pull-down assay of His-HAT1 (lane 1, 10% input), incubated with GST alone (lane 2) or GST-RAX1 (lane 3) proteins coupled with glutathione–sepharose. Western blots probed with anti-His antibody showed that His-HAT1 was present in the elution of GST-RAX1 pull-down and absent when using only GST.

3.1.1.3 Comparison of transcript accumulation of *HAT1* and *RAX1* in the vegetative apices

To explore the physiological relevance of the interaction between HAT1 and RAX1, co-localization of the two transcripts was investigated by *in situ* hybridization experiments. Plants were grown under short-day conditions and fixed 28 d after sowing. Longitudinal sections from apices of these plants were hybridized with antisense probes of *RAX1* (Fig. 3.1.1-2a) and *HAT1* (Fig. 3.1.1-2c, d) Probes for *RAX1* (Müler et al., 2006) and *HAT1* were derived from the non-conserved coding regions to avoid unspecific hybridizations. As shown in Fig. 3.1.1-2, *HAT1* transcripts accumulate in a domain at the adaxial base of young leaf primordia in vegetative shoot apices, very similar to that of *RAX1* (Müller et al. 2006). The transcript is also detectable in the middle of the abaxial side of differentiated leaf primordia (Fig. 3.1.1-2d, arrow). To this end, the co-localization of transcripts of *HAT1* and *RAX1* at the adaxial base of leaf primordia in the vegetative shoot apex indicated the physiological significance of their interactions in yeast.
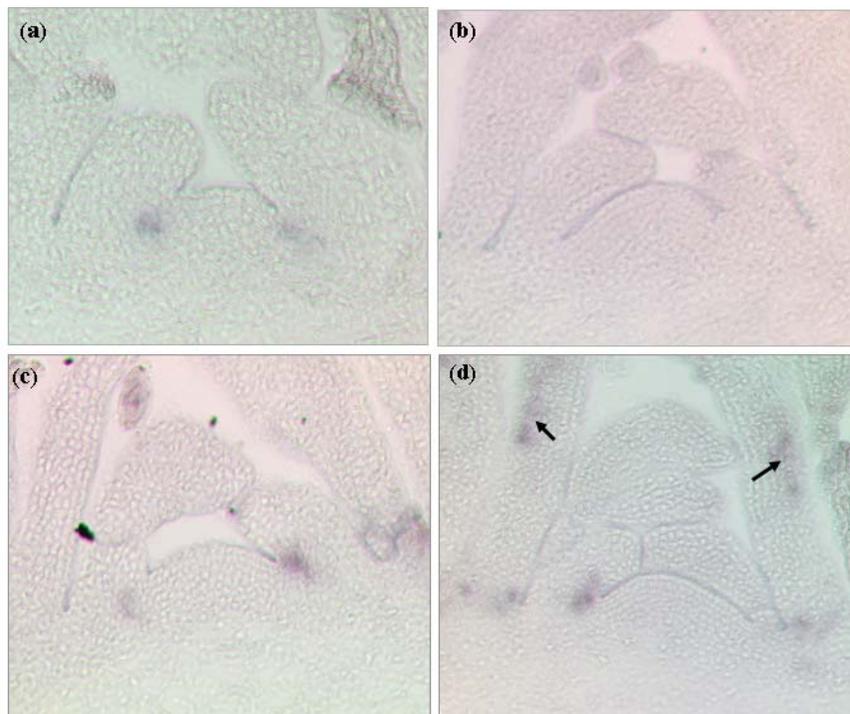
Fig. 3.1.1-2. **Patterns of transcript accumulation of *HAT1* and *RAX1* in vegetative apices.**. Longitudinal sections (a to d) through shoot apices of 28-day old Col-wt plants grown under short day conditions were hybridized with a *RAX1* antisense probe (a) and a *HAT1* antisense probe (c and d). The *HAT1* sense probe was used as a negative control (b). The sections of (c) and (d) are from two different apices. *HAT1* mRNA also accumulated in the middle of abaxial side of developing leaf primordia (arrow in d).

3.1.1.4 Analysis of the effect of *hat1-1* on the branching defect of *rax1-3*

HD-ZIP protein 1 (*HAT1*) belongs to the class II homeodomain leucine zipper (HD-ZIP) transcription factor family. Functions of the HD-ZIP II members are associated with controlling light responses in photosynthetic tissues, particularly in regulating shade avoidance response (Ariel et al., 2007). *HAT2*, the closest homolog of *HAT1* (Fig. 3.1.1-3a) has been shown to play opposite roles in the regulation of auxin-mediated morphogenesis in the shoot and root tissues (Sawa et al., 2002). To understand the possible role of *HAT1* in the process of development, its distribution in various tissues was analyzed by RT-PCR (Fig. 3.1.1-3b). Except in the root, the transcripts of *HAT1* were detectable in all tested tissues with lower expression level during the vegetative stage and higher level during the reproductive stage. This wide expression profile indicates a general function of *HAT1* (Fig. 3.1.1-3c).
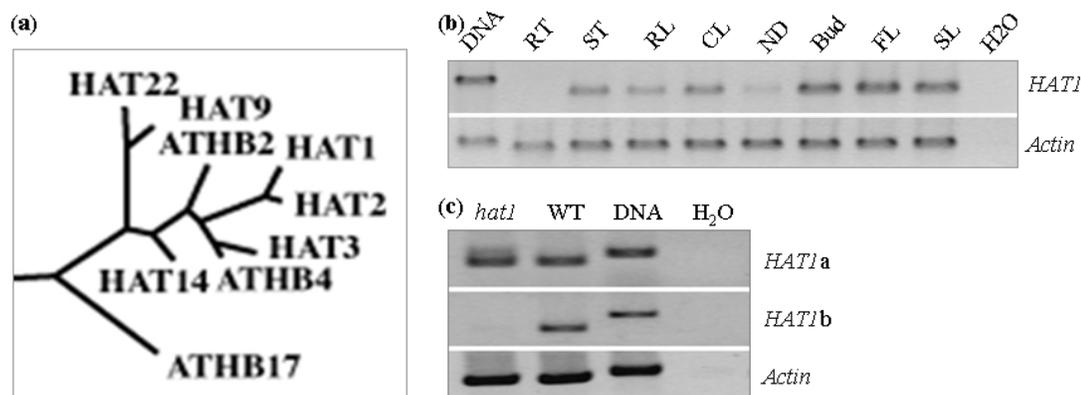
Fig. 3.1.1-3. The *Arabidopsis* homologues of *HAT1* and its expression in the wild type and T-DNA mutant backgrounds. (a) Phylogenetic tree of *Arabidopsis* HD-Zip II genes based on the alignment of full-length protein sequences. HAT2 shows 76% sequence similarity to HAT1. (b) The expression profile of *HAT1* in Col-wt background. The samples were harvested from the stems (ST), rosette leaves (RL), cauline leaves (CL), nodes (ND), floral buds (Bud), open flowers (FL) and siliques (SL) of main shoots of Col plants grown under short days for 4 weeks then shifted into long days. The roots (RT) were harvested from seedlings grown on agar medium. (c) A transcription of *HAT1* in shoot apices of the indicated backgrounds. *hat1* is a SALK line containing T-DNA insertion in the 2nd intron. The samples were harvested from vegetative shoot apices of 28d old short-day grown plants. The fragment *HAT1*a was amplified using gene-specific primers localized 5' of the insertion, and *HAT1*b was amplified using primers localized 5' and 3' of the insertion, demonstrating the absence of the transcription across the insertion in the *hat1* mutant background. The Actin amplification was done to control the templates and the genomic DNA of Col wt and H$_2$O were included as negative controls for PCR in b and c.

The interactions between HAT1 and RAX1 proteins and the co-localization of the two transcripts indicate a potential role of *HAT1* in the regulation of shoot branching. To further analyze the role of *HAT1* in this process, a knockout mutant allele, *hat1-1,* was isolated and investigated in detail. This mutant contains a T-DNA insertion in the 2nd intron (N506022 in the SALK stock center http://signal.salk.edu/cgi-bin/tdnaexpress). Gene-specific primers derived from the coding region 5' of the T-DNA insertion could amplify the N-terminal transcript of *HAT1*, whereas primers localized 5' and 3' of the insertion failed to amplify a transcript (Fig. 3.1.1-3c). However, *hat1-1* mutants did not display any branching defects when grown under any photoperiodic growth conditions. Next, the double mutant *hat1-1 rax1-3* was analyzed to look for a possible genetic interaction between these two genes. The morphology of *hat1-1 rax1-3* did not show an obvious deviation from Col-wt and *rax1-3* single mutant plants (Fig. 3.1.1-4a). Furthermore, stereomicroscopic analysis of the leaf axils demonstrated that the proportion of barren rosette leaf axils of *rax1-3* was not altered in *hat1-1 rax1-3* double mutants, and hence the branching pattern of double mutants was comparable to that observed in *rax1-3* (Fig. 3.1.1-4b). Therefore, *hat1-1* did not enhance the branching defect of *rax1-3*.
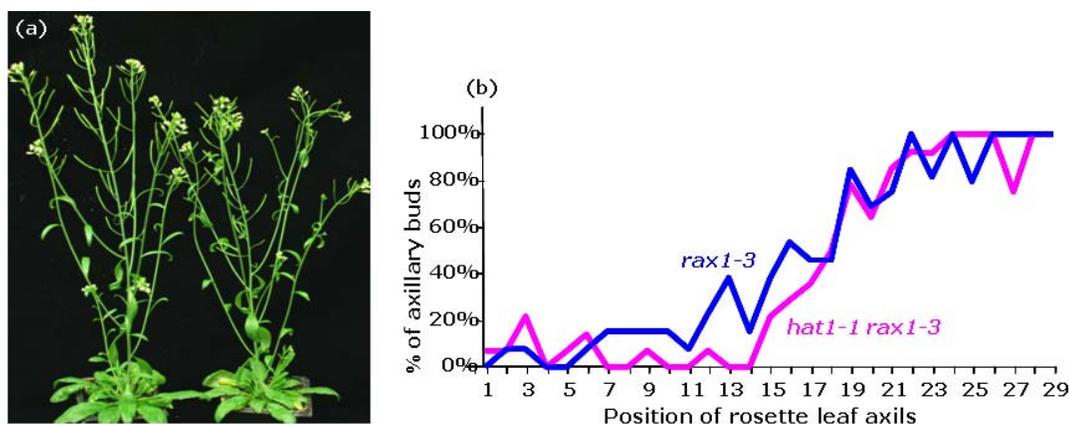
Fig. 3.1.1-4   Growth habit and branching pattern of *hat1-1   rax1-3* double mutants. (a) Morphology of a *hat1-1 rax1-3* double mutant (right) grown under short days for 4 weeks then shifted to long-day conditions to induce flowering, in comparison to a *rax1-3* single mutant (left). (b) Graphic representation of axillary bud formation in *hat1-1 rax1-3* mutants (n=14) in comparison with *rax1-3* single mutants (n=13). Leaf axils of plants were examined under a binocular microscope. Genotypes are indicated next to the graphs. The percentages of Y axis indicate the proportion of analyzed plants that show bud formation in a specific leaf axil. Position 1 corresponds to the oldest rosette leaf axil and position 29 corresponds to the youngest rosette leaf axil analyzed.

3.1.2 An apex cDNA library screening

Given that *RAX1* expression and function is required in the shoot apex (Keller et al., 2006; Müller et al., 2006) a yeast two-hybrid screen against an apex cDNA library (kindly supplied by Hans Sommer, MPIZ, Koeln) was performed to identify more potential interactors. The cDNA library was produced from mixed vegetative and reproductive shoot-tips of *Arabidopsis thaliana*. Bait strain Y187 expressing full-length RAX1 protein was mated to prey strain AH109 bearing the apex cDNA library. About 450 colonies from $1x10^6$ diploid yeast cells grew on the SD/-AHLW+5mM 3AT selective medium. Plasmids were rescued from randomly selected sixty colonies and were subjected to PCR. Forty-four amplified insertions of different sizes were subsequently sequenced. BLAST analysis against the *Arabidopsis* genome revealed 40 different insertions present in 42 tested clones. Based on their expression levels in the shoot apex (Genevestigator data https://www.genevestigator.ethz.ch/at/), the most interesting five candidates (Table 3.1.2) were selected for further analysis. All five clones were introduced with BD-RAX1 into AH109 and the growth of the transformed cells on the SD/-AHLW+5mM 3AT plates confirmed the interaction observed in the library screening. Among these five candidates,

Gene	Description	Expression pattern*
At2g45190	axial regulator *YABBY1* (*YAB1*) / abnormal floral organs protein (*AFO*) / filamentous flower protein (*FIL*)	highly expressed in the shoot apex (Sawa et al., 1999a; Siegfried et al., 1999)
At5g29350	two component phosphorelay mediator 1 (*ATHP1, AHP2*)	widely expressed (Tanaka et al., 2004)
At5g39340	two component phosphorelay mediator 2 (*ATHP2, AHP3*)	moderately expressed in the shoot apex
At4g02480	AAA-type ATPase family protein, ATP-dependent 26S proteasome regulatory subunit	highly expressed in the shoot apex
At5g65210	bZIP family transcription factor (*TGA1*)	moderately expressed in the shoot apex

* according to Genevestigator data

Table 3.1.2. List of the interesting putative interactors of RAX1 screened from the apex cDNA library. These five candidates show high expression levels in the shoot apex and could be shown to interact with RAX1 in preliminary Y2H screening.

YAB1/AFO/FIL (*YABBY1/ABNORMAL FLORAL ORGAN/FILAMENTOUS FLOWER*), a well-known axial regulator with high expression level in the shoot apex (Sawa et al., 1999a; Siegfried et al., 1999), was selected for further detailed analysis.

3.1.2.1 Y2H screening identified YAB1 as a potential partner of RAX1

The sequence of the *YAB1* clone isolated from the library screen did not contain the full open reading frame, but both the zinc finger-like domain and the YABBY domain were present (amino acids 30-185). After the initial yeast two-hybrid screen, the RAX1/YAB1 protein interaction was re-tested in yeast using the full length YAB1 coding region in the presence of an appropriate control (Fig. 3.1.2-1a). Yeast cells harbouring both AD-YAB1 and BD-RAX1 showed growth on the selective medium SD/-AHLW+5mM 3AT. However, yeast cells harbouring full length YAB1 protein had slower growth than cells harbouring only a fragment of YAB1 screened from the cDNA library. This result indicates that the sequences out of the zinc finger-like domain and the YABBY domain may contain an element suppressing the protein interaction of YAB1. Alternatively, Full length YAB1 protein has lower expression level in yeast cells than partial YAB1 protein.
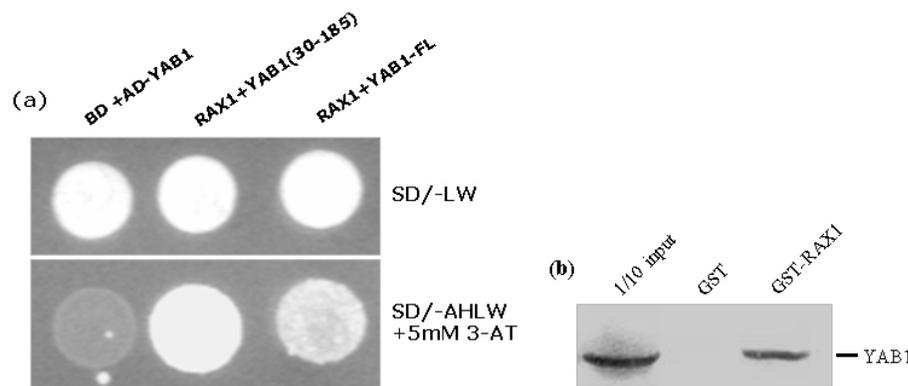
Fig. 3.1.2-2   The interaction between YAB1 and RAX1. (a) YAB1 showed interaction with RAX1 in yeast. Yeast cells transformed with the indicated plasmids grew on minimal medium for 3 days (upper panel) and were then transferred onto the selective plates (lower panel). The growth of cells harbouring BD-RAX1 and AD-YAB1 in contrast to the absence of growth of cells bearing AD-YAB1 and empty GAL4-BD vector indicated the interaction of two proteins. Whereas, the full length AD-YAB1 fusion protein together with BD-RAX1 protein led the transformed cells to grow slower than the cells bearing BD-RAX1 and a fragment of YAB1 (AA30-185) fused with GAL4-AD. (b) *In vitro* pull-down assay of His-YAB1 (lane 1, 10% supernatant as input), incubated with GST alone (lane 2) and the indicated GST-RAX1 (lane 3) proteins coupled with glutathione–Sepharose. Western blotting probed with anti-His antibody confirmed that His-YAB1 was present in the elution from GST-RAX1 pull-down assay and not pulled down by GST alone.

3.1.2.2 Confirmation of interaction between YAB1 and RAX1 by GST-pull down assay

To confirm the interaction between YAB1 and RAX1 identified in yeast, an *in vitro* pull down assay was performed. Full coding sequences of both, YAB1 and RAX1, were N-terminally fused with a His tag and a GST tag, respectively. In this assay, GST-RAX1 fusion protein was expressed in *E. coli* BL21 and purified with the help of glutathione beads (Material and Methods). However, it was not possible to purify His-YAB1 using Ni^{2+}-NTA beads under the tested conditions, and therefore the supernatant after sonication was subjected to a pull down assay. Antibodies against His-tagged fusion protein was able to detect specifically His-YAB1 used as input in supernatant (Fig. 3.1.2-2b, lane 1) and in the elution from the incubation in the presence of GST-RAX1 (Fig. 3.1.2-2b, lane 3), in contrast to lack of His-YAB1 in the elution from GST-only incubation (Fig. 3.1.2-2b, lane 2). This result demonstrates that YAB1 and RAX1 interact specifically *in vitro*.

3.1.2.3 Comparison of transcript accumulation of *YAB1* and *RAX1* in the shoot apex

YAB1 is initially expressed in leaf anlagen and the expression is confined to the abaxial regions of developing primordia later on (Siegfried et al., 1999). The earliest expression of *RAX1* is in the incipient leaf primordium, labeled P_0, and the transcript accumulates at the adaxial base of the developing lateral primordia (Keller et al., 2006; Müller et al., 2006). It is tempting to speculate that the transcripts of *YAB1* and *RAX1* have an overlapping expression domain in the region of the incipient primordium. To test this, consecutive sections of shoot apices from short-day grown plants were alternately hybridyzed with *YAB1* and *RAX1* antisense probes in parallel (Fig. 3.1.2-3). In apices of 45d old SD plants, *RAX1* and *YAB1* mRNAs were detected in partially overlapping domains in the region of incipient leaf primordium (Fig. 3.1.2-3a, b, arrow). The co-expression of *YAB1* and *RAX1* transcripts was also observed at the base of incipient primordium in the apices of 50d old SD plants (Fig. 3.1.2-3 c, d). These findings demonstrate that the

transcripts of *YAB1* and *RAX1* partially co-localize in the incipient leaf primordium.
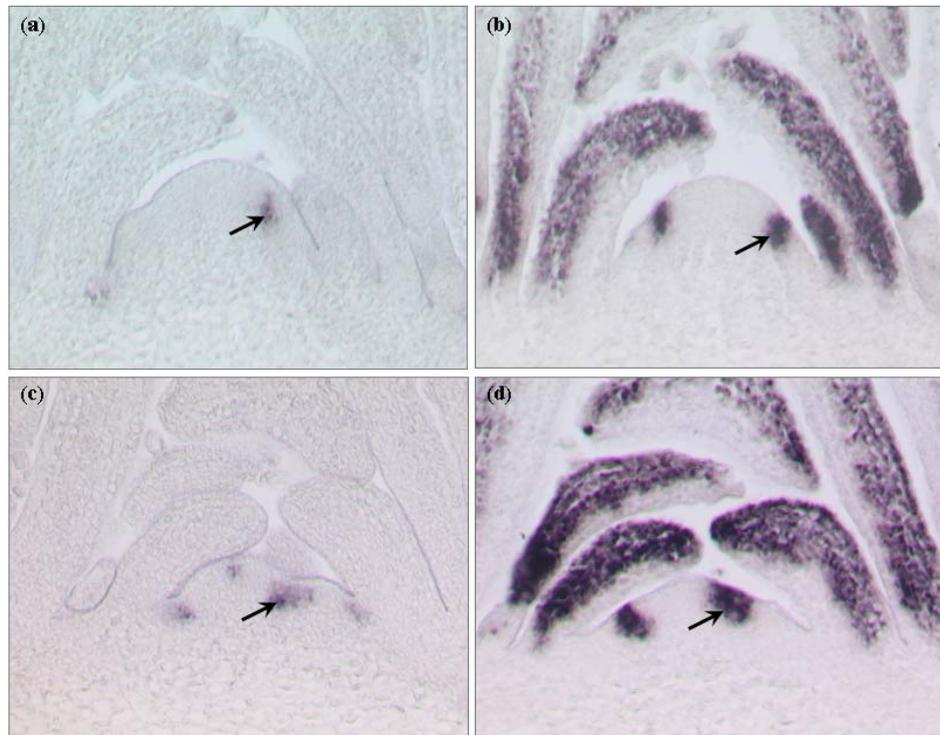
Fig.3.1.2-3. **Co-localization of *RAX1* and *YAB1* transcripts in the incipient leaf primordium**. Consecutive section ns through shoot apices of 45d old (a, b) or 50d old (c, d) Col plants grown under short day conditions were alternately hybridyzed with a *RAX1* antisense probe (a, c) and a *YAB1* antisense probe (b, d). Both transcripts were found to be co-localized in the incipient primordia in the tested apices of short-day-grown plants.

3.1.2.4 *YAB1* regulates axillary bud formation during the both vegetative and reproductive stages of development

YAB1 is a member of the plant-specific YABBY gene family comprising six members in *Arabidopsis* (Siegfried et al., 1999). Several lines of evidence demonstrate that YABBY gene family members promote abaxial cell fate in lateral organs (Eshed et al., 1999; Sawa et al., 1999b; Siegfried et al., 1999). *YABBY* genes are initially expressed throughout the incipient lateral primordium and are restricted to the abaxial side of all lateral primordia later on (Sawa et al., 1999b; Siegfried et al., 1999). It has been previously described that a loss-of-function mutation in *YAB1* or *YAB3* gene does not lead to a change of the vegetative morphology of a plant due to functional redundancy. *yab1 yab3* double mutants, on the other hand, developed striking phenotypes, characterized by linearized cotyledons and leaves and ectopic meristems developing occasionally on the adaxial

surfaces of leaves (Kumaran et al., 2002; Siegfried et al., 1999). *FIL* (*YAB1*) was named after the filamentous flower architecture caused by the *yab1* mutation. Sawa *et al*. described that *fil* mutants frequently failed to produce tertiary shoots, and the severity of this defect was strongly enhanced by low temperature growth conditions. However, secondary shoots were observed to grow normally under the standard growth conditions (Sawa et al., 1999a).
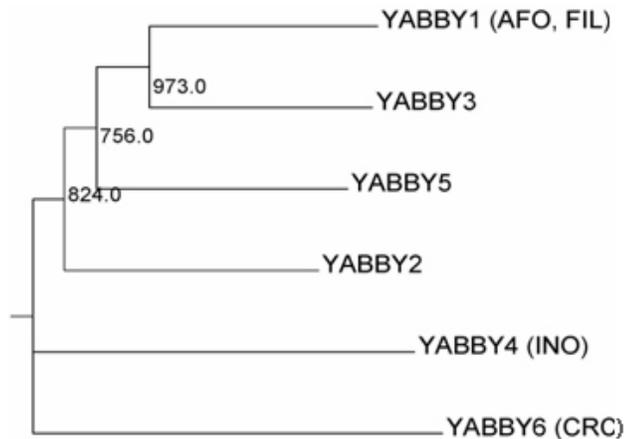
Fig. 3.1.2-4 Phylogenetic tree of the *Arabidopsis* YABBY genes. The alignment is based on full length protein sequences. YABBY3 (YAB3) shows the highest sequence similarity to YABBY1 (YAB1).

Given that the severity of the branching defects of *rax* mutants is strongly dependant on the day-length conditions (Müller et al., 2006), the branching phenotype of a knockout mutant allele of *yab1* in Ler background (*fil-8*, kindly supplied by Yuval Eshed) was analyzed by growing the plants to maturity under short-day conditions. *fil-8* contains a Ds insertion in the 4th exon within the YABBY domain, resulting in a deletion of the subsequent eighty-three amino acids (Kumaran et al., 1999). Stereomicroscopic analysis of leaf axils of *fil-8* mutants revealed a strong reduction in the formation of axillary buds in the topmost rosette leaf axils in comparison to the Ler wild type, whereas the older rosette leaf axils of *fil-8* showed no deviation in the development of axillary buds from wt (Fig. 3.1.2-5d, i). Defects in the axillary bud formation were also observed in cauline leaf axils of *fil-8* mutants (Fig. 3.1.2-5a, c, e, j). In addition, *fil-8* mutants developed an average of 17.8 cauline leaves (n=17) in comparison to the Ler wild type with an average of 10.7 cauline leaves (n=11), when the plants were grown in short photoperiods. In line with previous observations (Sawa et al., 1999a), *fil-8* mutants
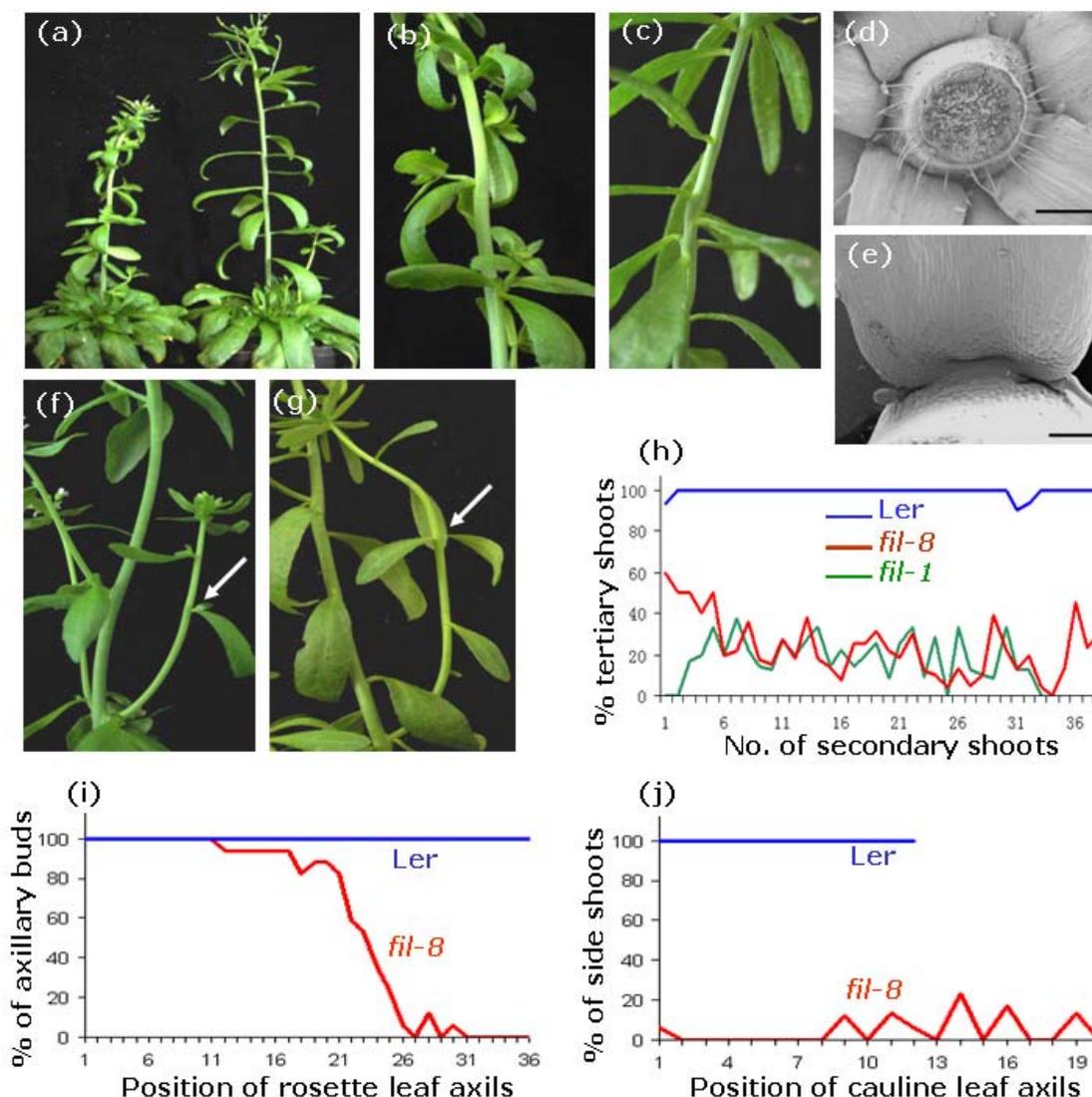
Fig.3.1.2-5. Growth habit and branching pattern of *fil-8* mutants grown under short day conditions. (a) Growth habit of a *fil-8* mutant (right) in comparison with a Ler wild-type (left) when grown to maturity in short days. (b, c) Close-ups of cauline leaf axils of Ler wild-type (b) and *fil-8* mutant (c). (d, e) SEM micrograph of the axils of the top of the rosette leaves (d) and a cauline leaf (e) of *fil-8* mutant. Scale bar: 1mm in (d) and 200µm in (e). (f, g) Close-ups of the leaf axils (arrows) of side shoots of Ler wild-type (f) and *fil-8* (g) mutant showing absence of the tertiary shoots in *fil-8*. (h, i, j) Graphic representation of axillary bud formation in *fil-8* mutants, in comparison with Ler wt plants. Leaf axils of plants were examined under a binocular microscope. Genotypes are indicated next to the graphs. (h) The percent values of Y axis indicate the proportion of the 36 secondary shoots (X axis) analyzed in *fil-8* mutants (n=6), *fil-1* mutants (n=5) and Ler wild-type plants (n=4) that show tertiary shoot formation. (i, j) The percent values of Y axis indicate the proportion of analyzed plants that show a bud in the specific leaf axil (n=17 in *fil-8*, n=11 in Ler). Position 1 corresponds to the oldest rosette leaf axil and position 38 corresponds to the uppermost rosette leaf axil in (i). Position 1 to 20 in (j) are positions of progressively younger cauline leaves. Ler wt plants analyzed in these experiments developed maximal 12 cauline leaves. The branching pattern analysis of *fil-8* was repeated at least once.

also showed a clear reduction in the formation of tertiary shoots (Fig. 3.1.2-5g,h). Interestingly, the branching defect of *fil-8* showed a high variability under different growth conditions. The defects in axillary bud formation in both rosette leaf axils and cauline leaf axils almost vanished when plants were grown to maturity in long photoperiod or when shifted to long days to induce flowering after 4-weeks growth in short days. Additionally, the branching defect of *fil-8* was more severe in winter than that observed in summer although plants were always grown under short photoperiods.

To confirm that the mutation in *YAB1* is the cause for the reduction of side shoot formation in the rosette and cauline leaf axils, a different mutant allele of *yabby1* (*fil-1*) was analyzed. *fil-1* contains a point mutation in the last nucleotide of the 4th intron resulting in a damage of the splicing site (Siegfried et al., 1999). *fil-1* mutants had normal vegetative growth, and barren cauline leaf axils were only present at a low frequency (21.3%, n=19) in comparison with the *fil-8* mutants (96%, n=17) when grown under the same short photoperiods. However, formation of tertiary shoots of *fil-1* was also strongly reduced and filamentous flowers were formed, similar to that observed in *fil-8* mutant (Fig. 3.1.2-5h).

Scanning electron microscope (SEM) inspection of the empty leaf axils of *fil-8* mutants did not reveal any axillary-bud-resembling morphological structure (Fig. 3.1.2-5d, e). This observation indicates that the cells of leaf axils lose their meristematic competence leading to a failure in axillary meristem initiation. Taken together, these observations suggest that the *YAB1* gene plays an important role in the control of axillary meristem formation in a day-length as well as a temperature dependent manner.

3.1.2.5 Analysis of the pattern of axillary meristem formation in *fil-8 rax1-3* double mutants

YAB1 was identified to interact with RAX1, which was supported by the partial co-localization of the two transcripts in incipient leaf primordia. More interestingly, the

mutations in both *YAB1* and *RAX1* affect lateral meristems formation during the vegetative phase of development. Müller *et al*. (2006) described that a loss-of-function allele of *rax1-3* led to a reduction in the axillary meristem formation in the old rosette leaf axils. To explore the biological relevance of the interaction of RAX1 and YAB1 proteins, *fil-8 rax1-3* double mutants were analyzed. *rax1-3* is a knockout allele in Col background, containing a T-DNA insertion close to the end of the ORF, and *fil-8* is in the Ler background. Under short-day growth conditions, *fil-8 rax1-3* double mutants showed a phenotype very similar to *fil-8* single mutants (Fig. 3.1.2.6a). These plants had a reduction in axillary bud formation at the topmost rosette leaf axils and in most of the cauline leaf axils. They also showed early flowering and formation of filamentous flowers. However, microscopic analysis revealed that the branching defect of *rax1-3* was suppressed in *fil-8 rax1-3* double mutants. Lateral buds developed in *fil-8 rax1-3* double mutants at a high frequency in the oldest 20 to 25 rosette leaf axils, in which *rax1-3* in the same mixed backgrounds showed a strong branching defect (Fig. 3.1.2-6b). The branching pattern of *fil-8* in the same mixed backgrounds did not change dramatically. Additionally, fil-8 rax1-3 flowered much earlier with an average of 36.4 rosette leaves (n=18) than *rax1-3* and *fil-8* with 56.4 (n=16) and 42.6 (n=14) average rosette leaves, respectively. In conclusion, the *fil-8* mutation reduced the proportion of barren rosette leaf axils of *rax1-3* during the early vegetative phase, but enhanced the early flowering phenotype of *rax1-3*.
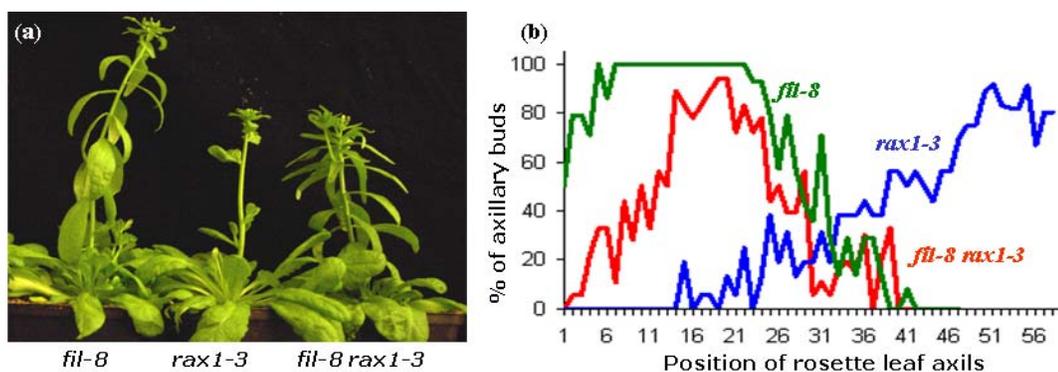
Fig 3.1.2-6: **Growth habit and branching pattern of *fil-8 rax1-3*.** (a) 75d old short-day grown *fil-8 rax1-3* double mutant in comparison with the control plants in the same mixed backgrounds. The genotypes are indicated. (b) Graphic representation of axillary bud formation in *fil-8 rax1-3* mutants (n=18) in comparison with control plants *fil-8* (n=14) and *rax1-3* (n=16). Position 1 corresponds to the oldest rosette leaf axil and position 58 corresponds to the uppermost rosette leaf axil. The branching pattern analysis of *fil-8 rax1-3* was repeated two times.

3.2 A role for *AtLAX* in shoot branching in *Arabidopsis thaniana*

Shoot branches are derived from the establishment and outgrowth of axillary meristems (AMs). Several transcription factors, like *LAS, RAX* and *CUC* function as gatekeepers for the initiation of axillary meristems (Greb et al., 2003; Müller et al., 2006; Keller et al., 2006; Hibara et al., 2006; Raman, 2006). The transcripts of these regulators accumulate in similar and/or overlapping domains in the developing leaf axils where axillary meristems will form. Loss-of-function mutations in these axillary meristem regulators result in absence of axillary meristem formation, demonstrating their important roles in the initiation of new meristems.

Recently, two other transcription factors *LAX PANICLE* (*LAX*) and *BARREN STALK1* (*BA1*), belonging to the basic helix-loop-helix (bHLH) family, have been shown to control the pattern of shoot and inflorescence branching in rice and maize, respectively (Gallavotti et al., 2004; Komatsu et al., 2003; Komatsu et al., 2001). The transcripts of both genes accumulate at the adaxial base of new meristems. Whereas the *LAX* activity is not detectable during the vegetative stage, *BA1* is expressed on the adaxial side of initiating axillary meristems during both vegetative and reproductive phases (Gallavotti et al., 2004; Komatsu et al., 2003). Accordingly, loss of *BA1* function leads to lack of tillers (vegetative branches), unbranched tassels and lack of ears (reproductive branches), while a mutation in the *LAX* gene results in a branching defect only during the reproductive stage. Plants homozygous for a strong knockout mutation in *LAX* are characterized by severely reduced panicle branches and a complete lack of lateral spikelets. Furthermore, the complete block of tiller formation in *lax spa* double mutants reveals an important role of *LAX* in regulating vegetative branching in a redundant fashion together with the *SMALL PANICLE* (*SPA*) gene (Komatsu et al., 2003). The comparison between LAX and BA1 amino acid sequence reveals 100% conserved bHLH domains and an overall protein identity of 62%. So far, a cognate homolog of *LAX* in *Arabidopsis* is not known yet. In this study, a *LAX*-related gene in *Arabidopsis* (*AtLAX*) was identified and its function in the process of axillary meristem formation was characterized.

3.2.1 Phylogenetic analysis of *LAX*-related genes in *Arabidopsis*

Basic helix-loop-helix (bHLH) transcription factors represent a family of proteins that contain a bHLH domain of approximately 50-60 amino acids (AA) in length (Murre et al., 1994). The bHLH domain consists of two functionally distinct regions: the basic region at the N-terminal end is involved in DNA binding and consists of 15 amino acids with a high number of basic residues, and the helix-loop-helix region at the C-terminal end functions as a dimerization domain (Ferre-D'Amare et al., 1994). Outside of the conserved bHLH domain, there is considerable sequence divergence among these genes (Atchley et al., 1999). In *Arabidopsis*, 162 bHLH genes in total are annotated and are classified into 21 subfamilies (Bailey et al., 2003). However, only 27 members have been functionally characterized.

BLAST analysis of the *Arabidopsis* genome demonstrated that a putative bHLH gene At5g01310, recently named *bHLH140*, shows the highest similarity to the rice *LAX* (*OsLAX*) and maize *BA1* (*ZmBA1*) genes within the bHLH domain. The annotated sequence for At5g01310 comprises six exons and five introns with a coding region containing 2739bp (http://www.arabidopsis.org/). Given that *LAX* and *BA1* are intron-less and have open reading frames (ORFs) with only 648bp and 660bp in length, respectively, the *AtLAX* gene is expected to have a short ORF with similar length to *LAX* and *BA1*. To prove this hypothesis, a reverse primer derived from the first intron of At5g01310 gene in combination with a forward primer specific for the putative start region of this gene could amplify a cDNA of 513bp. This result demonstrates that the annotation for At5g01310 (*bHLH140*) is wrong. Based on the high similarity to the rice *LAX* gene, *bHLH140* was designated *AtLAX* (Arabidopsis homolog of *LAX*) in this study. *AtLAX* encodes 171 amino acids with a bHLH domain spanning from position 44 to 92 (Fig. 3.2.1-1a). Within the bHLH domain, AtLAX shows 81% amino acid sequence identity to LAX and BA1, which is higher than all other bHLH genes (Fig. 3.2.1-1b). Outside of the bHLH domain, the sequences are highly divergent.

(a)

```
  1   ATGGATGATTTCAATCTTCGTAGCGAAAACCCTAATTCATCATCCACCACTTCCTCATCC
      M  D  D  F  N  L  R  S  E  N  P  N  S  S  S  T  T  S  S  S

 61   TCTTCCTCTTTCCACCGTCACAAGAGCGAAACCGGAAACACAAAACGGTCAAGGTCAACG
      S  S  S  F  H  R  H  K  S  E  T  G  N  T  K  R  S  R  S  T

121   TCCACGTTATCGACGGACCCTCAGAGCGTGGCGGCTCGCGACAGACGGCACCGAATTAGC
      S  T  L  S  T  D  P  Q  S  V  A  A  R  D  R  R  H  R  I  S

181   GACCGTTTCAAGATTTTACAAAGCATGGTCCCTGGTGGTGCGAAGATGGACACTGTATCT
      D  R  F  K  I  L  Q  S  M  V  P  G  G  A  K  M  D  T  V  S

241   ATGCTTGACGAAGCCATTAGCTACGTCAAGTTCTTGAAGGCTCAGATCTGGTATCACCAA
      M  L  D  E  A  I  S  Y  V  K  F  L  K  A  Q  I  W  Y  H  Q

301   AACATGCTTCTCTTCATAAACGACCACGAAACTACATCATCTTGTACTTACTCTCCCGGC
      N  M  L  L  F  I  N  D  H  E  T  T  S  S  C  T  Y  S  P  G

361   GCTGGAGAATTTGGACCGAAACTCTTTGGTTATGATGACGATTATGCCCCTATAATGGAC
      A  G  E  F  G  P  K  L  F  G  Y  D  D  D  Y  A  P  I  M  D

421   ACATATTCACAAGGCGTGCCACTTACGGTTGCGGACTCGAAGTATACGCCGTGGTTTGGT
      T  Y  S  Q  G  V  P  L  T  V  A  D  S  K  Y  T  P  W  F  G

481   TCGGTTGATGATGAGCAAGAACgtgactcgtcctag
      S  V  D  D  E  Q  E  R  D  S  S  *
```

(b)

```
                  *    *    *
LAX    STDPQSVAARERRHRISDRFRVLRSLVPGGSKMDTVSMLEQAIHYVKFL
BA1    STDPQSVAARERRHRISDRFRVLRSLVPGGSKMDTVSMLEQAIHYVKFL
AtLAX  STDPQSVAARDRRHRISDRFKILQSMVPGGAKMDTVSMLDEAISYVKFL
```

Fig. 3.2.1-1 Sequence of the *AtLAX* gene and its conserved bHLH domain. (a) Nucleotide sequence of *AtLAX* and its deduced amino acid sequence. *AtLAX* is an intronless gene and contains a bHLH domain spanning from position 44 to 92 (underline). The last 11 nucleotides (small letters) of the coding region are deduced from the first intron of the gene At5g01310, annotated in the TAIR database (http://www.arabidopsis.org/). (b) Comparison of the bHLH domains of the *LAX* gene in rice, the orthologous gene *BA1* in maize, and the most closely related gene *AtLAX* in *Arabidopsis*. The conserved 5-9-13 motif within the bHLH domain is represented by amino acids Q-A-R (asterisks), respectively (Heim et al., 2003).

AtLAX belongs to the group VIII of the bHLH gene family due to the presence of the conserved Q-A-R motif: Gln, Ala and Arg at positions 5, 9, and 13, respectively, within the bHLH domain (Heim et al., 2003). These conserved amino acids have been proven to be critical for the ability of bHLH proteins to bind DNA (Atchley et al., 1999; Ledent and Vervoort, 2001). Q-A-R motif search revealed a total number of 14 group VIII members. Based on the structural similarities, twelve members have been divided into VIIIa, b, c three subgroups without *AtLAX* and *bHLH139* (Heim et al., 2003). *bHLH139* can be classified into subgroup VIIIc, whereas AtLAX does not show structural similarity to any other group members. Therefore, it is clustered into a separate subgroup VIIId, together

with LAX and BA1 (Fig. 3.2.1-2). Phylogenetic analysis on the basis of the protein sequences of the bHLH domains reveals that *AtLAX* is the most closely related gene to the rice *LAX* and the maize *BA1* genes (Fig. 3.2.1-2), implying that *AtLAX* might have a similar function in shoot branching.
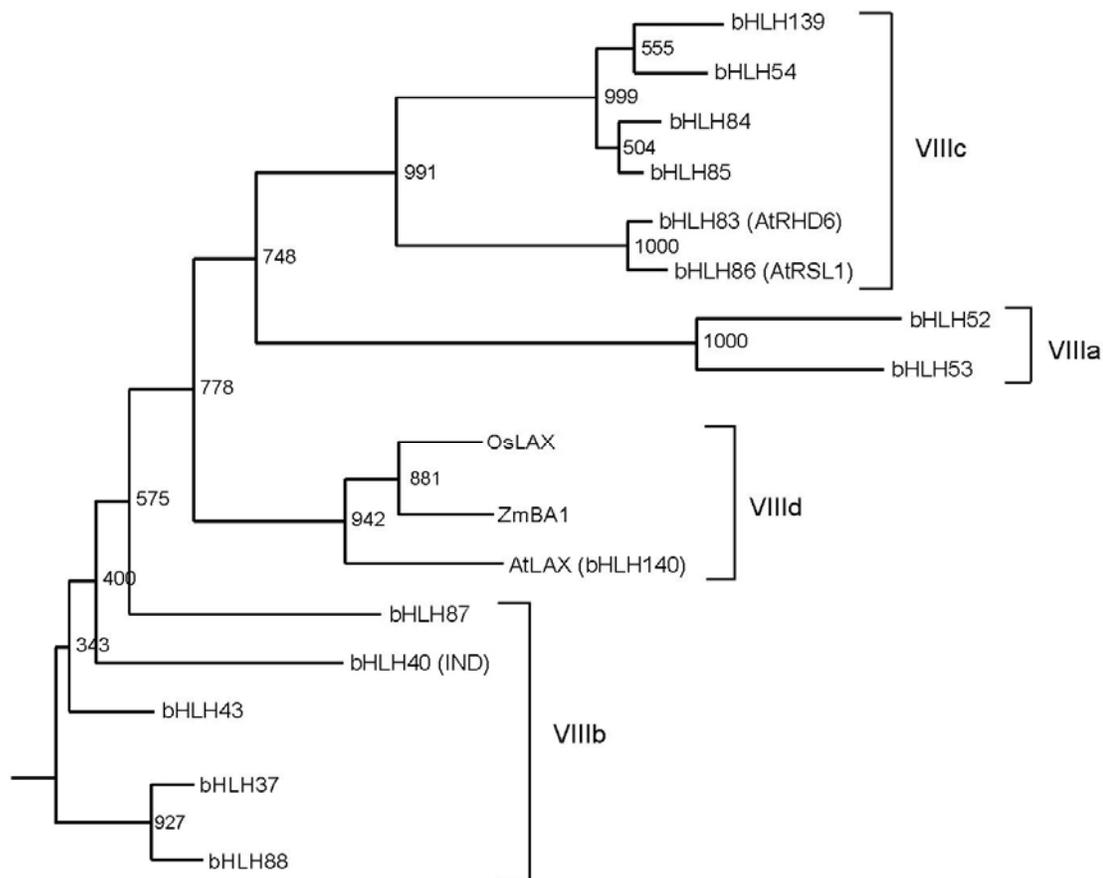
Fig. 3.2.1-2 Phylogenetic analysis based on the alignment of amino acid sequences within the bHLH domains. The conserved bHLH domain of bHLH140 (AtLAX), showing the highest sequence similarity to LAX in rice and BA1 in maize, was compared with thirteen Q-A-R motif containing bHLH genes from *Arabidopsis*. The tree was made using ClustalW software. Multiple sequence alignments were done using the bootstrap neighbor-Joining tree option with 1000 bootstraps. The synonyms of three functionally characterized members are given in the brackets. Os, *Oryza sativa*; Zm, *Zea mays*; At, *Arabidopsis thaliana.*

3.2.2 Expression profiles of the *AtLAX* subfamily members

To screen for candidate genes among the 14 bHLH-subfamily members with putative functions in apical and/or axillary meristems, the expression profiles of these genes were investigated by RT-PCR analysis. Total RNA was isolated from different tissues of Col-wt

plants, including roots of agar-grown plants, shoot tips of 28d old short-day-grown plants, rosette leaves, cauline leaves, cauline nodes, floral buds, open flowers and 1-3d old siliques from primary shoots. Due to the very small size of the Arabidopsis SAM, the harvested shoot tips include not only the SAM and leaf primordia, but also several young leaves. Total RNA was isolated and DNase digested to get rid of the genomic DNA contamination. Gene specific primers were designed across introns when possible. The expression profiles of the 14 group members are shown in Fig. 3.2.2. *bHLH83* (*AtRHD6, ROOT HAIR DEFECTIVE6*) and *bHLH86* (*AtRSL1, RHD SIX-LIKE1*) were found to be
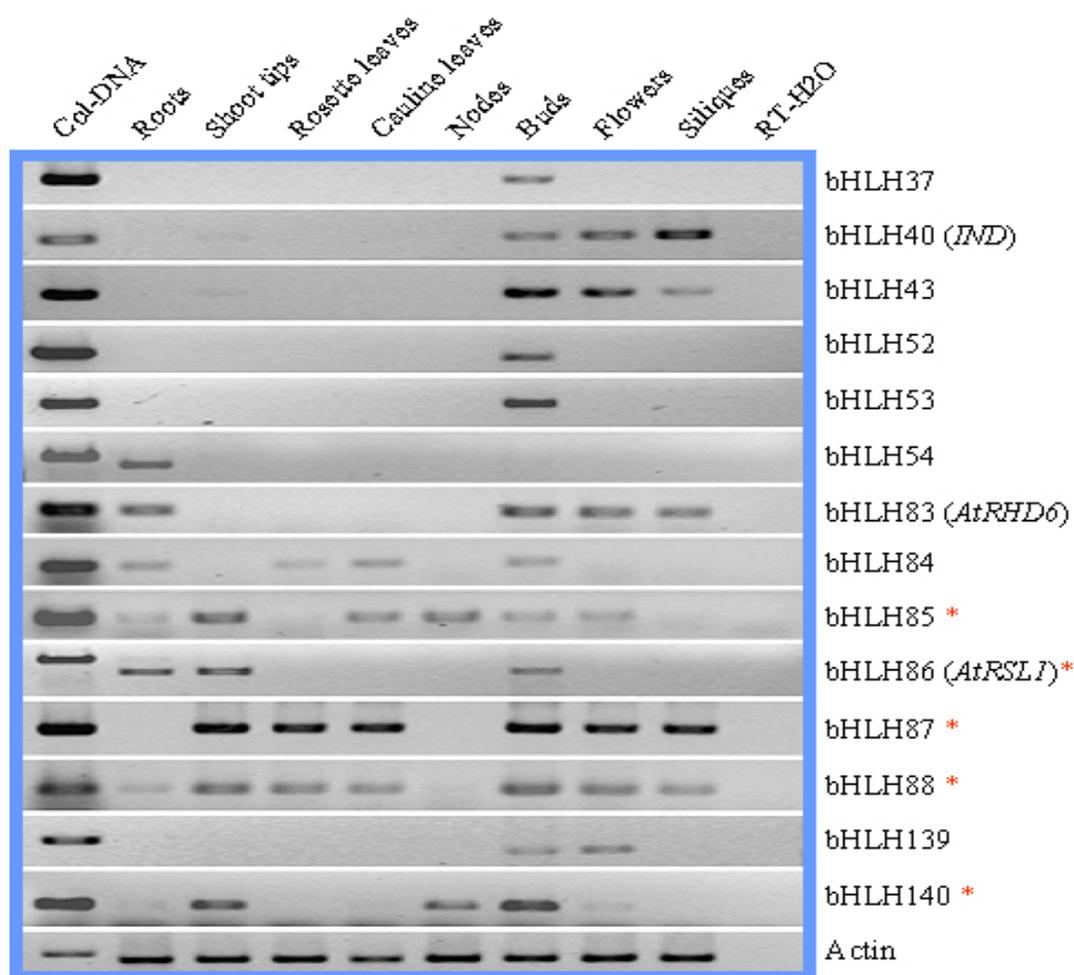
Fig. 3.2.2 The expression profiles of the *AtLAX* subfamily members. The tissues were harvested from roots of agar-grown seedlings, shoot tips of 28d old short-day-grown plants, rosette leaves, cauline leaves, cauline nodes, floral buds, open flowers and 1-3d old siliques from the primary shoots. 500ng total RNA of each sample was subjected to cDNA synthesis, and H_2O was used as a negative control for the transcriptions. The amplification for *ACTIN8* was included to control the amount of template, and the genomic-DNAs were used to control the PCR. Red asterisks mark the five subgroup members which have expression in the shoot tips.

expressed in roots, which corresponds to their functions in root hair development (Menand et al., 2007). *bHLH54* mRNA was exclusively detected in roots, consistent with the Genevestigator data. Therefore, *bHLH54* is supposed to function in roots. Interestingly, almost all the group members, except *bHLH54,* were active during reproductive developmental stage. For instance, *bHLH37*, *bHLH52, bHLH53* and *bHLH139* were specifically expressed in floral buds. *bHLH40* (*IND, INDEHISCENT*) showed the highest expression in siliques, tightly related to its role in fruit patterning (Liljegren et al., 2004). Transcripts of the genes *bHLH85, bHLH86* (*AtRSL1*)*, bHLH87, bHLH88* and *bHLH140 (AtLAX)* were detected in the shoot tips. Furthermore, mRNAs of *bHLH85* and *AtLAX* were also detected in the cauline nodes where the cauline leaf axils are located. Due to the fact that axillary meristems form at the adaxial base of leaf primordia, the genes showing mRNA accumulations in the shoot tips were selected for further analysis. Among those five candidate genes, *AtLAX* was the focus of this study considering its high sequence similarity to the rice *LAX* and the maize *BA1* genes.

3.2.3 Analysis of the expression pattern of *AtLAX* in the shoot apex

To further investigate the expression pattern of *AtLAX,* in situ hybridization experiments were conducted using tissue sections of Col wild type plants. An antisense probe derived from the nonconserved coding region (position 215bp from the ATG to the end) was used to avoid cross-hybridization with other members of the bHLH subfamily. In 25d to 35d old short-day-grown seedlings, *AtLAX* transcripts were detected at the adaxial base of leaf primordia (Fig. 3.2.3 a-c). A closer look at transverse sections revealed that the mRNA of *AtLAX* mainly accumulated in the center of the boundary between the SAM and young leaf primordia (arrow in Fig. 3.2.3 c). The expression domain was about 2-3 cell layers wide and 3-5 cell layers deep. *AtLAX* transcripts were detected from P_0 to P_{10}/P_{12}, including always the L3 layer, and were frequently excluded from the L1 or L1 and L2 layers of the SAM (Fig. 3.2.3b). Sections of reproductive apices were collected from plants grown under short days for 4 weeks and then shifted to long days for 4d, 6d or 10d to induce flowering. In these plants, *AtLAX* transcripts accumulated at the adaxial base of floral

primordia, frequently throughout the L1 and L2 layers and in the emerging floral primordia (arrows in Fig. 3.2.3d, e). In inflorescence meristems, *AtLAX* was expressed in the axils of stage 0 to stage 4 flower primordia (Smyth et al., 1990).
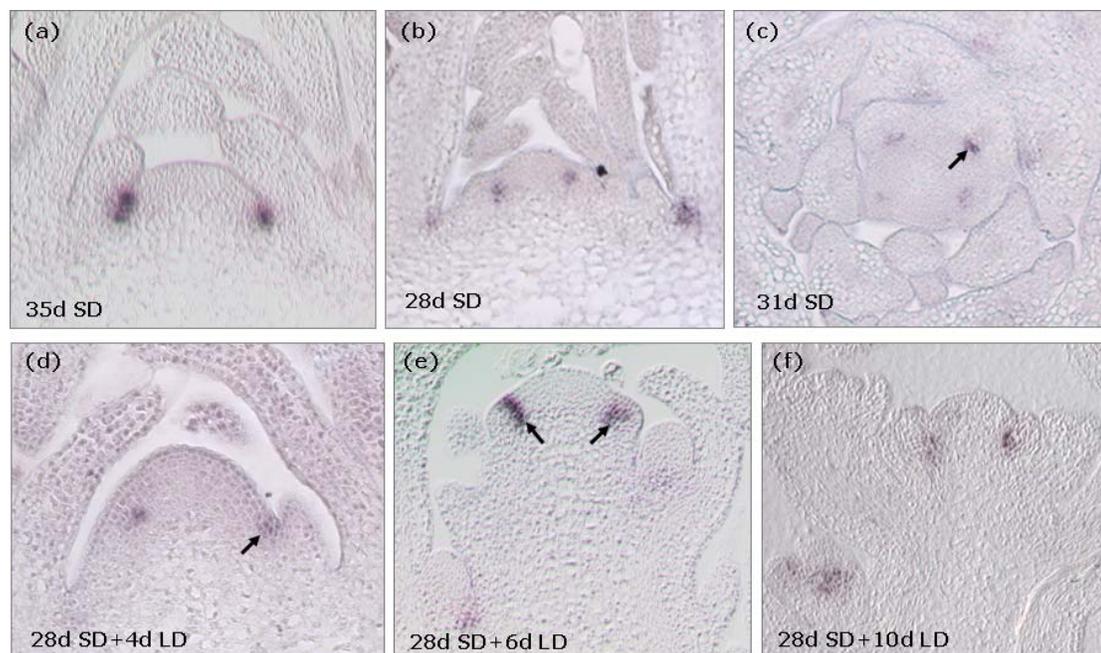
Fig. 3.2.3 Transcripts of *AtLAX* accumulated at the adaxial base of primordia. (a-c) Sections of vegetative shoot apices of 28d to 35d old Col plants grown under short-day conditions. Longitudinal sections showed that *AtLAX* mRNA was detectable in the axils of leaf primordia and frequently excluded from the L1 or L1 and L2 layers (b). A transverse section located around 24 μm below the top of the meristem demonstrated that *AtLAX* transcripts mainly accumulated in a ball-shaped domain in the center of the boundary region between the SAM and leaf primordia (c). (d-f) Longitudinal sections through reproductive shoot apices of Col plants grown for 28 days in short photoperiod and then shifted to long days for indicated number of days. In reproductive shoot apices, *AtLAX* were expressed at the adaxial base of floral primordia.

However, similar in situ experiments done in parallel with other specific probes could not detect transcripts of *bHLH85, bHLH86, bHLH87* and *bHLH88* in both vegetative and reproductive shoot apices. Hybridizations were performed using two different antisense probes for each of these four *bHLH* genes. The failure to detect any expression might be due to a very low level of transcripts that is undetectable using the in situ hybridization method. Low levels of *bHLH85, bHLH86* and *bHLH88* transcripts were indicated by the faint bands, obtained after 40 amplification cycles (Fig. 3.2.2).

3.2.4 Functional characterization of *AtlAX* in shoot branching

To unravel a gene function, one efficient way is to investigate the effect of a mutation in the gene on the phenotype of the corresponding mutant plant. However, the loss of function of a gene can often be compensated by the redundant function of its homolog(s) so that an informative phenotype is often failed to exhibit. Therefore, the phenotypes of mutants harboring mutations in different homologs are consequently necessary to analyze. On the other hand, a hint for the gene function can derive from the phenotype of plants in which the corresponding gene is mis-expressed.

3.2.4.1 Analysis of *bhlh* knockout mutants

The T-DNA insertion line collection from the SALK stock center was screened for knockouts in the genes *bHLH85, bHLH86, bHLH87, bHLH88* and *AtLAX* (see Methods). The transcripts of these genes were detected in the shoot tip as shown by RT-PCR and/or in situ hybridization experiment. The T-DNA insertion for each line is presented in Fig. 3.2.4-1a. Two independent insertion lines for *AtLAX* were characterized: *atlax-1* (N580565) and *atlax-2* (N524760) with a T-DNA insertion at the beginning of and behind the bHLH domain, respectively. Insertion points in these two lines were confirmed by sequencing PCR products obtained from plants homozygous for the respective insertion. *bhlh87-1* and *bhlh88-1* contain T-DNAs within the open reading frames, whereas the insertions in the *bHLH85 and bHLH86* genes are localized more than 100bp in front of their putative start codons. Transcript accumulation of each insertion allele was analyzed by RT-PCR using RNA isolated from plants homozygous for the corresponding T-DNA insertion. In the cases of *atlax* (Fig. 3.2.4-1b)*, bhlh*87-1 and *bhlh88-1*, gene-specific primers localized to 5' and 3' of the insertions did not yield amplification products, indicating that no functional transcripts could be detected. However, the transcripts of b*HLH85* and *bHLH86* in homozygous *bhlh85-1* and *bhlh86-1* mutants, respectively, did not show obvious alterations in comparison to that detected in Col-wt (data not shown). This data suggests that *bhlh85-1* and *bhlh86-1* might not be knockout mutants.
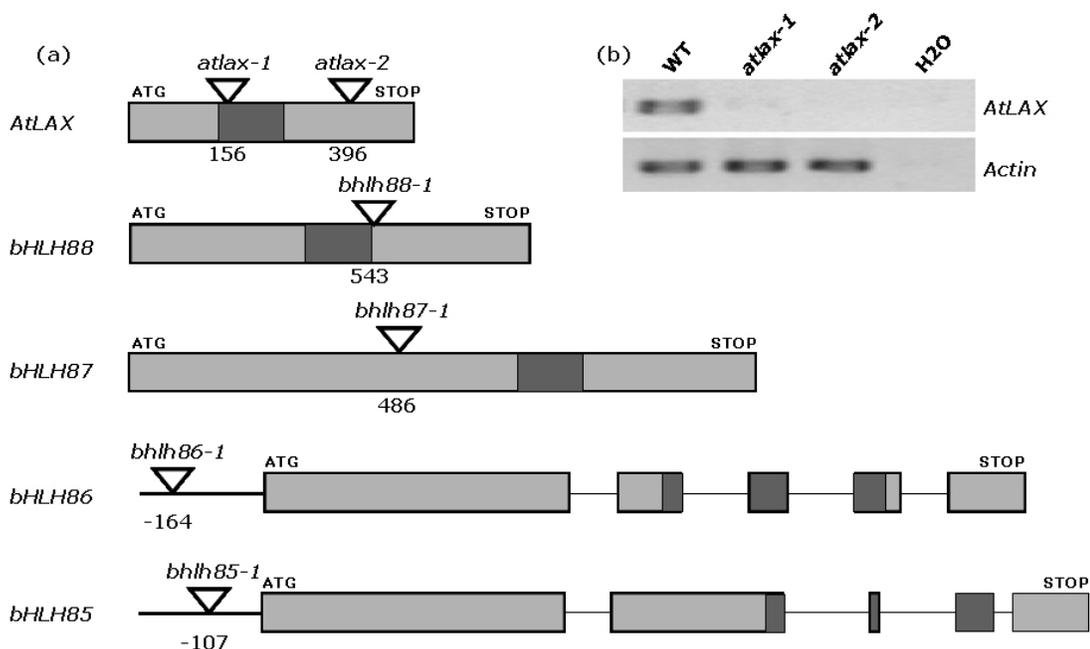
Fig. 3.2.4-1 Five bHLH genes with T-DNA insertions and their transcripts in the corresponding mutant alleles. (a) Schematic structure of bHLH genes showing the relative positions of T-DNA insertions. Numbers indicate the distance of the T-DNA insertion from the putative start of the open reading frame. Exons are presented by gray boxes. Introns and 5' UTR are indicated by black lines. The bHLH domains are indicated in dark gray. (b) RT-PCR shows that *atlax-1* and *atlax-2 alleles* contain RNA null mutations. The tissue were harvested from the floral buds of plants homozygous for *atlax-1* and *atlax-2.* Amplification of *AtLAX* from the wt floral buds was used as a PCR control.

The phenotype of plants carrying each mutant allele was investigated by growing plants under long- and short-day conditions given that the branching phenotypes of *rax* mutants are dependent on the day-length conditions (Müller et al., 2006). However, all plants homozygous for the mutations in *bHLH85, bHLH86, bHLH87 and bHLH88* had wild-type morphology under these growth conditions.

3.2.4.2   Analysis of *atlax* knockout mutants

Although the growth habit of *atlax-1* and *atlax-2* did not show an obvious difference from wild type, a weak branching defect could be observed in *atlax* by stereomicroscopic analysis of leaf axils (Fig. 3.2.4-2). In comparison with the Col wild type in which the lateral buds frequently failed to form during the early vegetative phase, *atlax* plants showed a more severe reduction in the number of axillary buds originating from the axils

of old rosette leaves. In *atlax-1* mutants, grown for 28 days in short photoperiods and then shifted to long days to induce flowering, lateral buds developed at a lower percentage than wild type at each axil of the oldest 10 rosette leaves (Fig. 3.2.4-2b). When grown to maturity in short photoperiods, empty leaf axils of *atlax-1* were found up to the 21st rosette leaf, whereas Col-wt plants showed a reduction in axillary bud formation only in the oldest 9 rosette leaves (Fig. 3.2.4-2c). During later vegetative stage and the reproductive stage, axillary bud formation in *atlax* mutants was not impaired. In addition, this weak branching defect of *atlax* vanished when plants were grown to maturity in long photoperiods.
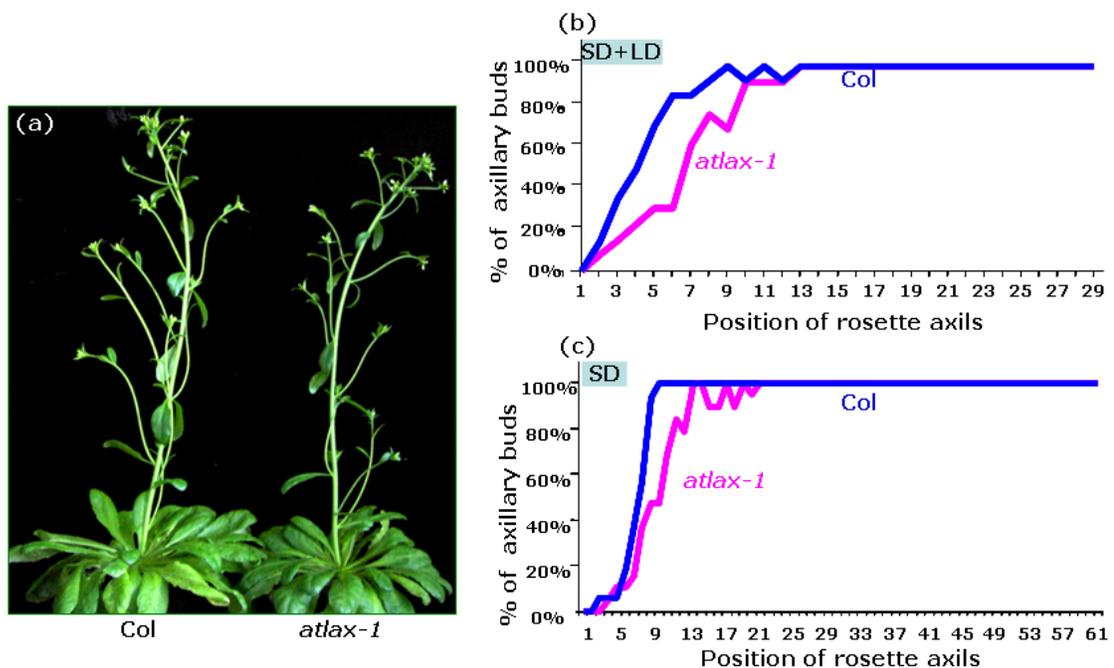
Fig. 3.2.4-2. Growth habit and the branching pattern of *atlax-1* mutants. (a) The *atlax-1* mutant did not show a different growth habit from the Col wt when grown in short photoperiods for 76 days. (b) and (c) Graphic representation of axillary bud formation of *atlax-1* mutants in comparison with Col wild-type plants. Leaf axils of plants were examined under a binocular microscope. Genotypes are indicated next to the graphs. The percent values of the Y axis indicate the proportion of analyzed plants that show a bud in a specific leaf axil ($n_{atlax-1}$=13, n_{Col}=14 in (b), and $n_{atlax-1}$=19, n_{Col}=16 in (c)). Position 1 corresponds to the oldest rosette leaf axil and position 29 or 61 corresponds to the uppermost rosette leaf axil in (b) and (c), respectively.

To unravel any possible functional redundancy, combinations of the different *bhlh* mutants were analyzed for their branching patterns. To this end, double *atlax-1 bhlh87-1* and triple *atlax-1 bhlh87-1 bhlh88-1* mutants did not show any obvious enhancement of the branching defect of *atlax-1* and their growth habits also did not deviate from wild type

plants. Considering the normal transcript level of *bHLH85* and *bHLH86* in their corresponding T-DNA insertion lines and the absence of visible defect in both *bhlh85-1* and *bhlh86-1* plants, they were excluded from the further double and triple mutant analysis.

3.2.4.3   Analysis of plants expressing the dominant repressor *AtLAXSRDX*

The weak branching defect of *atlax-1* and non-enhancement of this defect by two additional *bhlh* mutations indicate the presence of a putative functional redundancy from the remaining homologs. To prove this hypothesis, a chimeric repressor *AtLAX* was created by fusing with the SRDX domain (*AtLAXSRDX*) was created. The SRDX domain, derived from the EAR motif of *Arabidopsis SUPERMAN,* is a repression domain of 12 amino acids (LDLDLELRLGFA) length (Hiratsu et al., 2003; Hiratsu et al., 2004). A transcription factor fused with this domain has been shown to act as a transcriptional repressor and dominantly suppresses the expression of target gene(s), even in the presence of redundant transcription factors (Fig. 3.2.4-3a). In this study, a chimeric *AtLAXSRDX* repressor driven by the CaMV 35S promoter (*35S:AtLAXSRDX*) was introduced into Col wild type (Fig. 3.2.4-3b). After BASTA selection, a PCR using primers specific for the expression cassette was performed to ensure integration of the insertion into the Arabidopsis genome. Transgenic lines carrying single locus insertion were screened by BASTA resistance segregation in the T2 generation. To screen for putative single copy transgenic lines, families showing a 3:1 segregation were analyzed using primers derived from the left border (LB) and right border (RB) of T-DNA. Both LB and RB specific primers
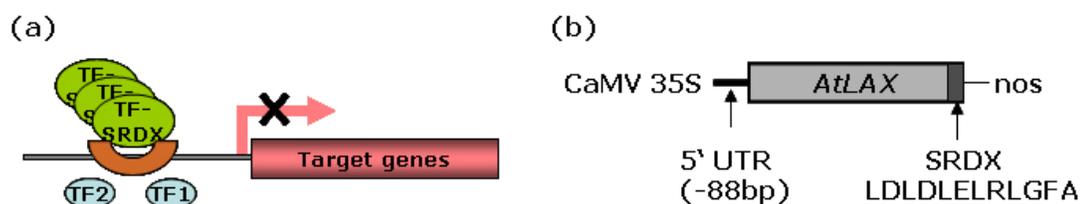
Fig. 3.2.4-3 Schematic drawing of AtLAXSRDX mediated suppression of target gene. (a) Schematic presentation showing suppression of the target gene(s) of a TF by the chimeric repressor *TFSRDX*, in the presence of its homologs TF1, TF2, etc. (b) Schematic representation of the *35S:AtLAXSRDX* transgene. CaMV 35S, 5' UTR (-88bp), SRDX, and nos represent the CaMV 35S promoter, the 5' UTR region of AtLAX (88bp before the ATG), the repression SRDX domain with 12AA, and the terminator sequence of the NOS gene, respectively.

are outward of the T-DNA. Since multiple T-DNAs frequently insert next to each other in one locus, the failure to amplify any PCR product in combination with a 3:1 segregation for resistance indicates one T-DNA copy in this locus.

The majority of transgenic plants (n=135) appeared wild type. However, ~33% of the plants showed a dwarf phenotype with varying severity (Fig. 3.2.4-4a). Plants with a moderate dwarf phenotype (semi-dwarf plants) were smaller as a result of slower growth than those of wild-type-like transgenic plants. These semi-dwarf lines bolted later than wild type and developed smaller leaves with normal petioles (Fig. 3.2.4-4c). In contrast, the severe dwarf plants displayed a stunted growth (Fig. 3.2.4-4b). They developed small and round leaves with very short petioles. The leaves were shrivelled so that the size of leaves was dramatically reduced (Fig. 3.2.4-4c). Most of these severe dwarfs did not bolt even after three months in short photoperiods, compared to the wild-type-like lines, which bolted in two months. The fertility of the dwarf plants was reduced although the morphologies of inflorescences and flowers were not altered (Fig. 3.2.4-4b, d, and e). RT-PCR analysis demonstrated that the severity of the dwarf phenotype was correlated with the transcript level of the transgene (Fig. 3.2.4-4f), indicating that high levels of the chimeric repressor are the reason for the dwarf phenotype.

Interestingly, the dwarf transgenic plants demonstrated a branching defect similar to that of *atlax* knockout mutants (Fig. 3.2.4-4g). In comparison with Col wt plants, These plants were characterized by a reduced number of side shoots in the axils of old rosette leaves, Dwarf plants carrying the 35S:*AtLAXSRDX* construct developed axillary buds at a much lower frequency in the axils of the first 15 to 17 rosette leaves, whereas wild type plants had empty axils up to the 10th rosette leaf. All the analyzed dwarf lines showed a similar reduction in axillary bud formation (Fig. 3.2.4-4g). Thus, the *AtLAXSRDX*-carrying plants mimic the *atlax* knockout mutants with respect to their branching pattern, suggesting that the *AtLAXSRDX* repressor protein was functional and the activity of *AtLAX* target gene(s) required for lateral meristem formation was suppressed in these transgenic plants. However, the *AtLAXSRDX*-expressing plants did not show an obviously stronger
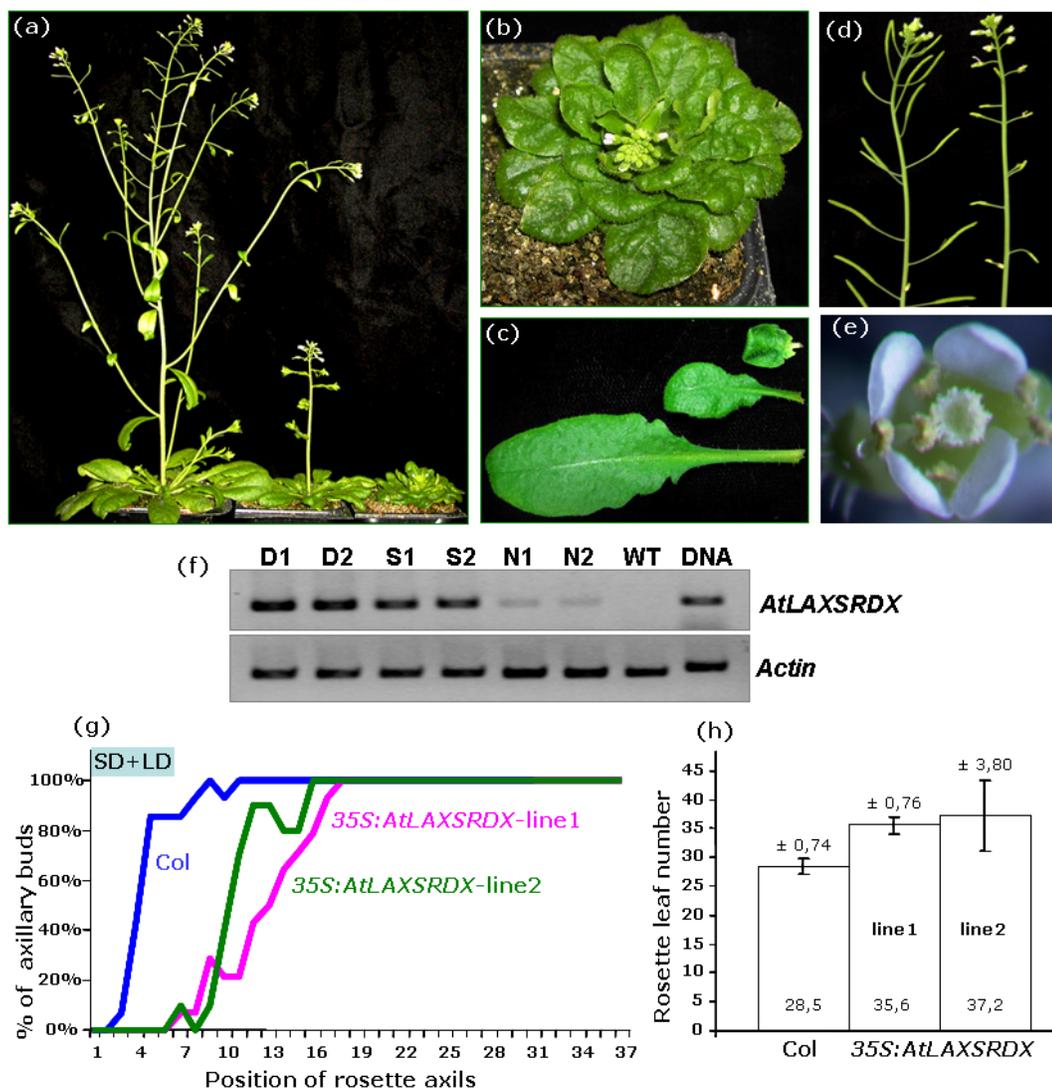
Fig. **3.2.4-4 Phenotypic analysis of transgenic plants carrying *35S:AtLAXSRDX*** (a) Three *35S:AtLAXSRDX*-carrying plants with wild-type-like, semidwarf, and dwarf phenotypes. Plants were grown for 28d in SD and then shifted to LD for 33d to induce flowering. (b) Close-up of the dwarf plant in (a) showing stunted growth and inflorescence with short stem. (c) Mature rosette leaves of transgenic plants in (a), showing contracted leaves in semidwarf and dwarf lines and very short petiole of rosette leaf of a dwarf plant. (d) and (e) Inflorescences of a Col-wt (left in b) and a dwarf plant (right in b) and a flower of dwarf plant (e). The dwarf plants have inflorescences with severely reduced fertility although the floral organs look like wild type (e). (f) Comparison of the transcript levels of transgene *AtLAXSRDX* in two independent lines which look like wild type (N1, N2), two semidwarf lines (S1, S2), and two dwarf (D1, D2) lines. The severity of dwarf phenotype is correlated with the transcript level of the transgene. (g) Graphic representation of axillary bud formation in two independent *35S:AtLAXSRDX*-harbouring dwarf lines and Col-wt plants grown for 28d in SD conditions and subsequently for 33 days in LD conditions (n=14 and 10 for two dwarf lines, respectively; n=14 for Col). Position 1 and 37 correspond to the oldest and the youngest rosette leaves, respectively. (h) Comparison of total rosette leaf number of two dwarf lines with the Col-wt plants analyzed in (g), showing that the dwarf plants are late flowering. Genotypes are indicated below the corresponding bars. The average rosette leaf numbers for each genotype are shown within the bars. The error bars and the accompanying numbers show the 95% confidence intervals.

branching defect than the *atlax* knockout mutants, indicating that *AtLAX* has no functionally redundant homologs. In addition, the dwarf plants were late flowering, leading to the formation of a significantly higher number of rosette leaves than wild type plants (Fig. 3.2.4-4h). Two independent dwarf lines formed 35.6 ± 0.76 (n=14) and 37.2 ± 3.80 (n=10) rosette leaves, respectively, whereas the Col wt developed on average 28.5± 0.76 (n=14) leaves.

3.2.4.4   Analysis of plants overexpressing *AtLAX*

As an alternative test for the function of *AtLAX*, the open reading frame of this gene was expressed under the control of the cauliflower mosaic virus 35S promoter (*35S:AtLAX-StrepII*) in the Col background. Among ~200 transgenic plants, about 50% showed a dwarf phenotype and displayed a loss of apical dominance (Fig. 3.2.4-5a). During the vegetative stage, the dwarf plants developed dark green small rosette leaves with downward-curling blades. This abnormal leaf phenotype was visible 10 days after germination. In comparison with the Col-wt, the dwarf plants produced small flowers with shorter sepals, petals, and stamens, which might be athe cause for the severely reduced fertility (Fig. 3.2.4-5b, c). RT-PCR analysis demonstrated that the *AtLAX-StrepII* transcripts accumulated to high levels in the leaves of these dwarf transgenic plants (Fig. 3.2.4-5d).

Most interestingly, all *AtLAX*-overexpressing dwarf plants produced accessory side shoots during both vegetative and reproductive stages of development, although there was a high variability in the frequency of rosette accessory paraclades. As revealed by SEM image of rosette leaf axils, accessory shoots were formed between the primary side shoot and the subtending rosette leaf (Fig. 3.2.4-5e). Stereomicroscopic analysis of a number of *35S:AtLAX-StrepII*-harbouring plants demonstrated that the younger rosette axils had a higher tendency to develop accessory shoots. In addition, most of the cauline leaf axils of the dwarf plants formed accessory side-shoots (Fig. 3.2.4-5f, g, h). Accessory bud formation was also observed in cauline leaf axils of secondary shoots. In many cases, there were two accessory buds/shoots developing in one cauline leaf axil (Fig. 3.2.4-5g,

arrow). In contrast, only a single axillary bud/shoot was found in all leaf axils of control plants. These findings suggest that AtLAX promotes the formation of lateral meristems.
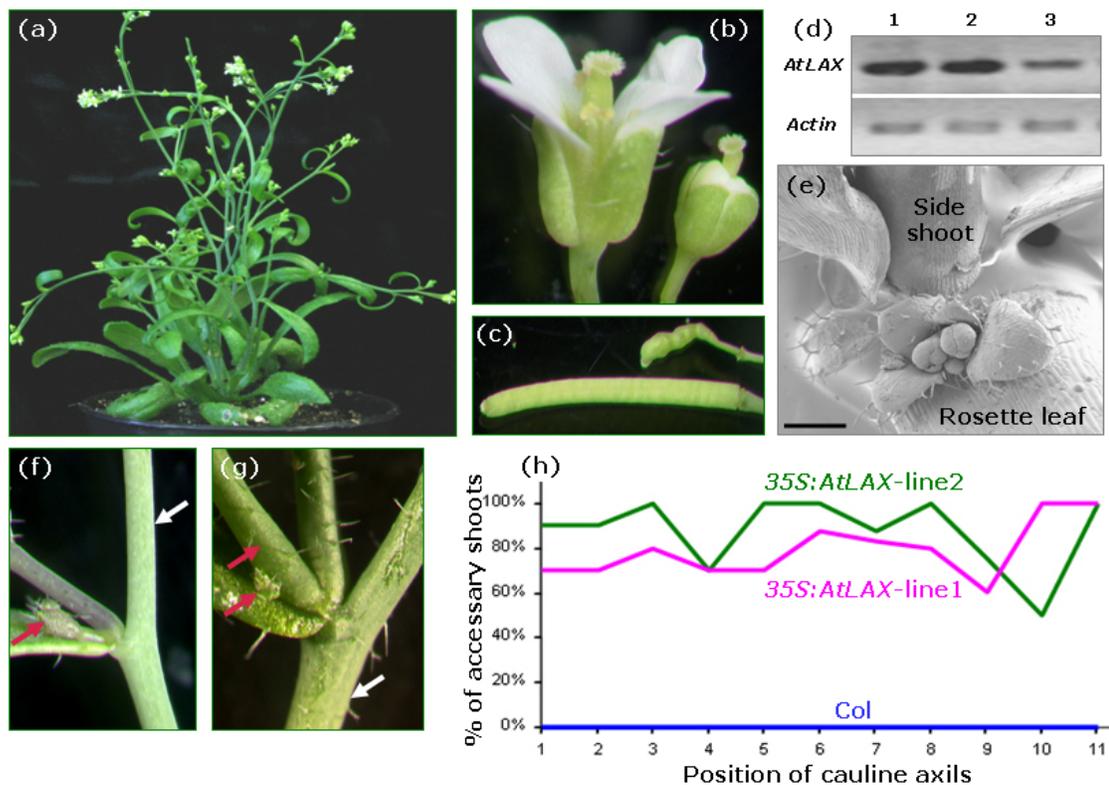
Fig. 3.2.4-5 Phenotype of *AtLAX*-overexpressing plants. (a) A *35S:AtLAX-StrepII* plant grown for 50d in LD showing a stunted growth and a loss of apical dominance. (b) Flowers of *35S:AtLAX-StrepII* plants (right) are reduced in size and have shorter sepals, petals, and stamens, in comparison with Col wild type (left). (c) Siliques of *35S:AtLAX-StrepII* plants (top) were underdeveloped and have a crinkled surface compared to a wild-type silique (bottom). (d) RT-PCR analysis showed that the transcripts of *AtLAX-StrepII* accumulated to higher amounts in the inflorescence (lane 1) and cauline leaves (lane 2) of a dwarf plant, in comparison to the level of endogenous *AtLAX* transcript in the infloresence of the Col wt (lane 3). (e) A SEM micrograph shows an accessory shoot forming between a side shoot and the subtending rosette leaf in a *35S:AtLAX-StrepII* plant. (f) and (g) Close-up of *35S:AtLAX-StrepII* nodes showing accessory shoots (red arrows) which developed in the axils of cauline leaves. The white arrows point out the primary shoots. Two accessory side-shoots frequently developed from a single cauline leaf axil (g). (h) Graphic representation of accessory side-shoot formation in cauline leaf axils of two independent *35S:AtLAX-StrepII* and Col plants (n=10). The plants were grown for 46 days in short photoperiods and subsequently for 24d under long day conditions.

3.2.5 Interaction between *AtLAX* and *RAX1*

From studies on several developmental processes it is well known that MYB proteins interact with bHLH proteins to perform their functions (Ramsay and Glover, 2005). A classical example is that *GLABRA3* (*GL3*) and *GLABRA1 (GL1)*, encoding bHLH and

R2R3-type MYB proteins, respectively, interact with each other to promote leaf trichome formation in *Arabidopsis* (Payne et al., 2000; Sawa, 2002; Zhang et al., 2003). TTG1, a WD40 protein, is also involved in this interaction to form a MYB-bHLH-WD40 complex regulating trichome cell fate (Larkin et al., 2003; Schiefelbein, 2003; Zhong and Ye, 2004). Another well-known example is the interaction of bHLH and MYB genes in the process of root hair patterning (Bernhardt et al., 2003; Esch et al., 2003; Larkin et al., 2003; Schiefelbein, 2003). The single MYB-type transcription factor, *CAPRICE /CPC*, is proposed to interact with GL3 and/or EGL3 in differentiating hair cells to trigger hair cell fate (Wada et al., 2002). WEREWOLF (WER), a R2R3 MYB protein, has also been shown to interact with GL3 and EGL3 by the yeast two-hybrid assay (Bernhardt et al., 2003). The cooperative action of R2R3-type MYB and bHLH proteins has been extensively studied in the process of anthocyanin biosynthesis (Grotewold et al., 2000; Morita et al., 2006). In maize, the transcriptional activation of anthocyanin biosynthesis genes by the R2R3 MYB proteins ZmC1 and ZmPl requires the involvement of bHLH proteins from the R/B gene family (Grotewold et al., 2000). A direct interaction between the MYB domain of ZmC1 and the N-terminal domain of the bHLH protein ZmB has been described (Goff et al., 1992).

Here, the genetic interaction between *AtLAX* and *RAX1* was tested to uncover their possible correlation in the process of axillary meristem development. *RAX1* is a R2R3-type MYB transcription factor and has been shown to regulate axillary meristem initiation (Keller et al., 2006; Müller et al., 2006).

3.2.5.1 Analysis of *atlax-1 rax1-3* double mutants

To explore a possible interaction between *AtLAX* and *RAX1*, a double mutant was generated by combining two loss-of-function mutations in these two genes, *atlax-1* and *rax1-3*. Overall, two aspects of the *rax1-3* mutant phenotype were modified by the *atlax* mutation, indicating their interconnection in the process of shoot development.

3.2.5.1.1   Analysis of branching pattern of *atlax-1 rax1-3* double mutant

The *rax1-3* mutant is characterized by a strong reduction in the number of axillary buds originating from the older rosette leaf axils, whereas a very high proportion of the younger rosette leaf axils produce axillary buds, leading to an acropetal gradient of axillary bud formation (Müller et al., 2006). Interestingly, a combination of the *rax1-3* and *atlax-1* alleles resulted in a strong enhancement of the branching defect observed in *rax1-3* plants (Fig. 3.2.5-1). The double mutants failed to form axillary buds in almost all of the rosette leaf axils during the early and middle vegetative phase, and lateral bud formation during the late vegetative stage of development was also reduced. When grown in short days for 4 weeks and then shifted to long days to induce flowering, *atlax-1 rax1-3* did not produce any axillary buds in the oldest twenty rosette leaf axils, whereas in *rax1-3* single mutants side shoots started to develop from the 6th–oldest rosette leaf axil onwards (Fig. 3.2.5-1b). As the severity of the branching defect of *rax1-3* is dependent on day-length condition, the pattern of axillary bud formation in *atlax-1 rax1-3* double mutants was also investigated by growing plants to maturity under short day conditions. A high proportion of the late rosette leaf axils of *rax1-3* mutants produced lateral buds while at the same developmental stage axillary bud formation of double mutants was still strongly reduced (Fig. 3.2.5-1c). For instance, *rax1-3* mutants developed 50-100% lateral buds in a zone between 27 to 51 rosette leaves, whereas only up to 35% leaf axils of *atlax-1 rax1-3* supported axillary bud formation. Furthermore, *atlax-1* plants showed the same enhancement on the branching defect of *rax1-3* when grown to maturity in long day conditions (Fig. 3.2.5-1d). During the reproductive stage, the formation of side shoots in cauline leaf axils of *atlax-1 rax1-3* double mutants did not deviate from the *rax1-3* single mutants, or from the Col wild type. Thus, *atlax-1* enhanced the defect of axillary bud formation of *rax1-3* during the vegetative phase.
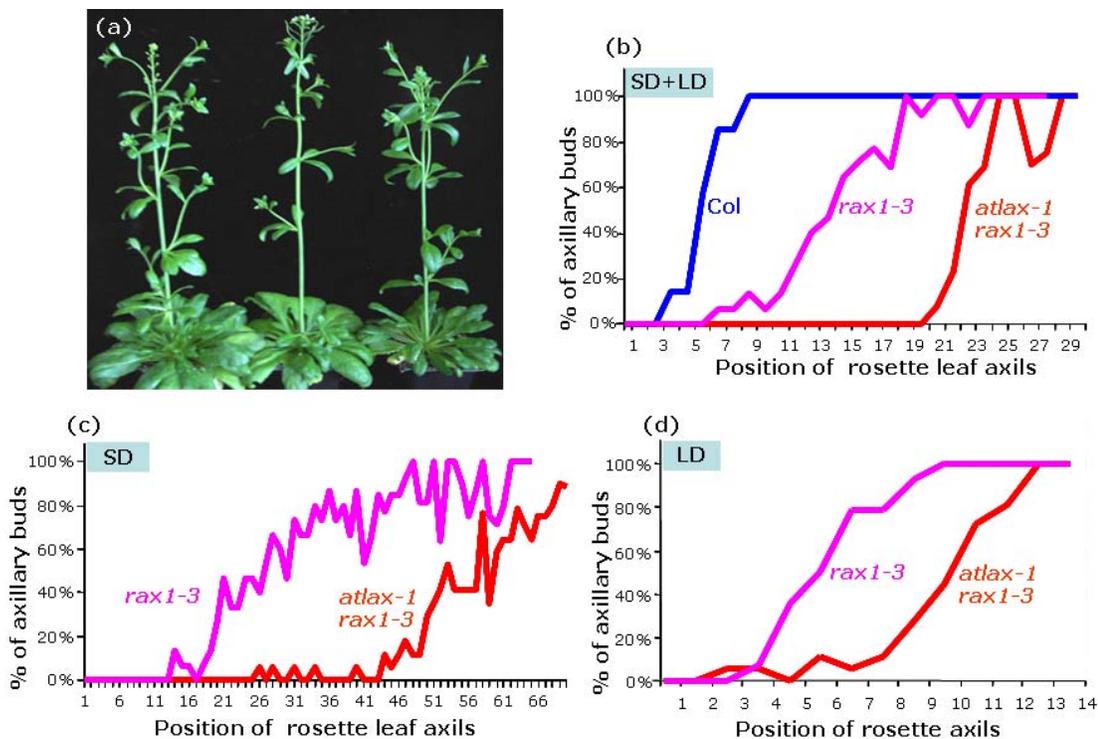
Fig. 3.2.5-1 Phenotypic analysis of the *atlax1 rax1-3* double mutants (a) Growth habit of a Col wild-type (left), an *rax1-3* mutant (middle), and an *atlax-1 rax1-3* double mutant (right) grown under short day conditions for 76d. (b-d) Graphic representations of axillary bud formation in *atlax-1 rax1-3* double mutant plants in comparison with *rax1-3* single mutant and Col wild-type plants (only in b). Plants were either grown for 28 days in short photoperiods and subsequently for 29 days in long photoperiods to induce flowering (b), or grown to maturity in short day conditions (c), or grown under long day conditions immediately after sowing (d). Genotypes are indicated next to the graphs. Position 1 corresponds to the oldest rosette leaf, and towards the right are positions of progressively younger rosette leaf axils. The percent values of the Y axes indicate the proportion of plants analyzed that formed an axillary bud in a specific position along the shoot axis (n=7, 15, and 13 for Col, *rax1-3*, and *atlax-1 rax1-3*, respectively, in (b); n=15 and 17 for *rax1-3* and *atlax-1 rax1-3*, respectively, in (c); n=14 and 18 for *rax1-3* and *atlax-1 rax1-3*, respectively, in (d)). Phenotype analysis of *atlax-1 rax1-3* double mutants was repeated at least once, except when plants were grown to maturity in long days since sowing.

The tertiary buds/shoots arise from the leaf axils of a secondary shoot. In *rax1-3* single mutants, tertiary buds formed in up to 82% of the leaf axils of each secondary shoot, whereas *atlax-1* had nearly a 100% ability to support tertiary shoot formation (Fig. 3.2.5-2b). In contrast, the formation of tertiary shoots in *atlax-1 rax1-3* double mutants was strongly reduced, with only up to 25% of the leaf axils of each secondary shoot developing axillary buds (Fig. 3.2.5-2). Thus, *atlax-1* also enhanced the branching defect of *rax1-3* during late reproductive phase of development.
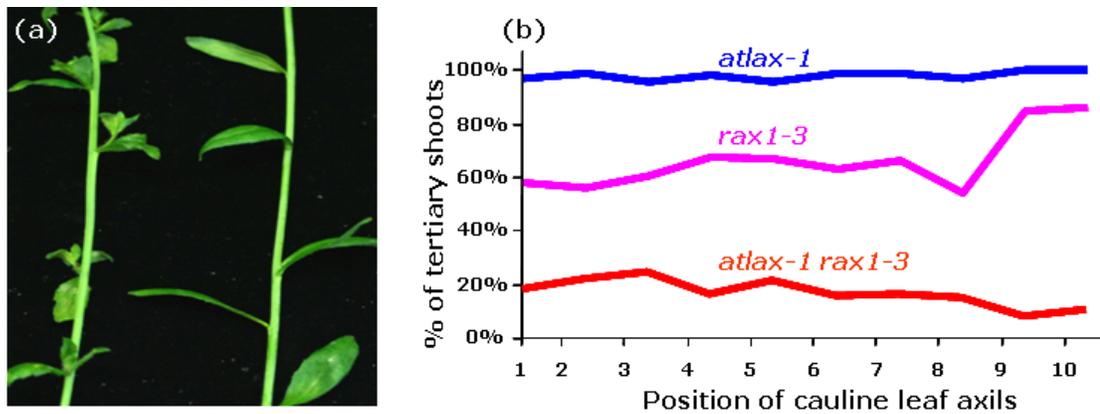
Fig. 3.2.5-2 The pattern of tertiary shoot formation in *atlax-1 rax1-3*. (a) Close-up of secondary shoots of an *atlax-1 rax1-3* double mutant (right) and a *rax1-3* single mutant. *atlax-1 rax1-3* double mutants had barren leaf axils in almost all the secondary shoots. (b) Graphic representation of tertiary shoot formation in *atlax-1 rax1-3* double mutants in comparison with *atlax-1* and *rax1-3* single mutant plants. Genotypes are indicated next to the graphs. Position 1 corresponds to the oldest cauline leaf axil, and position 10 corresponds to the youngest cauline leaf axil. The percent values of the Y axes indicate the proportion of leaf axils of secondary shoots that formed an axillary bud. The numbers of X axes represent the secondary shoots formed at the specific position of cauline leaf axils (n=11, 9, and 11 for *atlax-1, rax1-3*, and *atlax-1 rax1-3,* respectively). The experiment was repeated two times.

3.2.5.1.2   Analysis of flowering time of *atlax-1 rax1-3* double mutant

A loss of function mutation in *RAX1* causes not only a reduction in axillary meristem formation, but also early flowering, which is strongly enhanced in mutant combinations with its homologs (Keller et al., 2006; Müller et al., 2006). Flowering time is usually measured by the total number of rosette leaves produced by a plant or the number of days to flowering, both these characteristics being very tightly correlated (Koornneef et al., 1991). The precise number of rosette leaves developed until bolting was recorded by marking each newly formed leaf to avoid missing the oldest rotten rosette leaves. The days to flowering was obtained when the first flower opened. The seeds of all genotypes were harvested at a similar developmental stage and were imbibed in water at 4°C for 3 days to get an even germination. Under short day conditions, *rax1-3* plants developed an average of 33.6 ± 0.53 (n=18) rosette leaves, whereas *atlax-1 rax1-3* double mutants developed 49.4 ± 0.92 (n=24) rosette leaves, which was similar to *atlax-1* (50.3 ± 1.07, n=15) itself and the Col wild type control (50.0 ± 1.35, n=15) (Fig. 3.2.5-3a). Consistent with these observations, *atlax-1 rax1-3* double mutants flowered later than *rax1-3* plants

with an average of 51.2 ± 1.20 and 42.3 ± 0.52 days to the first open flower, respectively (Fig. 3.2.5-3b). Flowering time in atlax-1 was comparable to that in wt plants, with 55 ± 0.81 and 55.1 ± 1.14 days, respectively (Fig. 3.2.5-3b). Thus, *atlax-1* suppressed the early flowering phenotype of *rax1-3*.
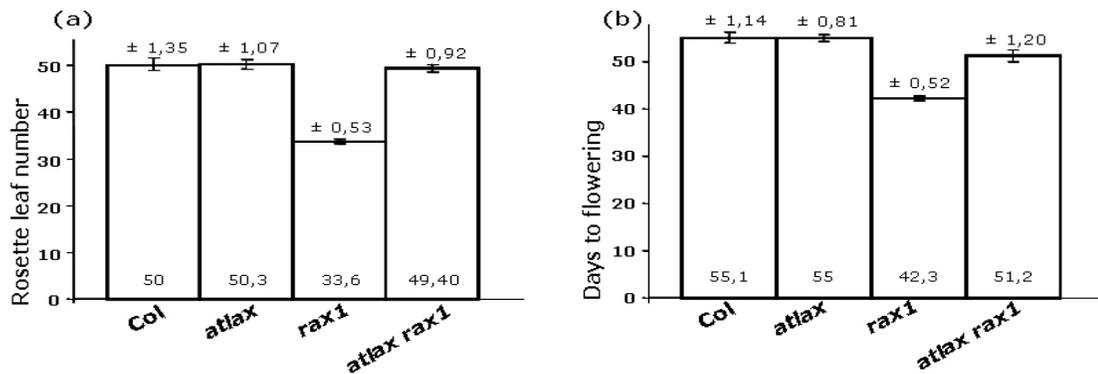
Fig. **3.2.5-3   Flowering time of *atlax-1 rax1-3* double mutants**. (a) and (b) Comparison of rosette leaf numbers (a) and the days to flowering (b) between *atlax-1 rax1-3* double mutants and control plants grown to maturity in short days. Genotypes are indicated below the corresponding bars. The average rosette leaf number and average days to flowering for each genotype are shown within the bars. The error bars and the neighboring numbers show the 95% confidence intervals (n=15, 15, 18, and 24 for Col, *atlax-1, rax1-3,* and *atlax-1 rax1-3*, respectively). The experiment was repeated two times.

3.2.5.2   Comparison of transcript accumulation of *AtLAX and RAX1* in the shoot apex

RAX1 transcripts accumulate at the boundary region between the SAM and leaf primordia from P0 to P10/P11, including always the L3 layer and frequently also the L1 and L2 layers of the SAM (Müller et al., 2006). In transverse sections, the *RAX1* expression is seen in a circular domain in the leaf axils, extending approximately 3-5 cell layers in the adaxial–abaxial and the tangential dimensions. RNA in situ hybridization experiments revealed that the *AtLAX* mRNA also specifically accumulated in the center of the boundary region between the SAM and leaf primordia, in a domain showing an almost complete overlap with that of *RAX1* (Fig. 3.2.5-4). Furthermore, the expression patterns of these two transcription factors were also very similar in the phase of reproductive development (Fig. 3.2.3d, e, f; Müller et al., 2006).

71
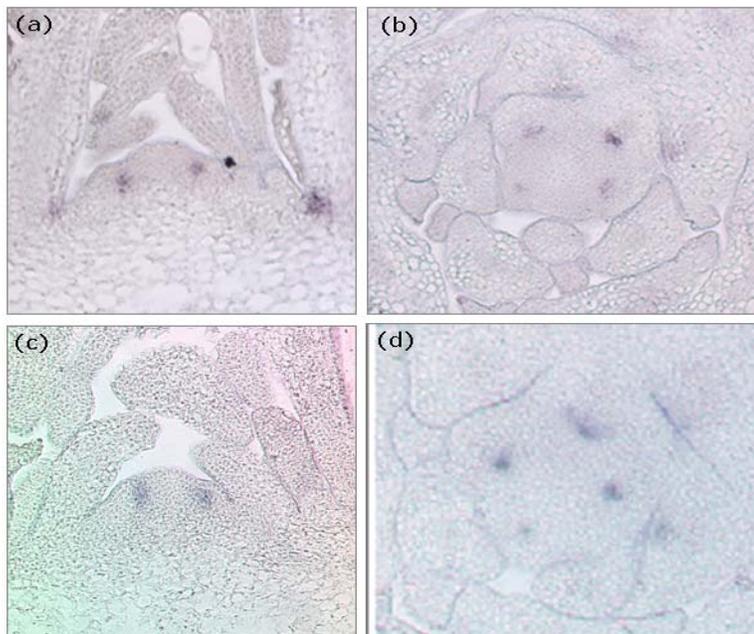
Fig. 3.2.5-4 Co-localization of *AtLAX* and *RAX1* transcripts in the center of boundary between the SAM and leaf primordia. (a) and (b) Longitudinal and transverse sections through shoot apices of 31d-old Col-wt plants grown under short day conditions were hybridyzed with an *AtLAX* antisense probe. (c) and (d) Longitudinal and transverse sections through shoot apices of 28d-old Col-wt plants grown under short day conditions were hybridyzed with a *RAX1* antisense probe (Müller D., 2006).

3.2.5.3   The interaction of AtLAX and RAX1 proteins

Inspired by the well-known model for interaction between bHLH and MYB proteins, as well as the co-localization of *AtLAX* and *RAX1* mRNAs, a possible proteins interaction between AtLAX and RAX1 was investigated. At first a yeast two-hybrid system was used. However, western blot analysis did not show the expression of AD-AtLAX in transformed yeast cells, whereas BD-AtLAX was expressed but demonstrated autoactivation in the yeast assay. Therefore, a GST-pull down assay was performed to test for an interaction between His-AtLAX and GST-RAX1 fusion proteins. Due to the failure to purify His-AtLAX, the supernatant of His-AtLAX containing cell suspension after sonication was subjected to a pull down assay. To this end, GST-RAX1 protein was found to specifically bind to His-AtLAX (Fig. 3.2.5-5). Similar results were obtained in pull-down assays using GST-tagged AtLAX and His-tagged RAX1. GST-AtLAX was able to pull His-RAX1 down whereas GST alone was not (data not shown). These data demonstrate the interaction of AtLAX and RAX1 proteins.

Fig. 3.2.5-5   Interaction between AtLAX and RAX1 proteins. In a pull-down assay, His-AtLAX supernatant was incubated with GST and GST-RAX1 proteins. Western blots probed with anti-His antibody confirmed that His-AtLAX was not pulled down by GST alone (lane 2), but was present in the elution of a GST-RAX1 pull-down assay (lane 3), (lane1, 10% of His-AtLAX supernatant as input).
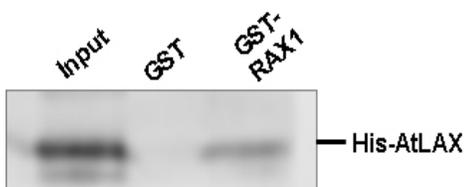
3.2.5.4   Analysis of the expression patterns of *RAX1* and *AtLAX* in *atlax-1* and *rax1-3* mutants

To further investigate the relationship between *AtLAX* and *RAX1*, the effect of *atlax* mutation on the transcript accumulation of *RAX1* was analyzed. In the *atlax-1* mutant, the mRNA of *RAX1* was found in a narrow domain in the youngest leaf primordium, extending across the L1, L2 and L3 layers of the SAM (Fig. 3.2.5-6b), comparable to that observed in wild type (Fig. 3.2.5-6b). *RAX1* transcripts were also detected in the axils of leaf primordia of *atlax-1* mutants. Thus, the cellular distribution of the *RAX1* transcript in *atlax-1* apices remains unaltered.

However, examination of *AtLAX* transcript accumulation in the *rax1-3* single and *rax1-3 rax2-1 rax3-1* triple mutant backgrounds revealed a clear downregulation of *AtLAX* during the vegetative stage. All in situ hybridizations for *AtLAX* were controlled by hybridizing comparable sections of wt and *rax* mutant apices side by side on the same slide. Apices were harvested from the plants grown for 25 d or 31 d in short photoperiods. In total twenty *rax* (*rax1-3* and *rax triple*) mutant apices were subjected to six independent in situ hybridizations. Whereas strong signals of *AtLAX* were seen on the sections from Col-wt apices (Fig. 3.2.5-6c), transcripts of *AtLAX* were rarely detectable on *rax* mutant apices (Fig. 3.2.5-6d-f). Only on three sections from two apices of *rax1-3 rax2-1 rax3-1* triple mutants, a very faint signal was found in the leaf axils (arrows, Fig. 3.2.5-6e, f). Since the activity of the axillary meristem marker *LAS* is shown to be unaltered in *rax1-3* mutants (Müller et al., 2006), a similar in situ hybridization experiment was performed for *LAS* using the same batch of *rax1-3* apices as used for *AtLAX* hybridization. *LAS* mRNA was
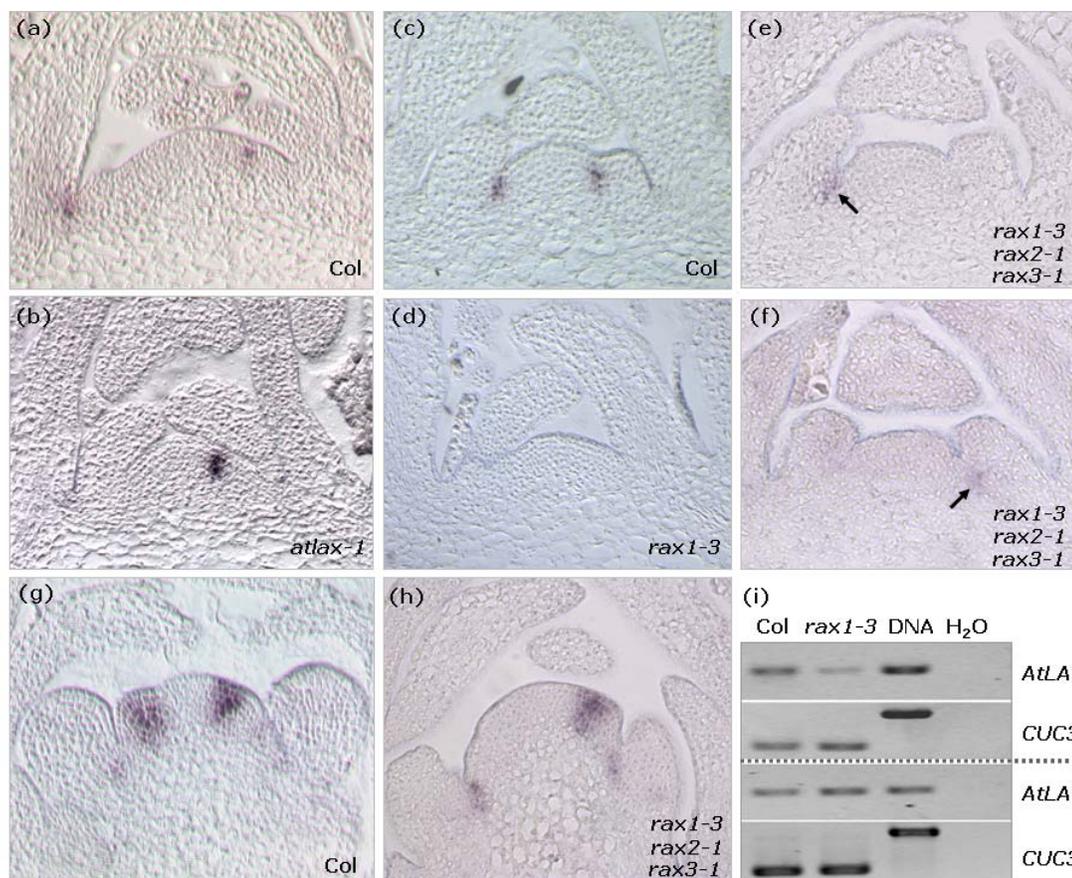
Fig. 3.2.5-6 Expression patterns of *RAX1* and *AtLAX* in *atlax-1* and *rax1-3* mutants, respectively. (a) and (b) Longitudinal sections through vegetative shoot apices of a 31d-old Col-wt plant (a) and an *atlax-1* mutant plant (b) grown under short day conditions were hybridized with a *RAX1* antisense probe. (c to f) Longitudinal sections through 28d-old shoot apices of a Col-wt plant (c) and *rax1-3* mutants (d, e, and f) grown under short day conditions were hybridized with an *AtLAX* antisense probe. (e) and (f) are two out of three sections in total from two different apices showing a very faint signal for *AtLAX* (arrow). In all other section from *rax1-3* vegetative shoot apices, *AtLAX* transcripts were not detectable, as shown in (d). (g) and (h) Longitudinal sections through reproductive shoot apices of a Col-wt plant and a *rax1-3* mutant were hybridized with an *AtLAX* antisense probe. The plants were grown for 28 days under short day conditions and then shifted to long days for 6 days. The transcript accumulation of *AtLAX* was not impaired in *rax1-3*. (i) RT-PCR analysis shows reduced mRNA levels of *AtLAX* in vegetative shoot tips of *rax1-3* (upper panel) and normal transcript level in floral buds of *rax1-3* mutants (lower panel), in comparison with Col wt. To harvest vegetative shoot tips, plants were grown for 28 days under short day conditions. To harvest floral buds, plants were grown for 28 days under short day conditions and then shifted into long days to induce flowering. *CUC3* transcripts were amplified as a control for a gene specifically expressed in axillary regions. Col-genomic DNA and H_2O were included as PCR controls. RT-PCR was repeated two times using different biological samples.

detected at the leaf axils of *rax1-3* (data not shown), showing that the axillary cell tissues were intact in this batch of *rax1-3* mutants. Conversely, during the reproductive phase of development, *AtLAX* transcript accumulated in the floral primordia and at the adaxial base

of floral primordia of triple *rax* mutants, in the same way as observed in Col wild type (Fig. 3.2.5-6g, h). RT-PCR analysis was performed to confirm the effect of the *rax1-3* mutation on *AtLAX* transcript accumulation during the vegetative developmental stage (Fig. 3.2.5-6i). Based on the result that *CUC3* transcript accumulation is unaltered in the *rax1* knockout mutant (Keller et al., 2006), *CUC3* mRNA was amplified as a control for a gene specifically expressed in axillary regions. *rax1-3* shoot tips contained less *AtLAX* transcripts than those of Col-wt plants (Fig. 3.2.5-6i). By contrast, the levels of *AtLAX* mRNAs in floral buds were indistinguishable between *rax1-3* and wt plants (Fig. 3.2.5-6i). Amplification of *RAX1* was also performed and showed that *RAX1* mRNA was absent in the tissues of *rax1-3* mutants used. These findings demonstrated that *AtLAX* transcript accumulation was impaired by loss of *rax1-3* only during the vegetative stage, but not during the reproductive phase of development.

3.2.6 Genetic interaction of *AtLAX*, *RAX1* and *LAS*

The phenotype of the *las* mutant and the specific accumulation of *LAS* transcripts in leaf axils have established it as a primary regulator of axillary meristem development (Greb *et al.,* 2003; Introduction 1.2.1.2). The lack of axillary buds during the vegetative phase of development in *las-4* is the result of the failure of leaf axil cells to retain their meristematic competence. In accordance with the mutant phenotype, *LAS* displays a band-shaped expression domain encompassing almost the whole boundary region between the SAM and the leaf primordia (Greb *et al.,* 2003). Genetic analysis has indicated that *LAS* and *RAX1* may be members of two independent pathways controlling axillary meristem formation in *Arabidopsis*. This hypothesis is based on the additive effect of *rax1-3* on the branching defect of *las-4* (Müller et al. 2006). In contrast to *las-4* mutants, in which lateral buds frequently develop in the axils of one to five uppermost rosette leaves, *las-4 rax1-3* double mutants do not produce any axillary buds from vegetative nodes. The oldest cauline leaves very often fail to support axillary bud formation. Similar results have been obtained through the analysis of *ls bl* double mutants

in tomato (Schmitz et al., 2002). Furthermore, the expression pattern of *RAX1* mRNA in *las-4* mutants did not show any deviation from that observed in the wild type, and vice versa (Müller et al. 2006).

3.2.6.1 Analysis of *atlax-1 las-4* and *atlax-1 rax1-3 las-4* mutants

AtLAX, the *Arabidopsis* ortholog of the *LAX* gene in rice, was shown to play a role in axillary meristem formation during the early vegetative stage in this study. To investigate a possible genetic interaction of *AtLAX* with *LAS*, an *atlax-1 las-4* double mutant was constructed. In comparison to *las-4* single mutants, the *atlax-1 las-4* double mutants had barren axils in all rosette leaves and frequently in the oldest one to three cauline leaves, showing a very similar branching defect as *las-4 rax1-3* double mutants (Fig. 3.2.6-1a, f). Interestingly, plants homozygous for *atlax-1, las-4* and *rax1-3* alleles not only failed to form a side shoot in rosette leaf axils, but also displayed an almost complete block in axillary bud formation in cauline leaf axils (Fig. 3.2.6-1f). Furthermore, *atlax-1 rax1-3 las-4* mutants developed more rosette leaves (56 ± 1.44, n=) than the control plants: *las-4, atlax-1 las-4* and *las-4 rax1-3* (Fig. 3.2.6-1g). However, this was not due to late flowering of the triple mutants, because the days to flowering were not increased in comparison to the control plants (Fig 3.2.6-1g). All mutants formed similar numbers of cauline leaves. This finding indicates that the rate of leaf primordia formation in *atlax-1 rax1-3 las-4* triple mutants is affected during the vegetative stage of development.
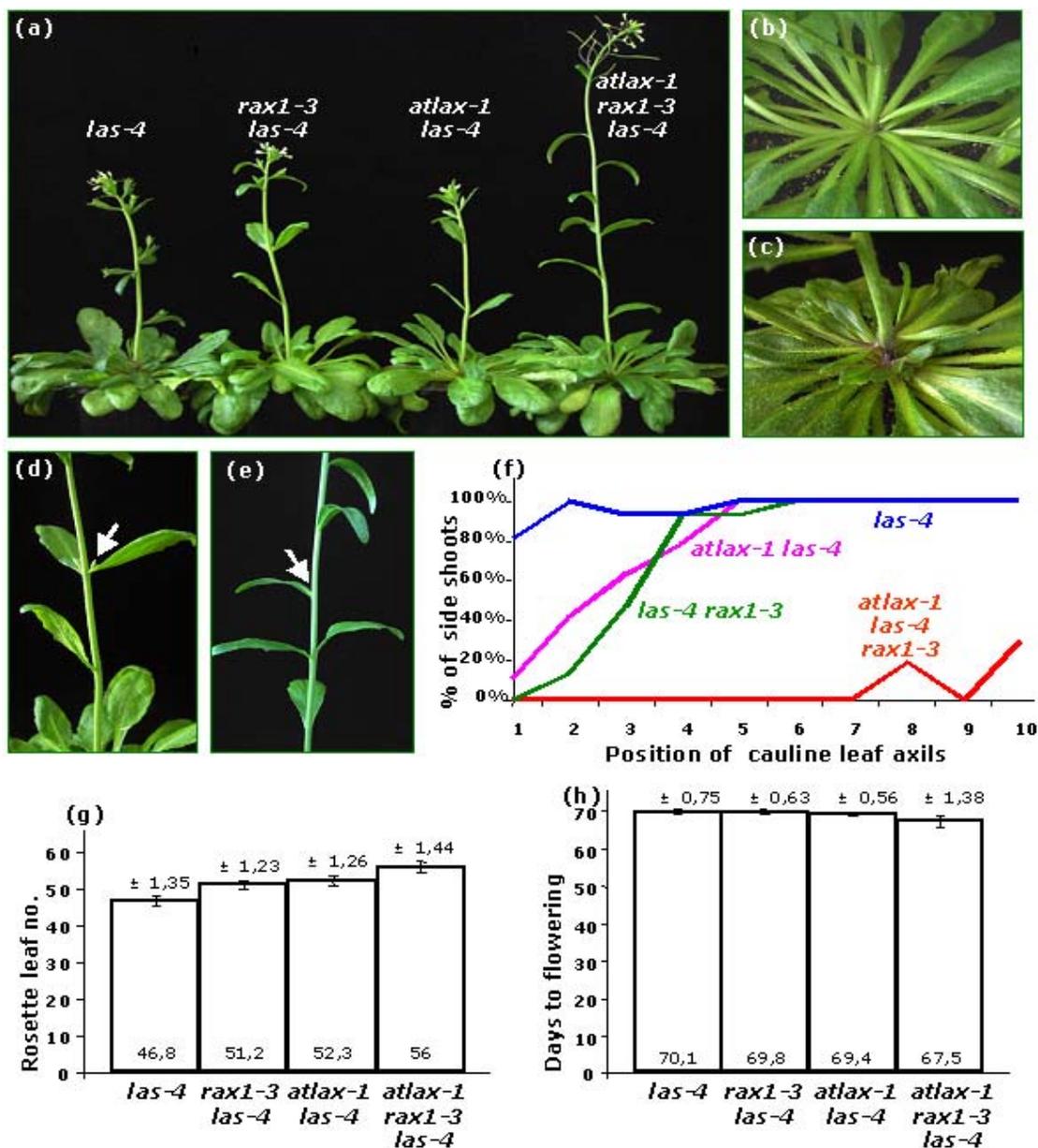
Fig. 3.2.6-1 Analysis of phenotypes of *las-4 rax1-3*, *atlax-1 rax1-3*, and *atlax-1 rax1-3 las-4* **double mutants**. (a) Growth habits of *las-4, las-4 rax1-3, atlax-1 rax1-3,* and *atlax-1 rax1-3 las-4* mutants grown for 60 days under short day conditions and subsequently for 12d in long days. Genotypes are indicated next to the plants. (b) and (c) Close-ups of rosettes of an *atlax-1 rax1-3 las-4* triple mutant (b) and a *las-4* single mutant (c). (d) and (e) Close-ups of bolts of a *rax1-3 las-4* double mutant (d) and an *atlax-1 rax1-3 las-4* triple mutant (e). Arrows indicate an axillary bud forming in *rax1-3 las-4* double mutant (d) and a barren leaf axil of *atlax-1 rax1-3 las-4* triple mutant (e). (f) Graphic representation of axillary bud formation in *atlax-1 rax1-3 las-4* triple mutants in comparison with control plants. Genotypes are indicated next to the graphs. Positions 1 to 10 correspond to the progressively younger cauline leaf axils (n=19, 15, 16, and 16 for *las-4, las-4 rax1-3, atlax-1 rax1-3, and* the *triple* mutants, respectively). (g) and (h) Comparison of rosette leaf numbers (g) and days to flowering (h) between *atlax-1 rax1-3 las-4* triple mutants and single and double mutants when grown until bolting in short days. The plant populations are the same as those used for reproductive branching pattern analysis in (f). The error bars and the accompanying numbers show the 95% confidence intervals.

3.2.6.2 Analysis of the expression patterns of *LAS* and *AtLAX* in *atlax-1* and *las-4* mutants

The transcripts of *LAS* accumulate in a band-shaped domain at the adaxial base of the primordia P1 to P21. The expression domain is about 3-5 cell layers deep and extends 1-2 cell layers in the adaxial-abaxial dimension (Greb *et al.,* 2003). In the vegetative apices of *atlax-1* mutants, the cellular distribution of *LAS* transcript was comparable to that observed in the Col wild-type (Fig. 3.2.6-2a).

By contrast, transcripts of *AtLAX,* as demonstrated by in situ hybridization experiments and RT-PCR analysis, were down-regulated in *las-4* mutant background during the vegetative stage of development (Fig. 3.2.6-2). Plants grown for 25-30 days under short-day conditions were fixed to collect the vegetative apices. The detection of *AtLAX* transcripts in the *las-4* mutant background was controlled by hybridizing sections from Col-wt apices on the same slide as those from *las-4* apices. Five independent hybridizations with eleven individual *las-4* apices did not reveal any signal from *AtLAX* (Fig. 3.2.6-2b), whereas the *AtLAX* transcripts were detectable in Col-wt apices in the same hybridization experiments (data not shown). In accordance with this, RT-PCR could amplify a fragment with expected size for *AtLAX* from Col shoot tip, whereas only a very faint band was seen when amplifying cDNA of *AtLAX* from *las-4* shoot tips (Fig. 3.2.6-2d, top panel). Based on the fact that *RAX1* transcript remains unaltered in *las-4* mutants (Müller et al., 2006), *RAX1* mRNA was amplified as a control for a gene specifically expressed in axillary regions. Three biological replicates showed a similar downregulation of *AtLAX* in *las-4* vegetative apices. However, during the reproductive phase of development, *AtLAX* transcripts were unaltered in *las-4* mutants revealed by in situ experiment. The expression pattern and intensity of *AtLAX* in *las-4* reproductive apex were comparable to that in the Col wt (Fig. 3.2.6-2c). Consistently, a normal amplification for *AtLAX* mRNA from the floral buds of *las-4* were obtained comparing to that in wt in RT-PCR analysis (Fig. 3.2.6-2d, lower panel). Thus, the downregulation of *AtLAX* transcripts caused by *las-4* mutation seems to be dependent on the developmental stage.
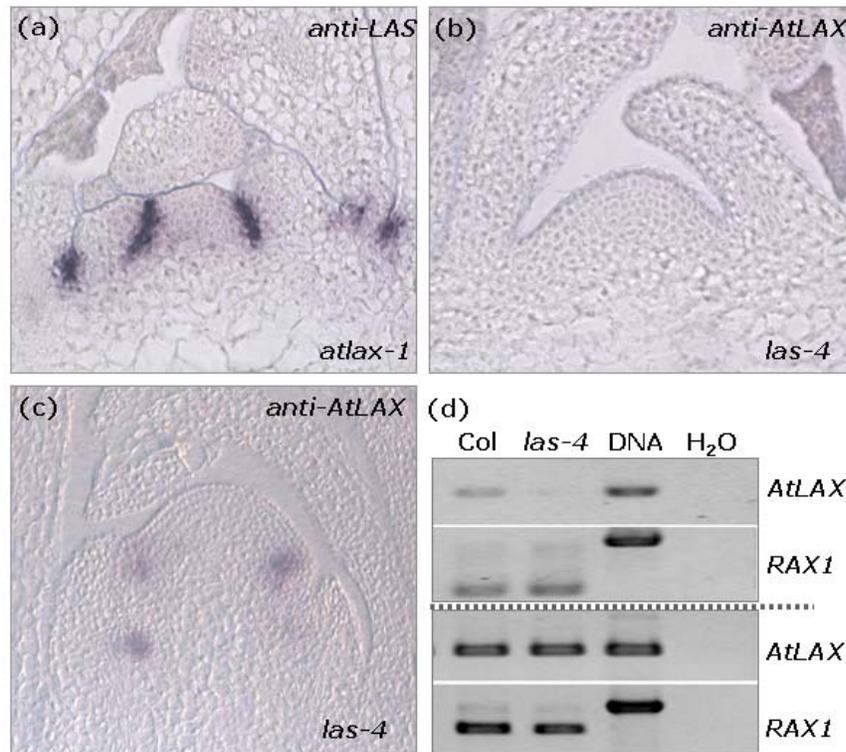
Fig. 3.2.6-2 **Expression pattern of *LAS* and *AtLAX* in *atlax-1* and *las-4* mutants, respectively**. (a) Longitudinal section through a vegetative apex of a 31d-old *atlax-1* mutant grown under short day conditions hybridized with an *LAS* antisense probe. (b) Longitudinal section through a 28d-old shoot apex of *las-4* mutant grown under short day conditions hybridized with an *AtLAX* antisense probe. (c) Longitudinal section through a reproductive apex of *las-4* hybridized with an *AtLAX* antisense probe. The mutant was grown for 28d under short day conditions and then shifted to long days for 6 days. (d) RT-PCR analysis shows reduced *AtLAX* transcript accumulation in vegetative shoot tips of *rax1-3* (upper panel) and normal mRNA level in floral buds of *rax1-3* mutants (lower panel), in comparison with Col wt. To harvest vegetative shoot tips, plants were grown for 28 days under short day conditions. To harvest floral buds, plants were grown for 28 days under short day conditions and then shifted into long days to induce flowering. *RAX1* transcripts were amplified as a control for a gene specifically expressed in axillary regions. Col-genomic DNA and H_2O were included as PCR controls. RT-PCR was repeated two times using different biological samples.

4. Conclusion and discussion

4.1 HAT1 and YAB1 are two putative interactors of RAX1

4.1.1 Two library screens produced different complexities of positive clones

To screen transcription factors interacting with RAX1, the REGIA transcription factor (TF) library was screened using yeast two-hybrid system. This screen identified more than one hundred positive colonies. However the sequence analysis revealed that there were only five different clones with different insertions present among those colonies. Several facts might contribute to this low complexity of TF library screen. Firstly, a low percentage (21.5%) of clones with correct full-length open reading frames (ORFs) is present in the TF library (http://genoplante-info.infobiogen.fr). Other clones have either partial ORFs, or no attB1 recombination sites, or no STOP codons, all of which result in the production of incorrect proteins. Secondly, the LR reactions were performed in a large scale instead of one by one. The presentation of different clones in the TF library may be skewed due to different LR efficiency of each clone. Some clones could not be subcloned into the expression vector and hence are lost before a yeast transformation. Thirdly, not all the clones can be transformed efficiently into the yeast cells during the generation of the prey strain. Finally, some clones could be lost during mating of yeasts due to the fact that not each prey cell has the ability to form diploids with a bait cell. These facts suggest that only a small proportion of prey clones with correct ORFs were subjected to an interaction test with RAX1.

By contrast, a large number of positive clones were identified from the apex cDNA library screening. About 450 colonies from 1×10^6 diploid yeast cells grew on the selective media. Furthermore, 40 out of 42 tested colonies were shown to contain different insertions, demonstrating a high complexity of this cDNA library, compared to the TF library. Only two out of more than 40 candidates were selected out and analyzed. By this other interesting ones, which have interactions and function together with RAX1, might be lost.

4.1.2 ***HAT1* may have a function in regulating axillary meristem formation during the vegetative stage of development**

HAT1 belongs to the class II subfamily of HD-Zip homeobox transcription factors comprising 9 members in *Arabidopsis* (Sessa et al., 1998). Some members of the HD-Zip II are shown to function in shade-avoidance responses which are tightly regulated by light signals, or affect auxin response (Ohgishi et al., 2001; Sawa et al., 2002). In a yeast two-hybrid screen, HAT1 was found to interact with RAX1 and the interaction was further confirmed by a pull down assay. In situ hybridization experiments revealed that *HAT1* mRNA accumulated in a domain very similar to that of *RAX1* at the adaxial base of leaf primordia. These findings imply that *HAT1* might interact with *RAX1* in the process of axillary meristem formation. However, plants homozygous for *hat1-1* did not display a deviation in branching pattern from the wild type. Due to the presence of a truncated transcript extending at least to the T-DNA insertion, the synthesis of a protein with a partial function cannot be excluded. More likely, the functional redundancy of *HAT1* homologs may contribute to the absence of a visible branching defect of *hat1-1*. Therefore, double- or multiple-mutants combining *hat1-1* with loss of function mutations in *HAT1* homologs need to be further investigated. In addition, RT-PCR analysis revealed a wide expression profile for *HAT1* (Fig. 3.1.1-3b), indicating its broad functions in the process of development. For instance, *HAT1* might play a role in the regulation of light response or auxin transport, similar to its closest homolog *HAT2* (Ohgishi et al., 2001; Sawa et al., 2002).

4.1.3 ***YAB1* is a regulator of axillary meristem formation**

YAB1 is a well-known regulator of abaxial cell identity of lateral organs (Sawa et al., 1999b; Siegfried et al., 1999). However, although *YAB1* is strongly expressed throughout the incipient leaf primordium, its role in the formation of axillary meristems has not been characterized. In this study, *YAB1* was shown to control the pattern of shoot branching during both vegetative and reproductive developmental phases. Loss of *YAB1* function led

to a strong reduction in the formation of axillary meristems at the topmost rosette leaf axils, as well as in most of cauline leaf axils when plants were grown to maturity under short day conditions. One of the hypotheses for the ontogeny of axillary meristems supports that they arise de novo from the adaxial side of leaf primordia (Lynn et al., 1999; McConnell and Barton, 1998). The supporting data is from the characterization of gain-of-function mutants *phb-1d* (*PHABULOSA*) (McConnell and Barton, 1998). These mutants develop axillary meristems around the entire basal circumference of adaxialized lateral organs. On the other hand, loss-of-function mutations in *PHB* and its closest homologs, *PHV* and *REV,* result in leaf abaxialization and loss of axillary meristem formation (Emery et al., 2003). The single mutants *fil-8* and *yab3-2* do not have any abnormal vegetative phenotype under normal growth conditions (Kumaran et al., 2002; Sawa et al., 1999b; Siegfried et al., 1999). They produce leaves similar to the wild type with respect to both adaxial and abaxial surfaces. *fil-5 yab3-1* double mutants develop strikingly abnormal leaves, but the polarity is not eliminated, at least in the rosette leaves forming at an early developmental stage (Kumaran et al., 2002; Sawa et al., 1999b; Siegfried et al., 1999). It is tempting to speculate that the partial absence of lateral meristems of *fil-8* at the late vegetative and the reproductive stages might be due to the partial loss of adaxial identity of leaf primordia which is tightly linked to the day-length conditions. Alternatively, loss of *YAB1* function might affect other adaxial identity regulators, which are also influenced by day-length conditions. In addition, another allele *fil-1*, which contains a point mutation at the end of the 4th intron (Kumaran et al., 1999), did not show a branching defect as strong as *fil-8*. This might be explained by the fact that the *fil-8* is a stronger loss-of-function allele. Nevertheless, *fil-1* displayed a strong reduction in tertiary shoot formation (Fig. 3.1.2-5h). To elucidate how the leaf polarity affect axillary meristem formation, the effect of *yab* mutation on other known axillary meristem regulators, such as *LAS, RAX* and *CUC*, is necessary to be investigated.

YAB1 was identified as an interactor of RAX1, an early regulator for axillary meristem initiation (Keller et al., 2006; Müller et al., 2006). The co-localization of *YAB1* and *RAX1* transcripts in incipient lateral primordia further indicates a physiological relevance in the

interaction between YAB1 and RAX1. Interestingly, the severity of branching defects of both *fil-8* and *rax1-3* is strongly dependent on the day-length conditions. The branching defect of *rax1-3* observed under short-day conditions was strongly diminished or vanished in long days (Müller et al., 2006). Similarly, *fil-8* mutants supported the formation of axillary buds in all leaf axils when grown in long photoperiods. These findings suggest that *YAB1* and *RAX1* cooperate to establish the identity of axillary meristem cells at a very early developmental stage in a day-length dependent manner. However, *fil-8 rax1-3* double mutants have a high proportion of rosette leaf axils forming side shoots in the zone where *rax1-3* shows severe branching defect. This partial reversion in the ability of *rax1-3* to support axillary meristem formation might be due to the mixed backgrounds or due to an epistatic effect of *fil-8*. To elucidate the genetic interaction between *RAX1* and *YAB1*, the phenotype of *fil rax1* double mutants in the same genetic background needs to be analyzed. It is also necessary to investigate the branching pattern of *rax1-3* in combination with other mutant alleles of *yab1*, as well as in combination with a loss of function allele of *YAB3*, the closest functionally redundant homolog of *YAB1*.

4.2   AtLAX is a regulator of axillary meristem formation

4.2.1 *AtLAX* is the closest homolog of the rice *LAX* gene in *Arabidopsis*

The orthologous *bHLH* genes, *LAX* and *BA1*, play crucial roles in the establishment of axillary meristems in rice and maize, respectively. LAX and BA1 contain bHLH domains sharing 100% sequence identity. Furthermore, they show a conserved molecular mechanism in controlling the pattern of reproductive branches. In this study, the *LAX*-related gene in *Arabidopsis* was identified.

Sequence blast analysis revealed that the *Arabidopsis* gene At5g01310, containing a bHLH domain, showed the highest sequence similarity to LAX and BA1 with 81% identity within the bHLH domain. However, the annotation of At5g01310 was shown to be wrong by cDNA amplification using a reverse primer against the first annotated intron. The first 513bp of the genomic sequence of gene At5g01310 were demonstrated to constitute the

complete ORF sequence of a functional gene, designated *AtLAX* in this study. *AtLAX* belongs to group VIII of the bHLH superfamily comprising 162 members in *Arabidopsis* (Heim et al., 2003; Toledo-Ortiz et al., 2003). In this study, a Q-A-R motif search within the bHLH domains demonstrated a total number of 14 group members. A phylogenetic tree based on an alignment of the bHLH domains classified *AtLAX* into the same subclade as *LAX* and *BA1*, and separated it from the other subclades (Fig. 3.2.1-2). The use of sequences outside of the bHLH domain did not change the overall picture (data not shown). These data indicate that *AtLAX* may have a similar function as *LAX* and *BA1* in the process of axillary meristem formation. It is also tempting to speculate that none of the other thirteen VIII-subgroup members have a redundant function with *AtLAX*. Thus, *AtLAX* seems to be a unique gene among these group VIII members.

In an effort to identify candidate gene(s) which might have a function in shoot branching, the expression profiles of all 14 subgroup members were analyzed using RT-PCR analysis. Overall, all group members except for *bHLH87* had rather low mRNA levels. Transcripts of all members, except *bHLH54,* accumulate in floral buds. This indicates functions in the process of flowering and/or floral organ formation, probably in a (partially) redundant manner, especially in the case of *bHLH52* and *bHLH53*. These two genes are exclusively expressed in floral buds and are classified into the same subgroup.

4.2.2 *AtLAX* plays a role in axillary meristem formation

LAX and *BA1* from rice and maize, respectively, are specifically expressed at the adaxial base of newly formed lateral meristems and control the establishment of shoot branches in a conserved manner (Gallavotti et al., 2004; Komatsu et al., 2003). *AtLAX* mRNA also accumulates at the adaxial base of leaf and floral primordia, but only in a narrow domain with up to 5 cell layers in the adaxial–abaxial and the tangential dimensions (Fig. 3.2.3). Therefore, together with its highest protein sequence similarity to *LAX* and *BA1*, it is strongly implied that *AtLAX* functions in the process of axillary meristem formation. In this study, phenotypic analysis of *AtLAX* loss-of-function and gain-of-function lines was

performed to investigate its possible role in the establishment of shoot branches.

The single knockout mutants *atlax-1* and *atlax-2* displayed a weak defect in axillary meristem formation, characterized by a reduction in the number of lateral buds formed in the old rosette leaf axils (Fig. 3.2.4-2b, c). Although not all old rosette leaf axils of Col-wt plants developed lateral buds (Aguilar-Martinez et al., 2007; Fig. 3.2.4-2b, c), the percentage of barren leaf axils in *atlax* mutants was significantly higher than in wt plants. In *atlax* mutants, empty leaf axils always extended to a later vegetative phase than in wild type plants. However, the block of axillary bud formation in *atlax* mutants was much weaker than that observed in both the *las* and *rax1* loss-of-function mutants (Greb et al., 2003; Keller et al., 2006; Müller et al., 2006). These observations demonstrate that loss of *AtLAX* activity does not strongly impair axillary meristem formation. Alternatively, redundant function(s) of its homolog(s) might be the cause for the weak branching defect of *atlax* mutants.

Since a transcription factor fused with a SRDX domain has been shown to be able to effectively suppress the activity of its target gene(s), even in the presence of functionally redundant genes, the influence of a chimeric repressor *AtLAXSRDX* on shoot development was investigated. It was speculated that if *AtLAX* acts as a transcription activator, a conversion into a transcriptional repressor would result in the repression of its target gene(s), and therefore phenocopy *atlax* as well as multiple mutants containing mutations in the redundant genes. To this end, the branching pattern of the *AtLAXSRDX*-carrying plants was found to be impaired (Fig. 3.2.4-4g). However, the block in axillary bud formation was again only observed at early vegetative stage. Axillary shoots formed in the rosette leaf axils during the late vegetative phase and in all cauline leaf axils. The similarity in the shoot branching patterns between *atlax* knockout mutants and *AtLAXSRDX*-expressing plants demonstrate that: 1) AtLAXSRDX is expressed and functioning in the transgenic lines; 2) *AtLAX* has a role, although a minor one, in the axillary meristem formation; 3) *AtLAX* functions as a transcriptional activator; and 4) *AtLAX* might have no functionally redundant homolog(s), which is also implied by its distinct grouping in the phylogenetic tree (Fig. 3.2.1-2). In addition, overaccumulation of

AtLAXSRDX resulted in pleiotropic phenotypes, leading to stunted growth and severely reduced fertility (Fig. 3.2.4-4a-e). The correlation between the severity of these pleiotropic phenotypes and the level of *AtLAXSRDX* transcript accumulation suggested that the chimeric repressor might be the direct cause for the dwarf phenotype as well as the branching defect observed in these plants. However, it cannot be excluded that the chimeric protein interferes with other bHLH genes. *AtLAXSRDX*-carrying dwarf lines also developed significantly more rosette leaves than wt plants (Fig. 3.2.4-4h). This observation suggests a role of *AtLAX* in the regulation of flowering time.

Considering that *AtLAX*-overexpressing plants developed significantly less rosette leaves in comparison to wt plants (data not shown), it is tempting to speculate that *AtLAX* has a role in flowering time. On the other hand, overexpressing *AtLAX* also caused a dwarf phenotype. These dwarf plants lost apical dominance and developed down-curling leaves and altered flowers, in contrast to *AtLAXSRDX*-expressing dwarf plants which had normal apical dominance, contracted leaves and normal inflorescence. Most importantly, *AtLAX*-overexpressor developed accessory shoots in the axils of almost all cauline leaves as well as in some young rosette leaves (Fig. 3.2.4-5). Frequently cauline leaf axils developed two accessory buds. These data further support a role of *AtLAX* in axillary meristem formation. Thus, *AtLAX* does not only have high sequence similarity to *LAX* and *BA1*, two axillary meristem regulators in rice and maize, respectively, but also shares the conserved expression pattern and function in controlling lateral meristem formation.

4.2.3 *AtLAX* interacts with *RAX1* in the process of axillary meristem formation

Phenotypic analysis has demonstrated that homozygous *atlax-1* plants are compromised in axillary bud formation during the early vegetative stage (Fig. 3.2.4-2). Likewise, *rax1-3* knockout mutants do not develop lateral buds in old rosette leaf axils and display moderate branching during the middle phase of vegetative development (Müller et al., 2006). In *atlax-1 rax1-3* double mutants, the block of axillary bud formation was extended towards the top of the rosette (Fig. 3.2.5-1). Formation of lateral buds in the

middle rosette zone of *rax1-3*, in which a rather high proportion of leaf axils support axillary bud formation, was completely blocked in *atlax-1 rax1-3*. The top of the rosette of *atlax-1 rax1-3* double mutants was also impaired in the formation of axillary buds. Although the branching pattern of the primary reproductive shoot was not altered compared to those observed in *atlax-1* and *rax1-3* single mutants, tertiary shoot formation in the leaf axils of secondary shoots of *atlax-1 rax1-3* plants was strongly reduced (Fig. 3.2.5-2). The additive effects of *atlax-1* and *rax1-3* mutations on the branching defect suggest that *AtLAX* and *RAX1* are members of two independent pathways controlling axillary meristem formation. Alternatively, these two regulators interact with each other. This hypothesis is originated from the well-known model in which bHLH proteins interact with MYB proteins to perform their functions (Ramsay and Glover, 2005). Both genetic and direct physical interactions suggest an intimate functional relationship between MYB and bHLH proteins. The compelling supports for the hypothesis that AtLAX might interact with RAX1 are derived from the overlapping expression pattern of the two transcripts (Fig. 3.2.5-4) and the interaction of the two proteins detected in a pull down assay (Fig. 3.2.5-5). *RAX1* transcripts accumulate in a spherical domain in the center of boundary region between the SAM and newly formed leaf primordia (Müller et al., 2006). *AtLAX* mimics this specific expression pattern (Fig. 3.2.3). These findings suggest that AtLAX and RAX1 may interact with each other to perform their functions in axillary meristem formation. However, due to general interaction abilities of bHLH with MYB proteins (Payne et al., 2000; Sawa, 2002; Zhang et al., 2003), it can not be excluded so far that the interaction of AtLAX with RAX1 shown by pull down assays does not happen in plant cells. Therefore, further investigations are required to elucidate their interaction in vivo and the specificity of this interaction between AtLAX and RAX1. For instance, interactions between AtLAX and two homologs of RAX1, RAX2 and RAX3 showing functional redundancy with RAX1, will be tested to find out whether the interaction is confined to AtLAX and RAX1. Similarly, the interaction tests between RAX1 and the homologs of AtLAX can also provide valuable information. The BiFC assay (also known as "split YFP") would help to unravel their interaction in vivo.

Additionally, the lack of side shoots in rosette leaf axils of *atlax-1 rax1-3* double mutants is not complete. Lateral buds were formed in a high proportion of the axils of the youngest rosette leaves of *atlax-1 rax1-3* double mutants (Fig. 3.2.5-1). Furthermore the cauline leaf axils of the primary shoot were not compromised in lateral bud formation. These observations can be attributed to redundant functions of the *RAX1* homologs, *RAX2* and *RAX3*. Müller et al. (2006) described that *RAX1* has a major role in axillary meristem formation during the early vegetative developmental stage, whereas *RAX2* and *RAX3* function mainly during late vegetative and reproductive stages in a redundant manner with *RAX1*. *rax1-3 rax2-1 rax3-1* triple mutants do not support axillary bud formation in almost all the leaf axils. Combinations of *atlax* with the mutations in all three *RAX* genes would be necessary to confirm this hypothesis. Alternatively, another yet-unknown pathway might also be responsible for the axillary meristem formation observed in *atlax-1 rax1-3* double mutants.

In addition, *RAX1* has also been shown to influence flowering time, as loss of *RAX1* function causes plants to flower earlier than wild type (Keller et al., 2006; Müller et al., 2006). In *atlax-1 rax1-3* double mutants, the early flowering phenotype of *rax1-3* was suppressed and nearly restored the wild type phenotype (Fig. 3.2.5-3). The opposite influences of *atlax-1* on *rax1-3* in the processes of shoot branching and flowering time could be contributed to another un-known regulator/interactor.

4.2.4   *AtLAX* acts downstream of *RAX1* and *LAS* in controlling axillary meristem formation

RAX1 and *LAS* have overlapping expression domains in the leaf axils, and mutations in these two genes cause branching defects with different severities during the vegetative stage of development (Greb et al., 2003; Müller et al., 2006). Double mutant and expression pattern analysis revealed that *LAS* and *RAX1* function in two independent pathways in axillary meristem formation (Müller et al., 2006; Results 3.2.6). In this study, *AtLAX* was shown to be regulated by both *RAX1*and *LAS*.

The expression pattern of *RAX1* remains unaltered in the apices of *atlax-1* mutants, whereas *AtLAX* transcripts were hardly detectable in vegetative apices of *rax1-3* single and *rax1-3 rax2-1 rax3-1* triple mutants (Fig. 3.2.5-6a-f). This downregulation of *AtLAX* caused by loss of *RAX1* transcripts was confirmed in a RT-PCR analysis by reduced amplification of *AtLAX* mRNA from *rax1-3* shoot tips (Fig. 3.2.5-6i). These data suggest that *RAX1, 2, 3* genes regulate *AtLAX* transcript accumulation during the vegetative stage. So far, it is not possible to propose that this regulation is direct or indirect. Together with the interaction between RAX1 and AtLAX proteins shown by pull down assay, it is tempting to speculate that *RAX1* and *AtLAX* have relationships not only in a hierarchical order but also as partners. Conversely, the accumulation of *AtLAX* transcripts in the reproductive apices of *rax1-3 rax2-1 rax3-1* triple mutants was compatible with that observed in the wild type, shown by in situ hybridization experiment (Fig. 3.2.5-6g, h). Furthermore, RT-PCR yielded a normal amplification for *AtLAX* from floral buds of *rax1-3* and *rax* triple mutants in comparison with wt (Fig. 3.2.5-6i). These findings indicate that *RAX* genes regulate *AtLAX* specifically during the vegetative developmental phase. Alternatively, another regulator might activate *AtLAX* during the reproductive stage independent on *RAX* genes.

In situ hybridization analysis revealed that the cellular distribution of *LAS* in *atlax-1* apices mirrors its expression pattern in the wild type (Fig. 3.2.6-2a). Conversely, *AtLAX* transcript was not detectable in vegetative apices of *las-4* mutants (Fig. 3.2.6-2b). RT PCR also could hardly amplify *AtLAX* mRNA from *las-4* vegetative shoot tips. However, the transcript of *AtLAX* was found to accumulate normally in reproductive apices of *las-4* mutants (Fig. 3.2.6-2c). RT-PCR analysis revealed a normal mRNA level for *AtLAX* in the *las-4* floral buds. These findings demonstrate that *LAS* regulates *AtLAX* in a similar way as *RAX1.* In addition, double *atlax-1 las-4* mutants have a very similar branching defect as *rax1-3 las-4* plants, characterized by the complete lack of side shoots in all rosette leaf axils and the failure to initiate axillary buds in the early cauline leaf axils (Müller et al., 2006). This result demonstrates that loss of *RAX1* and *AtLAX* transcripts leads to similar enhancement of the shoot branching defect of *las-4*. Combination of *atlax-1 with rax1-3*

and *las-4* results in nearly complete block of axillary meristem formation in all the leaf axils during vegetative and reproductive development (Fig. 3.2.6-1). This data indicates that all these three regulators, *AtLAX, LAS* and *RAX1*, have also important functions in controlling axillary meristem formation during reproductive development.

Taken together, these expression pattern studies and double and triple mutant analysis raise the possibilities that *RAX1* and *LAS* regulate *AtLAX,* and all these three genes regulate axillary meristem formation during both vegetative and reproductive development. Further experiments are needed to clarify whether *RAX1* and *LAS* regulate *AtLAX* directly or indirectly. DNA binding assay and yeast one-hybrid analysis would be helpful to unravel these interactions. In addition, the weak branching defect of *atlax* indicates that the two pathways, in which *LAS* and *RAX*, respectively, are involved, can also act independent on *AtLAX* in regulating axillary meristem formation. Further experiments are required to elucidate their genetic interactions.

5. Abstract

The architecture of flowering plants is largely determined by the formation and outgrowth of lateral branches during the postembryonic phase of development. Lateral branches originate from secondary meristems initiated in the axils of leaf primordia. The *REGULATOR OF AXILLARY MERISTEMS1 (RAX1)* gene has been shown to play an important role at an early stage of axillary meristem formation in *Arabidopsis* (Keller et al., 2006; Müller et al., 2006). The aim of this study was to identify interactors of RAX1 and characterize their roles in the process of axillary meristem initiation.

To identify functional partners of RAX1 in a large scale, a yeast two-hybrid screen was performed. Two candidates, HAT1 (HD-Zip protein 1) and YAB1 (YABBY1), were shown to interact with RAX1 in yeast and the interactions were confirmed by pull-down assays. Transcripts of *HAT1,* a HD-ZIP class II transcription factor, accumulated in a domain at the adaxial base of young leaf primordia, very similar to that of *RAX1*. Phenotypic analysis of *hat1-1* knockout mutant as well as *hat1-1 rax1-3* double mutants did not reveal any role of *HAT1* in the process of axillary meristem formation. This might be due to a functional redundancy of *HAT1* with its homologs. Co-localization of *YAB1* and *RAX1* transcripts in the incipient leaf primordia was demonstrated using consecutive sections for *RNA in-situ* hybridization. Loss of *YAB1* function (*fil-8*) resulted in a strong reduction in axillary bud formation when plants were grown in short photoperiods. *YAB1* was shown to regulate axillary meristem formation in a day-length dependent manner as the branching defect of *fil-8* was vanished in long days. The *rax1-3 fil-8* double mutant showed a similar branching defect as *fil-8*.

Another putative interactor of RAX1 is AtLAX, which was characterized in detail in this study. *AtLAX* is the closest homolog of the rice *LAX* and maize *BA1* genes in *Arabidopsis*.

LAX and *BA1* are shown to play crucial roles in the establishment of axillary meristems in rice and maize, respectively. *LAX, BA1* and *AtLAX* encode bHLH-type transcription factors with highly conserved bHLH domains. Phenotype analysis of *atlax* knockout mutants and transgenic plants carrying the *AtLAXSRDX* dominant repressor showed that: 1) *AtLAX* plays a role in the formation of axillary meristems; 2) *AtLAX* functions as a transcriptional activator; and 3) *AtLAX* probably has no functionally redundant homolog(s). The specific expression pattern of *AtLAX* at the adaxial domain of leaf primordia and accessory shoot formation in the *AtLAX*-overexpressing plants further support the role of *AtLAX* in axillary meristem formation. The idea of an interaction between AtLAX and RAX1, a R2R3-type MYB protein, is derived from the classical interaction model of bHLH and MYB proteins described for several developmental processes. The protein interaction between AtLAX and RAX1 is demonstrated in pull down assays and is supported by a nearly completely overlap of their domains of transcript accumulation. In addition, *AtLAX* mRNA accumulation is down-regulated in vegetative, but not in reproductive apices of *rax1-3* loss-of-function mutants, suggesting that *RAX1* regulates *AtLAX* in the process of axillary meristem initiation during the vegetative stage of development. Finally, analysis of the genetic interaction between *AtLAX, RAX1* and *LAS* (*LATERAL SUPPRESSOR*) demonstrates that these three regulators are necessary for the formation of axillary meristems during both vegetative and reproductive stages of shoot development.

6. Zusammenfassung

Die Architektur von Blütenpflanzen wird hauptsächlich durch die Bildung und das Auswachsen von Seitentrieben während der postembryonalen Phase der Entwicklung bestimmt. Seitentriebe entstehen aus sekundären Meristemen, die in den Achseln von Blattprimordien initiiert werden. Das *REGULATOR OF AXILLARY MERISTEMS1 (RAX1)*-Gen spielt in *Arabidopsis* eine wichtige Rolle in der frühen Phase der Achselmeristembildung (Keller et al., 2006; Müller et al., 2006). Das Ziel dieser Arbeit war es, Interaktionspartner von *RAX1* zu identifizieren und ihre Rolle im Prozess der Achselmeristeminitiation zu charakterisieren.

Um im großen Maßstab funktionelle Partner von *RAX1* zu identifizieren wurde ein Hefe Zwei-Hybrid Screening durchgeführt. Für zwei Kandidaten, HAT1 (HD-ZIP PROTEIN 1) und YAB1 (YABBY1), konnte eine Interaktion in Hefe gezeigt werden, die durch Pull-Down Assays bestätigt werden konnte. Der HD-ZIP-Klasse II-Transkriptionsfaktor HAT1 wird in einer engen Domäne an der adaxialen Basis junger Blattprimordien transkribiert, sehr ähnlich wie *RAX1*. Die phänotypische Analyse der *hat1-1*-Mutante sowie der *hat1-1 rax1-3* Doppelmutante, ergab keinen Hinweis auf eine Funktion von *HAT1* im Prozess der Achselmeristembildung. Dies könnte durch die funktionelle Redundanz von *HAT1* mit anderen homologen HD-ZIP-Klasse II-Transkriptionsfaktoren begründet sein. Durch RNA-In-Situ-Hybridisierungen aufeinander folgender Schnitte von Apices konnte eine Co-Lokalisation von *YAB1* und *RAX1* in entstehenden Blattprimordien gezeigt werden. Der Verlust der *YAB1*-Funktion (*fil-8*) führte zu einer starken Reduktion der Achselknospenbildung, wenn die Mutanten in kurzen Fotoperioden angezogen werden. Für *YAB1* konnte gezeigt werden, dass es die Achselmeristembildung tageslängenabhängig reguliert, da im Langtag kein Verzweigungsdefekt von *fil-8* erkennbar ist. Die *rax1-3 fil-8* Doppelmutante zeigte einen ähnlichen Verzweigungsdefekt wie *fil-8*.

Ein weiterer putativer Interaktionspartner von *RAX1* ist *AtLAX*, der in dieser Arbeit im Detail charakterisiert wurde. *AtLAX1* ist der nächste Homologe in *Arabidopsis* des *LAX*-Gens aus Reis und des *BA1*-Gens aus Mais. Es wurde gezeigt, dass *LAX* und *BA1* eine entscheidende Rolle in der Entstehung von Achselmeristemen in Reis bzw. Mais spielen. *LAX, BA1* und *AtLAX* kodieren für bHLH-Transkriptionsfaktoren, die sich durch eine hochkonservierte bHLH-Domäne auszeichnen. Die phänotypische Analyse von *atlax*-Mutanten und transgenen Pflanzen, die den dominanten *AtLAXSRDX*-Repressor exprimieren, zeigte: 1) *AtLAX* spielt eine Rolle in der Achselmeristembildung; 2) *AtLAX* wirkt als Transkriptionsaktivator; und 3) *AtLAX* hat wahrscheinlich keine funktionell redundanten Homologe. Des weiteren deuten das spezifische Expressionsmuster von *AtLAX* an der adaxialen Seite von Blattprimordien und die Bildung von akzessorischen Seitentrieben in *AtLAX*-überexprimierenden Pflanzen weiter auf eine Rolle von *AtLAX* in der Achselmeristembildung hin. Die Idee einer direkten Interaktion zwischen *AtLAX* und *RAX1*, einem MYB-Protein des R2R3-Typs, resultierte aus dem bekannten, klassischen Interaktionsmodell zwischen bHLH- und MYB-Proteinen, welches für verschiedene biologische Prozesse beschrieben ist. Die Proteininteraktion zwischen *AtLAX* und *RAX1* konnte durch Pull-Down-Assays gezeigt werden und ein Zusammenspiel in vivo wird durch die nahezu vollständige Überschneidung der Expressionsdomänen weiter untermauert. Des Weiteren ist die *AtLAX*-mRNA-Menge in *rax1-3*-Mutanten während der vegetativen Phase stark reduziert, in reproduktiven Apices allerdings auf Wildtypniveau, was dafür spricht, dass *RAX1* während der vegetativen Entwicklungsphase *AtLAX* im Prozess der Achselmeristementwicklung reguliert. Schließlich zeigt die Analyse der genetischen Interaktionen zwischen *AtLAX, RAX1* und *LAS (LATERAL SUPPRESSOR)*, dass diese drei Regulatoren eine wichtige Rolle in der Achselmeristembildung, sowohl in der vegetativen, als auch der reproduktiven Phase, der Sprossentwicklung spielen.

7. References

Aguilar-Martinez, J.A., Poza-Carrion, C., and Cubas, P. (2007). Arabidopsis BRANCHED1 acts as an integrator of branching signals within axillary buds. Plant Cell **19**, 458-472.

Aida, M., Ishida, T., Fukaki, H., Fujisawa, H., and Tasaka, M. (1997). Genes involved in organ separation in Arabidopsis: an analysis of the cup-shaped cotyledon mutant. Plant Cell **9**, 841-857.

Ariel, F.D., Manavella, P.A., Dezar, C.A., and Chan, R.L. (2007). The true story of the HD-Zip family. Trends Plant Sci **12**, 419-426.

Atchley, W.R., Terhalle, W., and Dress, A. (1999). Positional dependence, cliques, and predictive motifs in the bHLH protein domain. J Mol Evol **48**, 501-516.

Bailey, P.C., Martin, C., Toledo-Ortiz, G., Quail, P.H., Huq, E., Heim, M.A., Jakoby, M., Werber, M., and Weisshaar, B. (2003). Update on the basic helix-loop-helix transcription factor gene family in Arabidopsis thaliana. Plant Cell **15**, 2497-2502.

Benkova, E., Michniewicz, M., Sauer, M., Teichmann, T., Seifertova, D., Jurgens, G., and Friml, J. (2003). Local, efflux-dependent auxin gradients as a common module for plant organ formation. Cell **115**, 591-602.

Bennett, T., Sieberer, T., Willett, B., Booker, J., Luschnig, C., and Leyser, O. (2006). The Arabidopsis MAX pathway controls shoot branching by regulating auxin transport. Curr Biol **16**, 553-563.

Bernhardt, C., Lee, M.M., Gonzalez, A., Zhang, F., Lloyd, A., and Schiefelbein, J. (2003). The bHLH genes GLABRA3 (GL3) and ENHANCER OF GLABRA3 (EGL3) specify epidermal cell fate in the Arabidopsis root. Development **130**, 6431-6439.

Beveridge, C.A., Ross, J.J., and Murfet, I.C. (1994). Branching Mutant rms-2 in Pisum sativum (Grafting Studies and Endogenous Indole-3-Acetic Acid Levels). Plant Physiol **104**, 953-959.

Beveridge, C.A., Symons, G.M., and Turnbull, C.G. (2000). Auxin inhibition of decapitation-induced branching is dependent on graft-transmissible signals regulated by genes Rms1 and Rms2. Plant Physiol **123**, 689-698.

Beveridge, C.A., Murfet, I.C., Kerhoas, L., Sotta, B., Miginiac, E., Rameau, C. (1997a) The shoot controls zeatin riboside export from pea roots: evidence from the branching mutant *rms4* . *Plant J.* **11**, 339 345.

Beveridge, C.A., Symons, G.M., Murfet, I.C., Ross, J.J., Rameau, C. (1997b) The *rms1* mutant of pea has elevated indole-3-acetic acid levels and reduced root-sap zeatin riboside content but increased branching controlled by graft-transmissible signals . *Plant Physiol.* **115**, 1251 1258.

Booker, J., Sieberer, T., Wright, W., Williamson, L., Willett, B., Stirnberg, P., Turnbull, C., Srinivasan, M., Goddard, P., and Leyser, O. (2005). MAX1 encodes a cytochrome P450 family member that acts downstream of MAX3/4 to produce a carotenoid-derived branch-inhibiting hormone. Dev Cell **8**, 443-449.

Brand U, Fletcher JC, Hobe M, Meyerowitz EM, Simon R (2000). Dependence of stem cell fate in Arabidopsis on a feedback loop regulated by CLV3 activity. Science 289:617–619.

Brand, U., Grunewald, M., Hobe, M., and Simon, R. (2002). Regulation of CLV3 expression by two homeobox genes in Arabidopsis. Plant Physiol **129**, 565-575.

Byrne, M.E. (2006). Shoot meristem function and leaf polarity: the role of class III HD-ZIP genes. PLoS Genet **2**, e89.

Byrne, M.E., Simorowski, J., and Martienssen, R.A. (2002). ASYMMETRIC LEAVES1 reveals knox gene redundancy in Arabidopsis. Development **129**, 1957-1965.

Byrne, M.E., Barley, R., Curtis, M., Arroyo, J.M., Dunham, M., Hudson, A., and Martienssen, R.A. (2000). Asymmetric leaves1 mediates leaf patterning and stem cell function in Arabidopsis. Nature **408**, 967-971.

Cardon, G., Hohmann, S., Klein, J., Nettesheim, K., Saedler, H., and Huijser, P. (1999). Molecular characterisation of the Arabidopsis SBP-box genes. Gene *237*, 91-104.

Carles, C.C., and Fletcher, J.C. (2003). Shoot apical meristem maintenance: the art of a dynamic balance. Trends Plant Sci **8**, 394-401.

Chen, H., Banerjee, A.K., and Hannapel, D.J. (2004). The tandem complex of BEL and KNOX partners is required for transcriptional repression of ga20ox1. Plant J **38**, 276-284.

Chuck, G., Lincoln, C., and Hake, S. (1996). KNAT1 induces lobed leaves with ectopic meristems when overexpressed in Arabidopsis. Plant Cell **8**, 1277-1289.

Clark, S.E. (1997). Organ Formation at the Vegetative Shoot Meristem. Plant Cell **9**, 1067-1076.

Clark, S.E., Running, M.P., and Meyerowitz, E.M. (1993). CLAVATA1, a regulator of meristem and flower development in Arabidopsis. Development **119**, 397-418.

Clark, S.E., Williams, R.W., and Meyerowitz, E.M. (1997). The CLAVATA1 gene encodes a putative receptor kinase that controls shoot and floral meristem size in Arabidopsis. Cell **89**, 575-585.

Coen, E.S., Romero, J.M., Doyle, S., Elliott, R., Murphy, G., and Carpenter, R. (1990). floricaula: a homeotic gene required for flower development in antirrhinum majus. Cell **63**, 1311-1322.

Daimon, Y., Takabe, K., and Tasaka, M. (2003). The CUP-SHAPED COTYLEDON genes promote adventitious shoot formation on calli. Plant Cell Physiol **44**, 113-121.

Digby, J., T. H. Thomas and P. E. Wareing (1964) Promotion of cell division in tissue cultures by gibberellic acid. *Nature* 203: 547-548.

Doebley, J., Stec, A., and Hubbard, L. (1997). The evolution of apical dominance in maize. Nature **386**, 485-488.

Emery, J.F., Floyd, S.K., Alvarez, J., Eshed, Y., Hawker, N.P., Izhaki, A., Baum, S.F., and Bowman, J.L. (2003). Radial patterning of Arabidopsis shoots by class III HD-ZIP and KANADI genes. Curr Biol **13**, 1768-1774.

Endrizzi, K., Moussian, B., Haecker, A., Levin, J.Z., and Laux, T. (1996). The SHOOT MERISTEMLESS gene is required for maintenance of undifferentiated cells in Arabidopsis shoot and floral meristems and acts at a different regulatory level than the meristem genes WUSCHEL and ZWILLE. Plant J **10**, 967-979.

Esch, J.J., Chen, M., Sanders, M., Hillestad, M., Ndkium, S., Idelkope, B., Neizer, J., and Marks, M.D. (2003). A contradictory GLABRA3 allele helps define gene interactions controlling trichome development in Arabidopsis. Development **130**, 5885-5894.

Eshed, Y., Baum, S.F., and Bowman, J.L. (1999). Distinct mechanisms promote polarity establishment in carpels of Arabidopsis. Cell **99**, 199-209.

Eshed, Y., Baum, S.F., Perea, J.V., and Bowman, J.L. (2001). Establishment of polarity in lateral organs of plants. Curr Biol **11**, 1251-1260.

Eshed, Y., Izhaki, A., Baum, S.F., Floyd, S.K., and Bowman, J.L. (2004). Asymmetric leaf development and blade expansion in Arabidopsis are mediated by KANADI and YABBY activities. Development **131**, 2997-3006.

Ferre-D'Amare, A.R., Pognonec, P., Roeder, R.G., and Burley, S.K. (1994). Structure and function of the b/HLH/Z domain of USF. Embo J **13**, 180-189.

Fields, S., and Song, O. (1989). A novel genetic system to detect protein-protein interactions. Nature **340**, 245-246.

Fletcher, J.C., Brand, U., Running, M.P., Simon, R., and Meyerowitz, E.M. (1999). Signaling of cell fate decisions by CLAVATA3 in Arabidopsis shoot meristems. Science **283**, 1911-1914.

Fu, Y., Xu, L., Xu, B., Yang, L., Ling, Q., Wang, H., and Huang, H. (2007). Genetic interactions between leaf polarity-controlling genes and ASYMMETRIC LEAVES1 and 2 in Arabidopsis leaf patterning. Plant Cell Physiol **48**, 724-735.

Gallavotti, A., **Zhao, Q.**, **Kyozuka, J.**, **Meeley, R.B.**, **Ritter, M.K.**, **Doebley, J.F.**, **Pe, M.E.**, **and Schmidt, R.J.** (2004). The role of barren stalk1 in the architecture of maize. Nature **432**, 630-635.

Gallois, J.L., **Woodward, C.**, **Reddy, G.V.**, **and Sablowski, R.** (2002). Combined SHOOT MERISTEMLESS and WUSCHEL trigger ectopic organogenesis in Arabidopsis. Development **129**, 3207-3217.

Garcia, D., **Collier, S.A.**, **Byrne, M.E.**, **and Martienssen, R.A.** (2006). Specification of leaf polarity in Arabidopsis via the trans-acting siRNA pathway. Curr Biol **16**, 933-938.

Garrison, R. (1955) Studies in the development of axillary buds. . Am. J. Bot. 42, 257–66.

Goff, S. A., **Cone, K. C.**, **and Chandler, V. L.** (1992). Functional analysis of the transcriptional activator encoded by the maize B gene: evidence for a direct functional interaction between two classes of regulatory proteins. Genes Dev **6**, 864-875.

Golz, J.F. (2006). Signalling between the shoot apical meristem and developing lateral organs. Plant Mol Biol **60**, 889-903.

Golz, J.F., **Roccaro, M.**, **Kuzoff, R.**, **and Hudson, A.** (2004). GRAMINIFOLIA promotes growth and polarity of Antirrhinum leaves. Development **131**, 3661-3670.

Grbic, V., **and Bleecker, A.B.** (2000). Axillary meristem development in Arabidopsis thaliana. Plant J **21**, 215-223.

Greb, T., **Clarenz, O.**, **Schafer, E.**, **Müller, D.**, **Herrero, R.**, **Schmitz, G.**, **and Theres, K.** (2003). Molecular analysis of the LATERAL SUPPRESSOR gene in Arabidopsis reveals a conserved control mechanism for axillary meristem formation. Genes Dev **17**, 1175-1187.

Gross-Hardt, R., **and Laux, T**. (2003). Stem cell regulation in the shoot meristem. J Cell Sci **116**, 1659-1666.

Grotewold, E., **Sainz, M.B.**, **Tagliani, L.**, **Hernandez, J.M.**, **Bowen, B.**, **and Chandler, V.L.** (2000). Identification of the residues in the Myb domain of maize C1 that specify the interaction with the bHLH cofactor R. Proc Natl Acad Sci U S A **97**, 13579-13584.

Haecker, A., **and Laux, T.** (2001). Cell-cell signaling in the shoot meristem. Curr Opin Plant Biol **4**, 441-446.

Hay, A., **Kaur, H.**, **Phillips, A.**, **Hedden, P.**, **Hake, S.**, **and Tsiantis, M.** (2002). The gibberellin pathway mediates KNOTTED1-type homeobox function in plants with different body plans. Curr Biol **12**, 1557-1565.

Heim, M.A., **Jakoby, M.**, **Werber, M.**, **Martin, C.**, **Weisshaar, B.**, **and Bailey, P.C.** (2003). The basic helix-loop-helix transcription factor family in plants: a genome-wide study of protein structure and functional diversity. Mol Biol Evol **20**, 735-747.

Hempel, F.D., **and Feldman, L.J. (**1994). Bidirectional inflorescence development in Arabidopsis thaliana—Acropetal initiation of flowers and basipetal initiation of paraclades. Planta 192: 276–286.

Henriksson, E., **Olsson, A.S.**, **Johannesson, H.**, **Johansson, H.**, **Hanson, J.**, **Engstrom, P.**, **and Soderman, E.** (2005). Homeodomain leucine zipper class I genes in Arabidopsis. Expression patterns and phylogenetic relationships. Plant Physiol **139**, 509-518.

Hibara, K., **Karim, M.R.**, **Takada, S.**, **Taoka, K.**, **Furutani, M.**, **Aida, M.**, **and Tasaka, M.** (2006). Arabidopsis CUP-SHAPED COTYLEDON3 regulates postembryonic shoot meristem and organ boundary formation. Plant Cell **18**, 2946-2957.

Higuchi, M., **Pischke, M.S.**, **Mahonen, A.P.**, **Miyawaki, K.**, **Hashimoto, Y.**, **Seki, M.**, **Kobayashi, M.**, **Shinozaki, K.**, **Kato, T.**, **Tabata, S.**, **Helariutta, Y.**, **Sussman, M.R.**, **and Kakimoto, T.** (2004). In planta functions of the Arabidopsis cytokinin receptor family. Proc Natl Acad Sci U S A **101**, 8821-8826.

Hiratsu, K., **Matsui, K.**, **Koyama, T.**, **and Ohme-Takagi, M.** (2003). Dominant repression of target genes by chimeric repressors that include the EAR motif, a repression domain, in Arabidopsis. Plant J **34**, 733-739.

Hiratsu, K., **Mitsuda, N.**, **Matsui, K.**, **and Ohme-Takagi, M.** (2004). Identification of the minimal repression domain of SUPERMAN shows that the DLELRL hexapeptide is both necessary and sufficient for repression of transcription in Arabidopsis. Biochem Biophys Res Commun **321**, 172-178.

Horvath, D.P., **Anderson, J.V.**, **Chao, W.S.**, **and Foley, M.E.** (2003). Knowing when to grow: signals regulating bud dormancy. Trends Plant Sci **8**, 534-540.

Hu, W., Zhang, S., Zhao, Z., Sun, C., Zhao, Y., and Luo, D. (2003). The analysis of the structure and expression of Os TB1 gene in rice. J. Plant Physiol. Mol. Biol. 29: 507–514.

Hubbard, L., McSteen, P., Doebley, J., and Hake, S. (2002). Expression patterns and mutant phenotype of teosinte branched1 correlate with growth suppression in maize and teosinte. Genetics **162**, 1927-1935.

Itoh, J., Sato, Y., Nagato, Y., and Matsuoka, M. (2006). Formation, maintenance and function of the shoot apical meristem in rice. Plant Mol Biol **60**, 827-842.

Jackson, D., Veit, B. and Hake, S. (1994). Expression of maize knotted1-related homeobox genes in the shoot apical meristem predicts patterns of morphogenesis in the vegetative shoot. Development 129: 405–413.

Johri, M.M., and Coe, E.H., Jr. (1983). Clonal analysis of corn plant development. I. The development of the tassel and the ear shoot. Dev Biol **97**, 154-172.

Juarez, M.T., Twigg, R.W., and Timmermans, M.C. (2004). Specification of adaxial cell fate during maize leaf development. Development **131**, 4533-4544.

Kaelin, W.G. Jr, Pallas, D.C., DeCaprio, J.A., Kaye, F.J. & Livingston, D.M. (1991). Identification of cellular proteins that can interact specifically with the T/E1A-binding region of the retinoblastoma gene product. *Cell* **64**, 521–532.

Kayes, J.M., and Clark, S.E. (1998). CLAVATA2, a regulator of meristem and organ development in Arabidopsis. Development **125**, 3843-3851.

Kebrom, T.H., Burson, B.L., and Finlayson, S.A. (2006). Phytochrome B represses Teosinte Branched1 expression and induces sorghum axillary bud outgrowth in response to light signals. Plant Physiol **140**, 1109-1117.

Keller, T., Abbott, J., Moritz, T., and Doerner, P. (2006). Arabidopsis REGULATOR OF AXILLARY MERISTEMS1 controls a leaf axil stem cell niche and modulates vegetative development. Plant Cell **18**, 598-611.

Kerstetter, R.A., and Hake, S. (1997). Shoot Meristem Formation in Vegetative Development. Plant Cell **9**, 1001-1010.

Kerstetter, R.A., Laudencia-Chingcuanco, D., Smith, L.G., and Hake, S. (1997). Loss-of-function mutations in the maize homeobox gene, knotted1, are defective in shoot meristem maintenance. Development **124**, 3045-3054.

Klee, H.J.&Estelle, M. (1991) Molecular genetic approaches to plant hormone biology. *Annu. Rev. Plant Physiol. Plant Mol. Biol.* **42**, 529 551.

Klee, H.J.&Romano, C.P. (1994) The roles of phytohormones in development as studied in transgenic plants. *Crit. Rev. Plant Sci.* **13**, 311 324.

Komatsu, K., Maekawa, M., Ujiie, S., Satake, Y., Furutani, I., Okamoto, H., Shimamoto, K., and Kyozuka, J. (2003). LAX and SPA: major regulators of shoot branching in rice. Proc Natl Acad Sci U S A **100**, 11765-11770.

Komatsu, M., Maekawa, M., Shimamoto, K., and Kyozuka, J. (2001). The LAX1 and FRIZZY PANICLE 2 genes determine the inflorescence architecture of rice by controlling rachis-branch and spikelet development. Dev Biol **231**, 364-373.

Koornneef, M., Hanhart, C.J., and van der Veen, J.H. (1991). A genetic and physiological analysis of late flowering mutants in Arabidopsis thaliana. Mol Gen Genet **229**, 57-66.

Koyama, T., Furutani, M., Tasaka, M., and Ohme-Takagi, M. (2007). TCP transcription factors control the morphology of shoot lateral organs via negative regulation of the expression of boundary-specific genes in Arabidopsis. Plant Cell **19**, 473-484.

Kumaran, M.K., Bowman, J.L., and Sundaresan, V. (2002). YABBY polarity genes mediate the repression of KNOX homeobox genes in Arabidopsis. Plant Cell **14**, 2761-2770.

Kurakawa, T., Ueda, N., Maekawa, M., Kobayashi, K., Kojima, M., Nagato, Y., Sakakibara, H., and Kyozuka, J. (2007). Direct control of shoot meristem activity by a cytokinin-activating enzyme. Nature **445**, 652-655.

Kwiatkowska, D., and Dumais, J. (2003). Growth and morphogenesis at the vegetative shoot apex of Anagallis arvensis L. J Exp Bot **54**, 1585-1595.

Lang, G.A., **Early**, **J.D.**, **Martin**, **G.C.**, **and Darnell**, **R.L.** (1987). Endo-, para- and eco-dormancy: Physiological terminology and classification for dormancy research. Hortic. Sci. 22: 371–377.

Larkin, **J.C.**, **Brown**, **M.L.**, **and Schiefelbein**, **J.** (2003). How do cells know what they want to be when they grow up? Lessons from epidermal patterning in Arabidopsis. Annu Rev Plant Biol **54**, 403-430.

Laux, **T.**, **and Jurgens**, **G.** (1997). Embryogenesis: A New Start in Life. Plant Cell **9**, 989-1000.

Laux T, Schoof H (1997) Maintaining the shoot meristem — the role of *CLAVATA1*. Trends Plant Sci 2:325–327.

Laux, **T.**, **and Mayer**, **K.F.** (1998). Cell fate regulation in the shoot meristem. Semin Cell Dev Biol **9**, 195-200.

Ledent, **V.**, **and Vervoort**, **M.** (2001). The basic helix-loop-helix protein family: comparative genomics and phylogenetic analysis. Genome Res **11**, 754-770.

Lenhard, **M.**, **and Laux**, **T.** (2003). Stem cell homeostasis in the Arabidopsis shoot meristem is regulated by intercellular movement of CLAVATA3 and its sequestration by CLAVATA1. Development **130**, 3163-3173.

Lenhard, **M.**, **Jurgens**, **G.**, **and Laux**, **T.** (2002). The WUSCHEL and SHOOTMERISTEMLESS genes fulfil complementary roles in Arabidopsis shoot meristem regulation. Development **129**, 3195-3206.

Leyser, **H.M.O.**, **and Furner**, **I.J.** (1992). Characterisation of three shoot apical meristem mutants of Arabidopsis thaliana. Development 116, 397-403.

Leyser, **H.M.**, **Lincoln**, **C.A.**, **Timpte**, **C.**, **Lammer**, **D.**, **Turner**, **J.**, **and Estelle**, **M.** (1993). Arabidopsis auxin-resistance gene AXR1 encodes a protein related to ubiquitin-activating enzyme E1. Nature **364**, 161-164.

Li, **H.**, **Xu**, **L.**, **Wang**, **H.**, **Yuan**, **Z.**, **Cao**, **X.**, **Yang**, **Z.**, **Zhang**, **D.**, **Xu**, **Y.**, **and Huang**, **H.** (2005). The Putative RNA-dependent RNA polymerase RDR6 acts synergistically with ASYMMETRIC LEAVES1 and 2 to repress BREVIPEDICELLUS and MicroRNA165/166 in Arabidopsis leaf development. Plant Cell **17**, 2157-2171.

Li, **X.**, **Qian**, **Q.**, **Fu**, **Z.**, **Wang**, **Y.**, **Xiong**, **G.**, **Zeng**, **D.**, **Wang**, **X.**, **Liu**, **X.**, **Teng**, **S.**, **Hiroshi**, **F.**, **Yuan**, **M.**, **Luo**, **D.**, **Han**, **B.**, **and Li**, **J.** (2003). Control of tillering in rice. Nature **422**, 618-621.

Liljegren, **S.J.**, **Roeder**, **A.H.**, **Kempin**, **S.A.**, **Gremski**, **K.**, **Ostergaard**, **L.**, **Guimil**, **S.**, **Reyes**, **D.K.**, **and Yanofsky**, **M.F.** (2004). Control of fruit patterning in Arabidopsis by INDEHISCENT. Cell **116**, 843-853.

Lincoln, **C.**, **Britton**, **J.H.**, **and Estelle**, **M.** (1990). Growth and development of the axr1 mutants of Arabidopsis. Plant Cell **2**, 1071-1080.

Lincoln, **C.**, **Long**, **J.**, **Yamaguchi**, **J.**, **Serikawa**, **K.**, **and Hake**, **S.** (1994). A knotted1-like homeobox gene in Arabidopsis is expressed in the vegetative meristem and dramatically alters leaf morphology when overexpressed in transgenic plants. Plant Cell **6**, 1859-1876.

Lincoln Taiz and Eduardo Zeiger (2002). Plant physiology, Third Edition. Chapter 16. Fig16.28. p364

Long, **J.**, **and Barton**, **M.K.** (2000). Initiation of axillary and floral meristems in Arabidopsis. Dev Biol **218**, 341-353.

Long, **J.A.**, **Moan**, **E.I.**, **Medford**, **J.I.**, **and Barton**, **M.K.** (1996). A member of the KNOTTED class of homeodomain proteins encoded by the STM gene of Arabidopsis. Nature **379**, 66-69.

Lynn, **K.**, **Fernandez**, **A.**, **Aida**, **M.**, **Sedbrook**, **J.**, **Tasaka**, **M.**, **Masson**, **P.**, **and Barton**, **M.K.** (1999). The PINHEAD/ZWILLE gene acts pleiotropically in Arabidopsis development and has overlapping functions with the ARGONAUTE1 gene. Development **126**, 469-481.

Mande K. Kumaran · De Ye · Wei-Cai Yang. Megan E. Griffith · Abdul M. Chaudhury. Venkatesan Sundaresan (1999). Molecular cloning of ABNORMAL FLORAL ORGANS: a gene required for flower development in Arabidopsis. Sex Plant Reprod 12:118–122

Mayer, **K.F.**, **Schoof**, **H.**, **Haecker**, **A.**, **Lenhard**, **M.**, **Jurgens**, **G.**, **and Laux**, **T.** (1998). Role of WUSCHEL in regulating stem cell fate in the Arabidopsis shoot meristem. Cell **95**, 805-815.

McConnell, **J.R.**, **and Barton**, **M.K.** (1998). Leaf polarity and meristem formation in Arabidopsis. Development **125**, 2935-2942.

McConnell, **J.R.**, **Emery**, **J.**, **Eshed**, **Y.**, **Bao**, **N.**, **Bowman**, **J.**, **and Barton**, **M.K.** (2001). Role of PHABULOSA and PHAVOLUTA in determining radial patterning in shoots. Nature **411**, 709-713.

Mcdaniel, **C.N.**, **and Poethig**, **R.S.** (1988) Planta Cell-lineage patterns in the shoot apical meristem of the germinating maize embryo. 175, 13–22.

Medford, **J.I.**, **Behringer**, **F.J.**, **Callos**, **J.D.**, **and Feldmann**, **K.A.** (1992). Normal and Abnormal Development in the Arabidopsis Vegetative Shoot Apex. Plant Cell **4**, 631-643.

Menand, **B.**, **Yi**, **K.**, **Jouannic**, **S.**, **Hoffmann**, **L.**, **Ryan**, **E.**, **Linstead**, **P.**, **Schaefer**, **D.G.**, **and Dolan**, **L.** (2007). An ancient mechanism controls the development of cells with a rooting function in land plants. Science **316**, 1477-1480.

Meyerowitz, **E.M.** (1997). Genetic control of cell division patterns in developing plants. Cell **88**, 299-308.

Morita, **Y.**, **Saitoh**, **M.**, **Hoshino**, **A.**, **Nitasaka**, **E.**, **and Iida**, **S.** (2006). Isolation of cDNAs for R2R3-MYB, bHLH and WDR transcriptional regulators and identification of c and ca mutations conferring white flowers in the Japanese morning glory. Plant Cell Physiol *47*, 457-470

Müller, **D.**, **Schmitz**, **G.**, **and Theres**, **K.** (2006). Blind homologous R2R3 Myb genes control the pattern of lateral meristem initiation in Arabidopsis. Plant Cell **18**, 586-597.

Napoli, **C.** (1996). Highly Branched Phenotype of the Petunia dad1-1 Mutant Is Reversed by Grafting. Plant Physiol **111**, 27-37.

Navarro, **C.**, **Efremova**, **N.**, **Golz**, **J.F.**, **Rubiera**, **R.**, **Kuckenberg**, **M.**, **Castillo**, **R.**, **Tietz**, **O.**, **Saedler**, **H.**, **and Schwarz-Sommer**, **Z.** (2004). Molecular and genetic interactions between STYLOSA and GRAMINIFOLIA in the control of Antirrhinum vegetative and reproductive development. Development **131**, 3649-3659.

Nishimura, **C.**, **Ohashi**, **Y.**, **Sato**, **S.**, **Kato**, **T.**, **Tabata**, **S.**, **and Ueguchi**, **C.** (2004). Histidine kinase homologs that act as cytokinin receptors possess overlapping functions in the regulation of shoot and root growth in Arabidopsis. Plant Cell **16**, 1365-1377.

Ohgishi, **M.**, **Oka**, **A.**, **Morelli**, **G.**, **Ruberti**, **I.**, **and Aoyama**, **T.** (2001). Negative autoregulation of the Arabidopsis homeobox gene ATHB-2. Plant J **25**, 389-398.

Otsuga, **D.**, **DeGuzman**, **B.**, **Prigge**, **M.J.**, **Drews**, **G.N.**, **and Clark**, **S.E.** (2001). REVOLUTA regulates meristem initiation at lateral positions. Plant J **25**, 223-236.

Pautot, **V.**, **Dockx**, **J.**, **Hamant**, **O.**, **Kronenberger**, **J.**, **Grandjean**, **O.**, **Jublot**, **D.**, **and Traas**, **J.** (2001). KNAT2: evidence for a link between knotted-like genes and carpel development. Plant Cell **13**, 1719-1734.

Payne, **C.T.**, **Zhang**, **F.**, **and Lloyd**, **A.M.** (2000). GL3 encodes a bHLH protein that regulates trichome development in arabidopsis through interaction with GL1 and TTG1. Genetics **156**, 1349-1362.

Piehler, **J.** (2005). New methodologies for measuring protein interactions in vivo and in vitro. Curr Opin Struct Biol **15**, 4-14.

Poethig, **R.S.** (1997). Leaf morphogenesis in flowering plants. Plant Cell **9**, 1077-1087.

Prigge, **M.J.**, **Otsuga**, **D.**, **Alonso**, **J.M.**, **Ecker**, **J.R.**, **Drews**, **G.N.**, **and Clark**, **S.E.** (2005). Class III homeodomain-leucine zipper gene family members have overlapping, antagonistic, and distinct roles in Arabidopsis development. Plant Cell **17**, 61-76.

Raman (2006). Genetic Analysis of Axillary Meristem Development in Arabidopsis: Roles of MIR164, CUC1, CUC2, CUC3 and LAS, and identification of novel regulators. *Inaugural-Dissertation zur Erlangung des Doktorgrades der Mathematisch-Naturwissenschaftlichen Fakultät der Universität zu Köln.*

Ramsay, **N.A.**, **and Glover**, **B.J.** (2005). MYB-bHLH-WD40 protein complex and the evolution of cellular diversity. Trends Plant Sci **10**, 63-70.

Reinhardt, **D.**, **Mandel**, **T.**, **and Kuhlemeier**, **C.** (2000). Auxin regulates the initiation and radial position of plant lateral organs. Plant Cell **12**, 507-518.

Reinhardt, **D.**, **Pesce**, **E.R.**, **Stieger**, **P.**, **Mandel**, **T.**, **Baltensperger**, **K.**, **Bennett**, **M.**, **Traas**, **J.**, **Friml**, **J.**, **and Kuhlemeier**, **C.** (2003). Regulation of phyllotaxis by polar auxin transport. Nature **426**, 255-260.

Riefler, M., **Novak**, O., **Strnad**, M., **and Schmulling**, T. (2006). Arabidopsis cytokinin receptor mutants reveal functions in shoot growth, leaf senescence, seed size, germination, root development, and cytokinin metabolism. Plant Cell **18**, 40-54.

Rojo, E., **Sharma**, V.K., **Kovaleva**, V., **Raikhel**, N.V., **and Fletcher**, J.C. (2002). CLV3 is localized to the extracellular space, where it activates the Arabidopsis CLAVATA stem cell signaling pathway. Plant Cell **14**, 969-977.

Sakamoto, T., **Kamiya**, N., **Ueguchi-Tanaka**, M., **Iwahori**, S., **and Matsuoka**, M. (2001). KNOX homeodomain protein directly suppresses the expression of a gibberellin biosynthetic gene in the tobacco shoot apical meristem. Genes Dev **15**, 581-590.

Sawa, S. (2002). Overexpression of the AtmybL2 gene represses trichome development in Arabidopsis. DNA Res **9**, 31-34.

Sawa, S., **Ito**, T., **Shimura**, Y., **and Okada**, K. (1999a). FILAMENTOUS FLOWER controls the formation and development of arabidopsis inflorescences and floral meristems. Plant Cell **11**, 69-86.

Sawa, S., **Ohgishi**, M., **Goda**, H., **Higuchi**, K., **Shimada**, Y., **Yoshida**, S., **and Koshiba**, T. (2002). The HAT2 gene, a member of the HD-Zip gene family, isolated as an auxin inducible gene by DNA microarray screening, affects auxin response in Arabidopsis. Plant J **32**, 1011-1022.

Sawa, S., **Watanabe**, K., **Goto**, K., **Liu**, Y.G., **Shibata**, D., **Kanaya**, E., **Morita**, E.H., **and Okada**, K. (1999b). FILAMENTOUS FLOWER, a meristem and organ identity gene of Arabidopsis, encodes a protein with a zinc finger and HMG-related domains. Genes Dev **13**, 1079-1088.

Schiefelbein, J. (2003). Cell-fate specification in the epidermis: a common patterning mechanism in the root and shoot. Curr Opin Plant Biol **6**, 74-78.

Schiefelbein, J.W., **Masucci**, J.D., **and Wang**, H. (1997). Building a root: the control of patterning and morphogenesis during root development. Plant Cell **9**, 1089-1098.

Schmitz, G., **and Theres**, K. (2005). Shoot and inflorescence branching. Curr Opin Plant Biol **8**, 506-511.

Schmitz, G., **Tillmann**, E., **Carriero**, F., **Fiore**, C., **Cellini**, F., **and Theres**, K. (2002). The tomato Blind gene encodes a MYB transcription factor that controls the formation of lateral meristems. Proc Natl Acad Sci U S A **99**, 1064-1069.

Schneeberger, R., **Tsiantis**, M., **Freeling**, M., **and Langdale**, J.A. (1998). The rough sheath2 gene negatively regulates homeobox gene expression during maize leaf development. Development **125**, 2857-2865.

Schoof, H., **Lenhard**, M., **Haecker**, A., **Mayer**, K.F., **Jurgens**, G., **and Laux**, T. (2000). The stem cell population of Arabidopsis shoot meristems in maintained by a regulatory loop between the CLAVATA and WUSCHEL genes. Cell **100**, 635-644.

Schulze (2007). Charakterisierung *HAIRY MERISTEM*-ähnlicher Gene und Identifizierung neuer Regulatoren der Seitentriebentwicklung in *Arabidopsis thaliana. Inaugural-Dissertation zur Erlangung des Doktorgrades der Mathematisch-Naturwissenschaftlichen Fakultät der Universität zu Köln.*

Schumacher, K., **Schmitt**, T., **Rossberg**, M., **Schmitz**, G., **and Theres**, K. (1999). The Lateral suppressor (Ls) gene of tomato encodes a new member of the VHIID protein family. Proc Natl Acad Sci U S A **96**, 290-295.

Sessa, G., **Steindler**, C., **Morelli**, G., **and Ruberti**, I. (1998). The Arabidopsis Athb-8, -9 and -14 genes are members of a small gene family coding for highly related HD-ZIP proteins. Plant Mol Biol **38**, 609-622.

Siegfried, K.R., **Eshed**, Y., **Baum**, S.F., **Otsuga**, D., **Drews**, G.N., **and Bowman**, J.L. (1999). Members of the YABBY gene family specify abaxial cell fate in Arabidopsis. Development **126**, 4117-4128.

Sinha, N.R., **Williams**, R. E., **and Hake**, S. (1993) Overexpression of the maize homeobox gene, KNOTTED-1, causes a switch from determinate to indeterminate cell fates. Gene Dev. 7, 787–795.

Smith, L.G., **Greene**, B., **Veit**, B., **and Hake**, S. (1992) A dominant mutation in the maize homeobox gene, Knotted-1, causes its ectopic expression in leaf cells with altered fates. Development 116, 21–30.

Smyth, D.R., **Bowman**, J.L., **and Meyerowitz**, E.M. (1990). Early flower development in Arabidopsis. Plant Cell **2**, 755-767.

Snow, **M.**, **and Snow**, **R**. (1942). The determination of axillary buds. New Phytol. 41, 13–22.

Snowden, **K.C.**, **Simkin**, **A.J.**, **Janssen**, **B.J.**, **Templeton**, **K.R.**, **Loucas**, **H.M.**, **Simons**, **J.L.**, **Karunairetnam**, **S.**, **Gleave**, **A.P.**, **Clark**, **D.G.**, **and Klee**, **H.J.** (2005). The Decreased apical dominance1/Petunia hybrida CAROTENOID CLEAVAGE DIOXYGENASE8 gene affects branch production and plays a role in leaf senescence, root growth, and flower development. Plant Cell **17**, 746-759.

Sorefan, **K.**, **Booker**, **J.**, **Haurogne**, **K.**, **Goussot**, **M.**, **Bainbridge**, **K.**, **Foo**, **E.**, **Chatfield**, **S.**, **Ward**, **S.**, **Beveridge**, **C.**, **Rameau**, **C.**, **and Leyser**, **O.** (2003). MAX4 and RMS1 are orthologous dioxygenase-like genes that regulate shoot branching in Arabidopsis and pea. Genes Dev **17**, 1469-1474.

Steeves, **T.A.**, **and Sussex**, **I**. **M.** (1989) Patterns in Plant Development. Cambridge University Press 2nd edition Cambridge, UK.

Stirnberg, **P.**, **Chatfield**, **S.P.**, **and Leyser**, **H.M.** (1999). AXR1 acts after lateral bud formation to inhibit lateral bud growth in Arabidopsis. Plant Physiol **121**, 839-847.

Stirnberg, **P.**, **van De Sande**, **K.**, **and Leyser**, **H.M.** (2002). MAX1 and MAX2 control shoot lateral branching in Arabidopsis. Development **129**, 1131-1141.

Sun, **Y.**, **Zhou**, **Q.**, **Zhang**, **W.**, **Fu**, **Y. and Huang**, **H**. (2002). ASYMMETRIC LEAVES1, an Arabidopsis gene that is involved in the control of cell differentiation in leaves. Planta 214: 694–702.

Sussex, **I.M.** (1955) Morphogenesis in solanum tuberosum l.: experimental investigation of leaf dorsiventrali and orientation in the juvenile shoot. Phytomorphology 5, 286–300.

Sussex IM: Morphogenesis in *Solanum tuberosum* L. (1995). Experimental investigation of leaf dorsoventrality and orientation in the juvenile shoot. *Phytomorphology*, 5:286-300.

Sussex, **I.M.**, **and Kerk**, **N.M.** (2001). The evolution of plant architecture. Curr Opin Plant Biol **4**, 33-37.

Takada, **S.**, **Hibara**, **K.**, **Ishida**, **T.**, **and Tasaka**, **M.** (2001). The CUP-SHAPED COTYLEDON1 gene of Arabidopsis regulates shoot apical meristem formation. Development **128**, 1127-1135.

Takeda, **T.**, **Suwa**, **Y.**, **Suzuki**, **M.**, **Kitano**, **H.**, **Ueguchi-Tanaka**, **M.**, **Ashikari**, **M.**, **Matsuoka**, **M.**, **and Ueguchi**, **C**. (2003). The OsTB1 gene negatively regulates lateral branching in rice. Plant J **33**, 513-520.

Talbert, **P.B.**, **Adler**, **H.T.**, **Parks**, **D.W.**, **and Comai**, **L.** (1995). The REVOLUTA gene is necessary for apical meristem development and for limiting cell divisions in the leaves and stems of Arabidopsis thaliana. Development **121**, 2723-2735.

Tanaka, **Y.**, **Suzuki**, **T.**, **Yamashino**, **T.**, **and Mizuno**, **T.** (2004). Comparative studies of the AHP histidine-containing phosphotransmitters implicated in His-to-Asp phosphorelay in Arabidopsis thaliana. Biosci Biotechnol Biochem **68**, 462-465.

Theodoris, **G.**, **Inada**, **N.**, **and Freeling**, **M.** (2003). Conservation and molecular dissection of ROUGH SHEATH2 and ASYMMETRIC LEAVES1 function in leaf development. Proc Natl Acad Sci U S A **100**, 6837-6842.

Timmermans, **M.C.**, **Hudson**, **A.**, **Becraft**, **P.W.**, **and Nelson**, **T**. (1999). ROUGH SHEATH2: a Myb protein that represses knox homeobox genes in maize lateral organ primordia. Science **284**, 151-153.

Toledo-Ortiz, **G.**, **Huq**, **E.**, **and Quail**, **P.H**. (2003). The Arabidopsis basic/helix-loop-helix transcription factor family. Plant Cell **15**, 1749-1770.

Trotochaud, **A.E.**, **Hao**, **T.**, **Wu**, **G.**, **Yang**, **Z.**, **and Clark**, **S.E.** (1999). The CLAVATA1 receptor-like kinase requires CLAVATA3 for its assembly into a signaling complex that includes KAPP and a Rho-related protein. Plant Cell **11**, 393-406.

Turnbull, **C.G.**, **Booker**, **J.P.**, **and Leyser**, **H.M.** (2002). Micrografting techniques for testing long-distance signalling in Arabidopsis. Plant J **32**, 255-262.

Vernoux, **T.**, **Kronenberger**, **J.**, **Grandjean**, **O.**, **Laufs**, **P.**, **and Traas**, **J.** (2000). PIN-FORMED 1 regulates cell fate at the periphery of the shoot apical meristem. Development **127**, 5157-5165.

Vollbrecht, **E.**, **Reiser**, **L.**, **and Hake**, **S**. (2000). Shoot meristem size is dependent on inbred background and presence of the maize homeobox gene, knotted1. Development **127**, 3161-3172.

Vroemen, C.W., Mordhorst, A.P., Albrecht, C., Kwaaitaal, M.A., and de Vries, S.C. (2003). The CUP-SHAPED COTYLEDON3 gene is required for boundary and shoot meristem formation in Arabidopsis. Plant Cell **15**, 1563-1577.

Wada, T., Kurata, T., Tominaga, R., Koshino-Kimura, Y., Tachibana, T., Goto, K., Marks, M.D., Shimura, Y., and Okada, K. (2002). Role of a positive regulator of root hair development, CAPRICE, in Arabidopsis root epidermal cell differentiation. Development **129**, 5409-5419.

Waites, R., Selvadurai, H.R., Oliver, I.R., and Hudson, A. (1998). The PHANTASTICA gene encodes a MYB transcription factor involved in growth and dorsoventrality of lateral organs in Antirrhinum. Cell **93**, 779-789.

Walter, M., Chaban, C., Schutze, K., Batistic, O., Weckermann, K., Nake, C., Blazevic, D., Grefen, C., Schumacher, K., Oecking, C., Harter, K., and Kudla, J. (2004). Visualization of protein interactions in living plant cells using bimolecular fluorescence complementation. Plant J **40**, 428-438.

Ward, S.P., and Leyser, O. (2004). Shoot branching. Curr Opin Plant Biol **7**, 73-78.

Weigel, D., and Jurgens, G. (2002). Stem cells that make stems. Nature **415**, 751-754.

Witte, C.P., Noel, L.D., Gielbert, J., Parker, J.E., and Romeis, T. (2004). Rapid one-step protein purification from plant material using the eight-amino acid StrepII epitope. Plant Mol Biol **55**, 135-147.

Wu, H. Mori, A. Jiang, X. Wang Y.X. and Yang M. (2006) The INDEHISCENT protein regulates unequal cell divisions in *Arabidopsis* fruit. *Planta*, 224, 971-979.

Zhang, F., Gonzalez, A., Zhao, M., Payne, C.T., and Lloyd, A. (2003). A network of redundant bHLH proteins functions in all TTG1-dependent pathways of Arabidopsis. Development **130**, 4859-4869.

Zhong, R., and Ye, Z.H. (2004). Amphivasal vascular bundle 1, a gain-of-function mutation of the IFL1/REV gene, is associated with alterations in the polarity of leaves, stems and carpels. Plant Cell Physiol **45**, 369-385.

Die vorliegende Arbeit wurde am Max-Planck-Institut für Züchtungsforschung in Köln durchgeführt.

8.   Erklärung

Ich versichere, dass ich die von mir vorgelegte Dissertation selbständig angefertigt, die benutzten Quellen und Hilfsmittel vollständig angegeben und die Stellen der Arbeit – einschließlich Tabellen, Karten und Abbildungen -, die anderen Werken im Wortlaut oder dem Sinn nach entnommen sind, in jedem Einzelfall als Entlehnung kenntlich gemacht habe; dass diese Dissertation noch keiner anderen Fakultät oder Universität zur Prüfung vorgelegen hat; dass sie - abgesehen von unten angegebenen Teilpublikationen - noch nicht veröffentlicht worden ist sowie, dass ich eine solche Veröffentlichung vor Abschluss des Promotionsverfahrens nicht vornehmen werde. Die Bestimmungen dieser Promotionsordnung sind mir bekannt. Die von mir vorgelegte Dissertation ist von Priv. Doz. Dr. Klaus Theres betreut worden.

Köln, 20 Dezember 2007

Fang Yang